TYROSINE-DERIVED POLYMERIC NANOCARRIERS: AN INNOVATIVE APPROACH FOR TOPICAL DRUG DELIVERY IN ACNE THERAPY

by

TANNAZ RAMEZANLI

A Dissertation Submitted to the

Graduate School-New Brunswick

Rutgers, The State University of New Jersey

In partial fulfillment of the requirements

For the degree of

Doctor of Philosophy

Graduate Program in Pharmaceutical Sciences

Written under the direction of

Professor Bozena Michniak-Kohn, Ph.D.

And approved by

_____

_____

_____

_____

New Brunswick, New Jersey

May, 2016

ABSTRACT OF THE DISSERTATION

Tyrosine-Derived Polymeric Nanocarriers: An Innovative Approach for Topical Drug Delivery in Acne Therapy

By TANNAZ RAMEZANLI

Dissertation Director: Professor Bozena Michniak-Kohn

The importance of nanotechnology in the field of drug delivery has been dramatically increased and nanocarriers are finding potential applications in many areas of medicine. The unique physico-chemical properties of nanoparticles allow them to overcome some biological barriers and hence, improve the bioavailability of their payload. In this thesis, a platform technology has been described based on amphiphilic biocompatible ABA triblock copolymers that self-assemble to form polymeric nanomicelles (TyroSpheres) to address the need of a suitable carrier system for enhancing the topical delivery of lipophilic actives and their solubility as well as stability in the formulation. Our goal was to investigate the applicability of TyroSpheres for follicular drug delivery and develop an aqueous-based gel formulation of drug-TyroSphere for acne therapy. In addition, we explored other biological properties of this carrier system for drug delivery, including cytotoxicity, genotoxicity and skin irritation to ensure the safety of the carriers/formulation for short-term and long-term applications.

Our selected anti-acne drug was adapalene, a third generation retinoid with a logP of 8.2. Adapalene-TyroSphere formulations were characterized for carrier particle size, binding efficiency, drug loading, drug release, sebum partitioning, crystallinity, and finally follicular delivery. Gel formulations of adapalene-TyroSpheres were also prepared using different thickening agents and analyzed for content uniformity, rheology, particle agglomeration and skin irritation. A preclinical mouse acne model was employed to test the efficacy of the adapalene treatment via TyroSpheres and compare it with the commercial product, Differin®.

Another highly lipophilic active that was formulated with TyroSpheres was Vitamin D3, which is sensitive to many environmental factors and hence, is an unstable compound. TyroSpheres were able to protect Vitamin D3 against hydrolysis and photodegradation and significantly enhance the stability of this active in the aqueous formulation.

In summary, our findings show that TyroSpheres lack short-term cytotoxicity and genotoxicity. These nanoparticles can accumulate in hair follicles and enhance drug delivery through intercellular and follicular pathways, which can benefit treatment of dermatological disorders, such as acne. The comedolytic properties of the retinoid were preserved after being encapsulated in TyroSpheres. The novel oil-free and alcohol-free aqueous-based formulation of adapalene can be potentially used in management of acne by delivering the drug where the disease originates, while reducing drug/vehicle-related skin irritation.

Acknowledgments

I would like to express my deep gratitude to the people and organizations that contributed to my dissertation projects or played a part in my graduate study.

I would like to thank Department of Pharmaceutics at Ernest Mario School of Pharmacy to give me an opportunity to pursue my Ph.D. in Pharmaceutical Sciences, all the professors who thought me and all the colleagues, labmates and classmates for their assistance and friendship.

My foremost gratitude goes to my advisor, Dr. Bozena Michniak-Kohn who admitted me to the Laboratory of Drug Delivery in September 2011, introduced me to skin research, and supported me intellectually. She let me choose my own research path and has been always supportive of the decisions that I made in my research projects.

I would like to thank Division of Life Sciences at Rutgers University and specially Dr. Garry Merrill who offered me a TA position at Systems Physiology and funded my education for the past four years. It was an absolute honor to work for Dr. Merrill. I truly admire his wisdom and manners.

I want to take this opportunity to thank the past and current members at New Jersey center for Biomaterials who assisted me with my research. Dr. Joachim Kohn, for allowing me to use his facility and his polymer; Dr. Ritu Goyal, Dr. Yong Mao, Dr. Murat Guvendiren, and Koustubh Dube for sharing their knowledge and experience with me; and most importantly Dr. Zheng Zhang for all his assistance and inputs in TyroSphere project.

I would like to thank all the past and current members of the Drug Delivery Laboratory, especially Pei-Chin Tsai, Krizia Karry, Dina Ameen, Mania Dorrani, and Golshid Keyvan for making our lab a wonderful place to work in and assisting me whenever I needed them. I will definitely miss their company.

I am also very grateful to Dr. Marianne Polunas at Research Pathology Services, Rutgers University for assisting me with histological analyses; Dr. Gregory Voronin and Mariel Nigro for their valuable input in the animal protocol and teaching me all the required techniques for the animal study; Valentine Starovoytov for helping me with TEM and SEM studies; and Dr. Frank Romanski from BASF for sending us samples of their polymers.

I would like to thank my thesis committee members, Dr. Tamara Minko, Dr. Leonid Kagan, and Dr. Amy Pappert for taking the time out of their busy schedules to review my thesis. Your critiques, comments, and guidance have truly been appreciated.

I am very grateful to the administrative staff at department of Pharmaceutics, Division of Life Sciences, and Center for Biomaterials, especially Hui Pung, Jana Curry, Louli Kourkounakis and Carol Lenardson.

I would like to thank my beloved relatives in the United States for their love and support during the past 6 years that I was far away from my parents and hometown. Especially, my aunt Fathieh Kiai who petitioned for me and my family to receive US Green Card. She and her kind husband, Hormoz Kiai took care of me while I was living in California

and treated me like their own child. I will always be grateful for all their support and kindness. My kind and caring cousin, Farnaz Absalan, who introduced me to Rutgers. I was very lucky to have her close to me when I first moved to New Jersey and didn't know anyone.

I also want to thank all the wonderful people that I met and became friends with at Rutgers (so many to list but I am sure you know who you are). I am thankful for their friendship, support and all the wonderful memories that we created together.

Finally, no words can express my love to my dearest parents and brother. Without their unconditional love, support, and encouragement none of my achievements have been possible. My dad is my roll model. He encouraged and supported me to pursue higher education. Even though we lived 6,000 miles apart, I knew I could count on him whenever I needed assistance or a second opinion. My mom is my angel. She has made a lot of sacrifices for her children. This journey was as hard on her as it was on me. Her love and affection have sustained me throughout my life. My wonderful brother and best friend Sam, who also studied at Rutgers and was beside me throughout the whole journey. He has been a great source of peace and comfort in my happy days and sad days and lit me up whenever I was down. I am truly blessed to have him in my life.

Dedications

I dedicate this thesis to my family. My parents, Mohammad Ramezanli and Fetneh Reyhanlou for their constant love and support. All I have and will accomplish are only possible due to their love and sacrifices. My brother, Sam Ramezanli who stood by me for this entire journey.

Table of Contents

List of Tables

List of Illustrations

Chapter 1. Background and Specific aims

1.1. Skin

Skin is one of the largest and most accessible organs of the body (approximately 1.8 m^2 surface area), which functions as a protective barrier against exogenous materials and dehydration, assisting in the maintenance of homeostasis by excreting water and salts and regulating body temperature, and also serving as an essential sensory organ for tactile and thermal stimuli.[1] Skin is composed of three main layers of epidermis, dermis and hypodermis (from top to bottom). The epidermis, the thinnest layer of the skin (a few hundred micrometers), consists of stratum corneum (SC), a granular layer, a spinous layer and a basal/suprabasal layer. The combination of the last three layers is known as the viable epidermis (Figure 1.1). The cellular components of the viable epidermis are the keratinizing epithelial cells, melanocytes, Langerhans cells, and Merkel cells.[2]

The topmost layer of epidermis, the SC, forms the interface with the environment. The average thickness of human SC is less than 20 μm and is the main contributor to the skin's barrier properties. This layer contains corneocytes —flattened dead cell bodies of terminally differentiated keratinocytes— and intercellular lipid lamellae. Intercellular lipids are sandwiched between corneocytes, forming a brick-and-mortar structure in SC.[3-4]

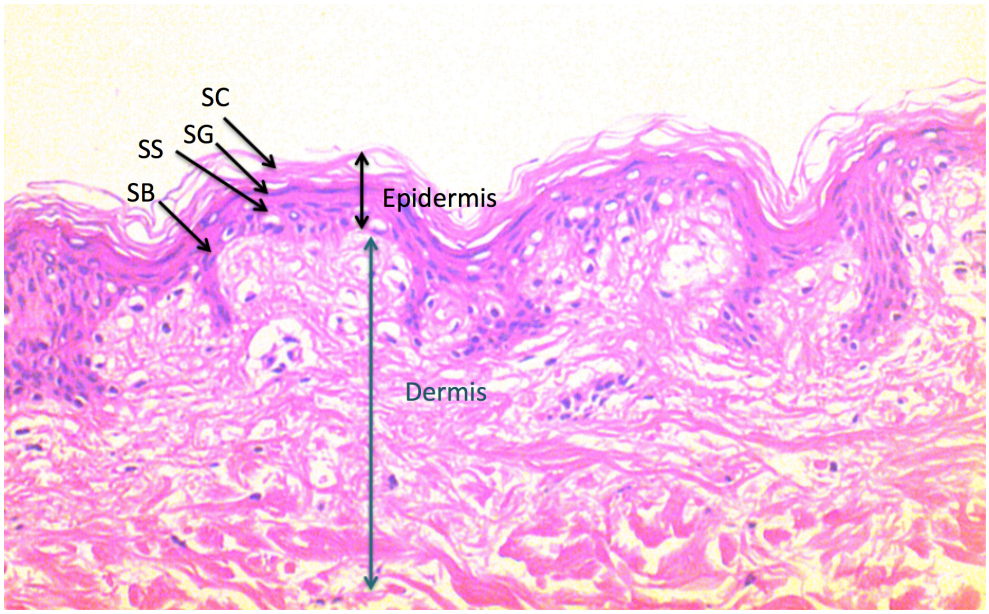

Figure 1.1. Cross section view of the human skin stained with haematoxylin and eosin. Epidermis layers are shown with arrows: stratum corneum (SC), stratum granulosum (SG), stratum spinosum (SS), and stratum basale (SB).

The dermis is a thick layer (3-5 mm) of fibrous and elastic tissue that is located underneath the epidermis. Collagen, elastin, and fibrillin are the main components of elastic connective tissue that provides flexibility and strength of the skin. Fibroblasts, endothelial cells, and mast cells exist in the dermis and are embedded with blood vessels, nerve endings, lymphatic vessels, sebaceous glands, sweat glands and hair follicles. The lowest layer of the skin that attaches it to the underlying structures is the hypodermis. The hypodermis contains a network of adipocytes (fat cells) and serves as thermal insulation, an energy storage area, a protective padding, and provides shock absorption.[5]

Skin appendages are skin-associated structures that exist within the epidermis and extend down into the hypodermis. In human skin, some of the common skin appendages are: hair follicles (that contains the hair shaft), sebaceous glands (that secrete an oily mixture called sebum into follicular cavity), arrector pilli muscles (that are connected to the hair follicle), eccrine glands (that secrete sweat and therefore regulate body

temperature), apocrine sweat glands and nails. Hair follicles contain several types of stem cells that not only produce hair, but also play an important role in re-epithelialization of skin and wound healing. The combination of hair shaft, hair follicle, sebaceous gland, and arrector pilli muscle connected to the follicle is commonly referred to as the pilosebaceous unit.[6-7]

1.2. Skin: a route for drug delivery

Due to its large surface area and easy accessibility, skin can be used as a potential site of application for drug delivery. This delivery avenue is both applicable for 1) delivery of chemicals to the skin strata to treat local dermatological conditions (topical delivery) and/or delivery to the blood vessels in the dermis that transfers the drug to the systemic circulation (transdermal delivery).[8] The process of transdermal drug delivery includes partitioning and diffusion through the mainly lipophilic SC, which provides the rate limiting step; partitioning into the viable epidermis, which is more hydrophilic than the SC in nature; and finally into the capillary network of the dermis.[9] Topical or transdermal delivery offers several advantages over other conventional routes of delivery (oral and intravenous injection) such as minimal or no first pass metabolism, non-invasive and painless delivery, self-administration of the dosage form, and possibilities of controlled or pulsatile drug delivery.[10] Moreover, in some skin disorders, such as psoriasis, atopic dermatitis, and melanoma, the target sites are within the skin. Hence, the skin layers affected by the diseases are closer to the SC providing a shorter pathway for the therapeutic drug to transverse to reach its target.[7, 9]

Generally, there are three main penetration pathways through the epidermis: 1) intercellular route, where the compounds penetrate via the lipid bilayers around the

corneocytes through the SC. This is the main penetration pathway for lipophilic and amphiphilic molecules; 2) transcellular (paracellular) route that permits drug penetration through corneocytes and 3) transappendageal which is mostly through the hair follicles, (surrounded by dense network of capillaries).[11-12]

The cutaneous delivery of drug molecules through intercellular pathway is guided by passive diffusion in one dimension and can be described most simply by Fick's first law of diffusion:

$$J = D\frac{\partial \varphi}{\partial x} = \frac{\partial \mathrm{M}}{A \times \partial \mathrm{t}}$$

In the equation above, J, the diffusion flux, is the amount of compound going through a unit area during a small interval of time; D is the diffusion coefficient of the compound in the membrane; $\partial\varphi/\partial x$ is concentration gradient; A is membrane surface area; and M is mass of the compound.[7,13]

The unique structure of the human skin, especially SC, prevents penetration of many xenobiotics, which imposes challenges for topical/transdermal drug delivery. A variety of strategies have been studied in the past few decades to overcome the barrier and optimize the cutaneous delivery of drugs. These approaches can be categorized into passive and active penetration enhancement techniques.[7] The passive penetration enhancement methods usually entail optimization of the drug carrier and formulation to increase the penetration flux across the skin. For example, using chemical penetration enhancers that reversibly alter the lipid structure of the SC to compromise skin barrier properties hence, allowing the drug transport passively across the skin; using a prodrug with better physicochemical characteristics for skin permeation; and/or using particulate systems for drug encapsulation to increase residence time of the formulation on the skin

and assist with partitioning of the drug to the SC.[2, 14] The active penetration enhancement methods involve bypassing, removing or disrupting the SC. These methods are suited for high molecular weight polar or hydrophilic compounds (e.g. peptides and genes) that do not have adequate properties to passively permeate to the skin. Examples for active penetration enhancement techniques are abrasion, microneedles, electroporation and iontophoresis.[7, 15-16] Different passive and active penetration enhancement techniques are listed in Figure 1.2.

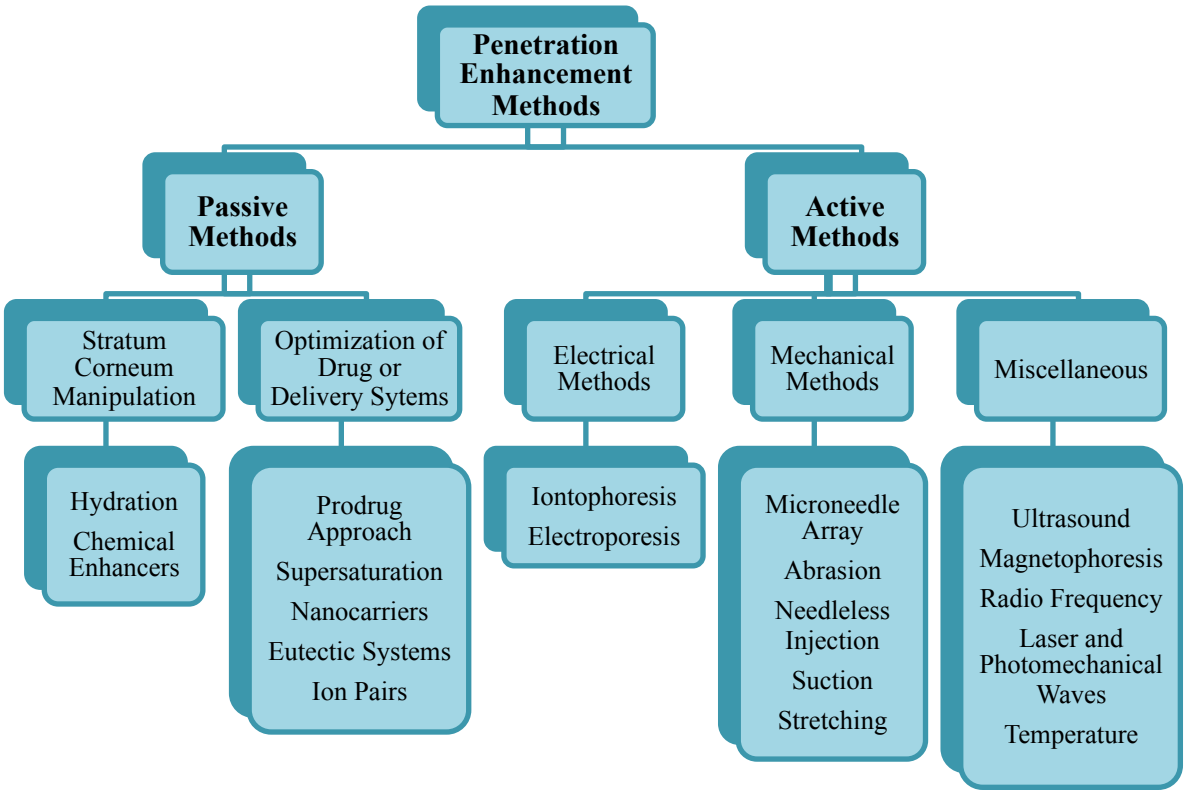

Figure 1.2. An overview of passive and active skin penetration enhancement techniques.[7]

1.3. Hair follicles, a route for drug delivery

The mammalian hair follicles have a complex structure, where various epithelial cell types, immunocompetent cells, and stem cells coexist.[17] The structure of the pilosebaceous unit is shown in Figure 1.3. The cells at the hair bulb are responsible for regulating hair growth. Each hair follicle is associated with one or more sebaceous glands, which produce a fungistatic and bacteriostatic mixture of waxes, triglycerides, and short chain fatty acids called sebum. Sebum is discharged into the upper third of the follicular canal and travel upwards to the surface of the skin. Sebum protects and lubricates the skin and helps maintaining its acidic pH (which is about 5).[12]

The follicular pathway has recently drawn a lot of attention in the field of skin delivery. Hair follicles can function as portal of entry for micro-sized particles and polar substances that cannot penetrate through SC at normal physiological conditions.[18] Hair follicles are surrounded by dense network of capillaries that can enhance systemic delivery rate of the topically applied chemicals.

Transfollicular pathway in comparison with transepidermal pathway is associated with faster absorption rate. In a study performed using caffeine, its absorption rate for hair follicles was about 10 times higher than for the SC.[19] Additionally, recent findings have revealed that as opposed to SC that only provides a short-term reservoir function, hair follicles represent efficient long-term reservoirs (up to 10 days) for topically applied compounds and particles, which can provide the possibility of retarded delivery. That is due to slow processes of hair growth, sebum production and sebum flow rate inside the follicles.[20]

The pilosebaceous unit is the target site for drug delivery in treatment of hair follicle-related disorders.[21] For instance, the sebaceous glands are involved in the etiology of both acne and androgenic alopecia (as conversion of testosterone to its active form, 5α-dihydrotestosterone occurs in sebaceous gland cells).[22] Follicular penetration was partially ignored by many investigators in the past, because it was assumed that hair follicles occupy less than 0.1% of the total skin area.[11] However, later it was realized that hair follicle density varies in different areas of human skin and also that some delivery occurs preferentially through follicles (especially with using techniques like iontophoresis[23]). There are locations such as palms and lips, where no hair grows and parts such as scalp and face that follicular openings may represent up to 10% of the skin area.[21]

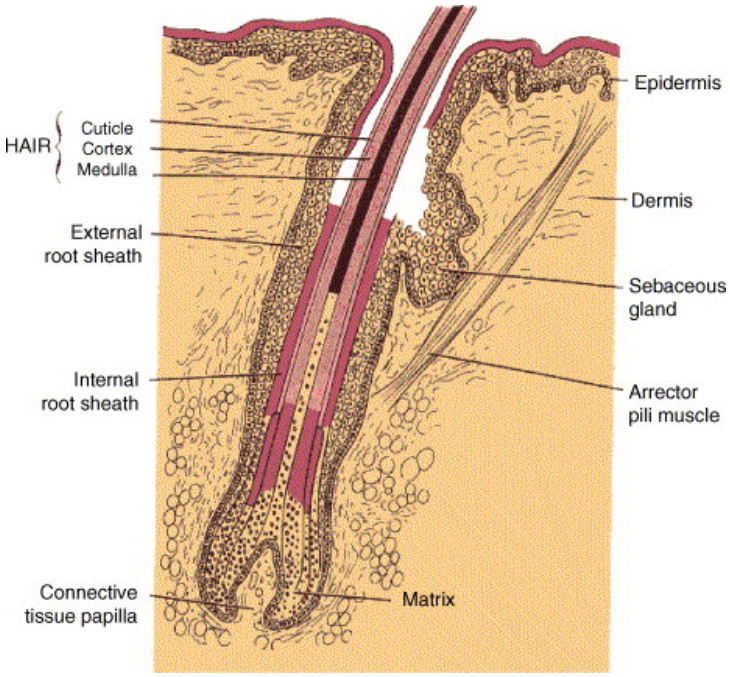

Figure 1.3. Structure of pilosebaceous unit.[21]

1.4. Acne and the medications for acne therapy

Acne is a chronic inflammatory disorder involving the pilosebaceous unit and it is one of the most common skin diseases in the young population. It is associated with hyperkeratinization, increased sebum production, change in the quality of sebum lipids, dysregulation of the hormone microenvironment, inflammation, and bacterial colonization within the pilosebaceous unit. Even though acne is not a lethal disease, it has severe consequences for the personality development of young people. In addition, much of the older population that are beyond puberty suffer acne problems including pregnant women. A high prevalence of depression and suicide are reported to be associated with this skin disorder.[22-24]

The early and non-inflammatory stage of acne usually features comedones, where the abnormal desquamation of follicular epithelium, increased cohesiveness of corneocytes, and androgen-driven activation of sebum secretion occur. Hyperkeratinization of follicular epithelium prevents normal shedding of follicular keratinocytes. As a result the pilosebaceous canal is partially or completely clogged with excess keratin and the drainage of sebum to the surface of the skin is obstructed.[25-26] These result in accumulation of keratin and sebum in the follicular cavity and formation of microcomedones, which can enlarge to form open or closed comedones (also known as black heads and white heads).[27] *Propionibacterium acnes* (*P. acnes*) is a microaerophilic Gram-positive bacteria and is part of the microbiota of the pilosebaceous unit. *P. acnes* plays a significant role in formation of inflammatory lesions (pustules and cysts) in acne vulgaris and contributes to the inflammation and irritation associated with this disease.[27-28]

Various medications are employed to target one or more processes occurring in acne (comedone formation, sebaceous activity, androgen production, *P. acnes,* or the inflammatory/immune response). Topical retinoids are the first-line therapy for treatment of comedones.[29] Retinoids are Vitamin A derivatives that bind to the retinoic acid nuclear receptor (RAR) and activate genes responsible for cellular differentiation. They also have anti-proliferative effects on the sebocytes and as a result decrease sebum production.[30-31] They inhibit formation and reduce number of both microcomedones and inflammatory acne lesions. The drugs in this family include: tretinoin (all trans retinoic acid and first topical retinoid approved for acne therapy), isotretinoin (13-cis retinoic acid), adapalene (derived from naphtoic acid) and tazarotene (acetylenic retinoid).[32]

Other topical treatment options for comedones include benzoyl peroxide, salicylic acid, sulfur, and azelaic acid. Topical and oral antibiotics, benzoyl peroxide, sulfur, and azelaic acid are also used in later stages of acne due to their anti-inflammatory effect. Anti-androgen drugs, such as oral contraceptive are also prescribed in androgen-induced acne. Oral isotretinoin is a potent retinoid with several harsh adverse effects that is used in severe and inflammatory acne. This chemical can shrink sebaceous glands and highly reduce sebum secretion.[27]

1.5. Nanoparticles for topical delivery

In the past few decades, tremendous efforts have been devoted to the field nanotechnology for drug delivery. Nanocarriers are generally sub-micron-sized colloidal particles/vesicles that can encapsulate/entrap drug molecules within their lipidic/polymeric matrix or adsorb/conjugate them to their surface.[33] Currently, there are

different definitions for the term “nanoparticle” based on the dimension range. However, the British Standards Institution (BSI) has set the external diameter range of 1-100 nm for nanoparticles and any particles larger than 100 nm are considered to be microparticles.[34] There is no official definition of nanotechnology established by U.S. Food and Drug Administration (FDA); however, there are two criteria for evaluating the use of nanotechnology in FDA-regulated products: 1) the materials have at least one dimension in the nanoscale range of 1-100 nm. 2) The materials exhibit certain physico-chemical/biological properties that are attributable to their small dimensions.[35-36]

Nano-sized carriers can be composed of degradable or non-degradable polymers, lipids, metals, sugars, and organic or inorganic subtances.[37] Nanoparticles can benefit drug delivery by providing 1) increased solubility of lipophilic agents for intravascular delivery and improving oral bioavailability; 2) chemical and physical protection of the therapeutic agents and enhancing their stability in the formulation; 3) sustained and controlled release of drugs; 4) enhanced permeation and retention (EPR) effect which results in higher drug localization in tumors; 5) targeted cell/tissue-specific drug delivery.[7, 33]

Nanotechnology platforms were first applied to develop injectables and oral dosage forms and later it also drew attention for potential use in the field of topical and transdermal delivery. In order to develop a successful nanoparticle-based topical delivery system, it is critical to understand nanoparticles’ interactions with the skin and their transport mechanisms. Depending on their size and physicochemical properties and surface charge, nanoparticles may be able to translocate intact into the skin or can be degraded on skin surface and release the incorporated therapeutic agents into the skin.

Nevertheless, there is convincing evidence in the literature that irrespective of nanomaterial used, most particles (especially particles larger than 20 nm) do not penetrate to viable tissues in healthy skin and the transappendageal pathway seems to be the dominant route of nanoparticle entry into skin.[37-38].

A broad spectrum of particles (including liposomes[39], solid lipid nanoparticles[40-41] polymeric micelles[42], microemulsions[43]) have been studied for enhancing therapeutic/cosmetic actives biodistribution in the skin. Figure 1.4 depicts various nanocarrier systems that have been used for dermal/transdermal drug delivery. There are various mechanisms that explain at least in part the penetration enhancement effects of nanocarriers.

Lipid carriers have been widely studied in the field of dermatopharmaceutics. Apart from the transappendegeal pathway, there are a few reports on penetration of some types of liposomes into the skin. The formation of a trans-epidermal osmotic gradient is claimed to be one mechanism explaining their penetration into epidermis.[44] Moreover, the dermal penetration enhancement effect can also be due to adhesion of lipid vesicles to the skin surface followed by destabilization of liposomes and their fusion with the SC lipid matrix.[37] Some recently developed lipid vesicles known as “transferosomes” have surfactants in their composition that act as an ”edge activator” and give elasticity to the vesicle. Transferosomes are claimed to overcome the skin barrier by squeezing themselves along the intracellular sealing lipids of SC. Lipid nanoparticles with diameter size of less than 200 nm can tightly adhere to the surface of the skin. They can form a hydrophobic monolayer on the skin that has occlusive action and increase skin hydration leading to enhanced drug permeation.[37, 45]

Polymeric nanoparticles can be made from natural or synthetic polymers. Natural polymers (e.g. chitosan) vary in purity and often lack the batch-to-batch consistency. It is often easier to obtain reproducible particle size/shape and controlled release pattern for the encapsulated drug(s) from synthetic polymers than natural polymers.[33] Commonly used synthetic polymers for drug delivery applications include biodegradable aliphatic polyesters such as polylactide (PLA), poly(lactide-co-glycolide) copolymers (PLGA), and poly(ε-caprolactone) as well as non-degradable polymers such as poly(methyl methacrylate) and polyacrylates.[7] The intact polymeric nanoparticles bigger than 20nm are only able to penetrate into the superficial layers of the SC, where the drug is released; thus, enhanced cutaneous penetration is obtained from increasing the concentration gradient. There is also sufficient evidence that polymeric nanoparticles can accumulate in the hair follicles and provide high local concentration of the drug in the follicular cavity, which then can be absorbed to viable skin layers.[37] Particles with diameters less than 100 nm showed the deepest penetration in the hair follicles and in some cases they were able to diffuse to the dermis via follicular route.[34]

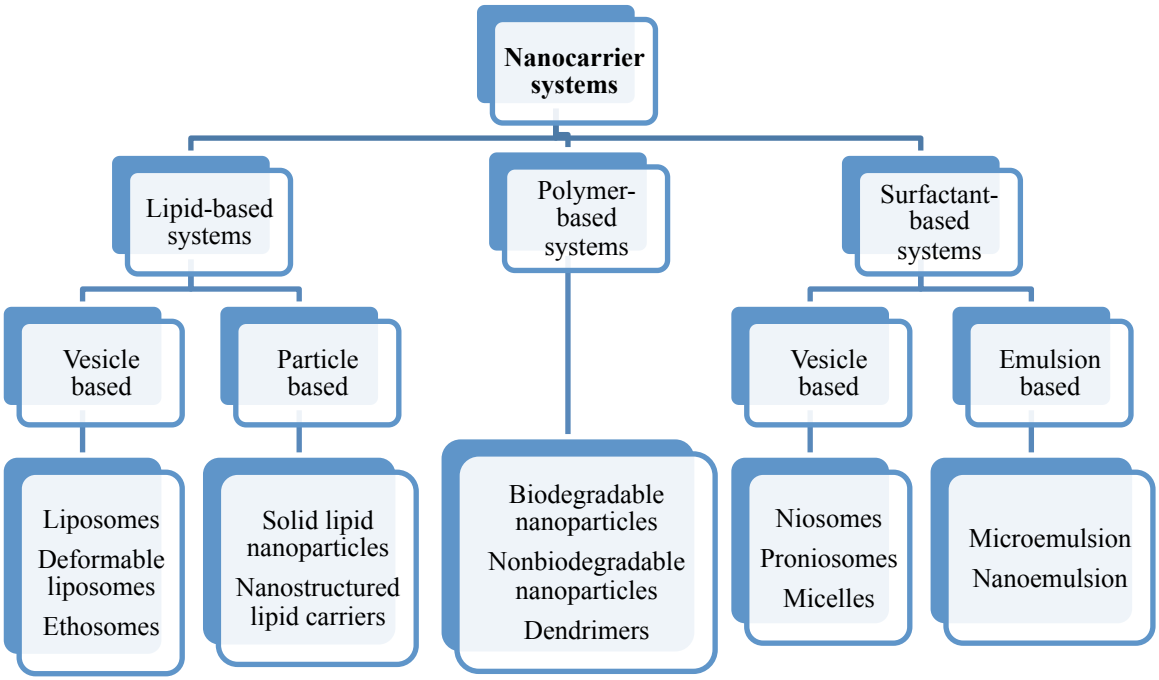

Figure 1.4. Nanocarriers used for cutaneous drug delivery.[46, 47]

1.6. Tyrosine-derived polymeric nanoparticles for topical delivery (a summary of previous studies)

A unique class of polymeric nanospheres, made of a family of biocompatible, amphiphilic tyrosine-derived ABA-triblock copolymers has been developed at The New Jersey Center for Biomaterials, Rutgers-The State University of New Jersey. The chemical structure of these copolymers is composed of hydrophobic B-block oligomers of desaminotyrosyl-tyrosine esters (DTR) and diacids (XA) —made from naturally occurring metabolites— and hydrophilic poly(ethylene glycol) (PEG) A-blocks. Tyrosine-derived copolymers, which are biocompatible and not cytotoxic have been developed and explored for medical applications by Kohn et al. at the New Jersey Center for Biomaterials.[48] These PEG-*b*-oligo(DTR-XA)-*b*-PEG triblocks (Figure 1.5) are in

general amorphous with Tg range of –32 to –34ºC, and a melting transition between 47 and 54ºC. Following addition of this copolymer to an aqueous environment it self-assembles into polymeric micelles referred to as TyroSpheres. The hydrophilic PEG segments and the amorphous oligo(DTR-XA) segment have flexible structures, ensuring the self-assembly of the copolymers into a dynamic and non-frozen structure in aqueous media.[49-50]

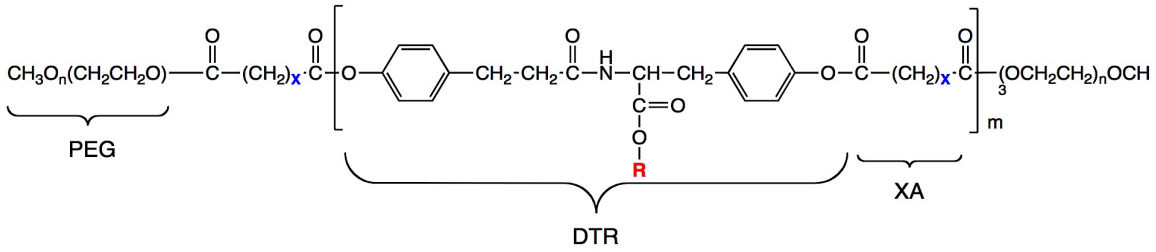

Figure 1.5. The chemical structure of PEG-*b*-oligo(DTR-XA)-*b*-PEG triblock copolymers.

Evaluation of this family of polymers has shown that the triblock polymer PEG_{5K}-b-oligo(desaminotyrosyl-tyrosine octyl ester suberate)-b-PEG_{5K} (DTO-SA/5K) is optimal for encapsulation efficiency, has the lowest polydispersity index (<0.18), a reproducible hydrodynamic diameter of 60-70 nm, and very low critical aggregation concentration (2.6×10^{-7} g/mL measured by Static Light Scattering), making this polymer the lead candidate evaluated for nanosphere applications. The cytotoxicity of TyroSpheres was examined on a variety of cell lines and these nanospheres were found not toxic at concentrations up to 11.5 mg/ml.[50-51]

TyroSpheres are fabricated by solvent displacement method as depicted in Figure 1.6.[51-52] There are several advantages with the fabrication process of TyroSpheres: The process is generally simple and easy to scale up. The chlorinated solvent and high temperature are avoided in the preparation of nanoparticles. The PEG segments of the

block copolymers (positioned at the periphery of the nanoparticles) can stabilize the nanosphere dispersion; therefore, external surfactants/ stabilizers are not used in the fabrication of TyroSpheres.

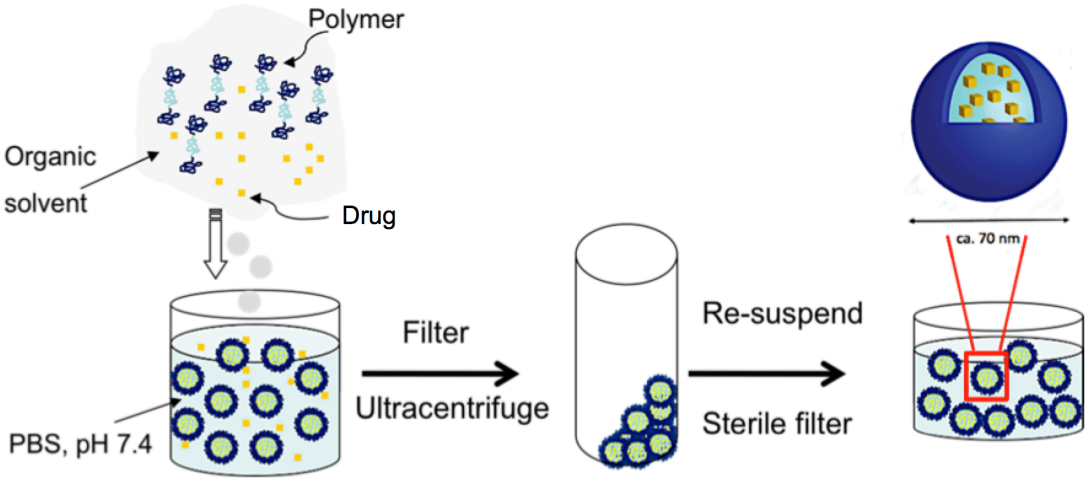

Figure 1.6. Schematic representation of TyroSpheres preparation process.

Scientists at the New Jersey Center for Biomaterials have investigated the applicability of TyroSpheres as a suitable carrier system for several hydrophobic compounds including paclitaxel, Nile Red, curcumin, diclofenac sodium, vitamin D3 and cyclosporine A. Incorporation of these chemicals into TyroSpheres did not show significant impact on the particle size. In a previous study by Costache et al.[53] computational modeling was employed to study drug-polymer interactions in TyroSpheres. The authors demonstrated that the binding affinity of drug to (DTO-SA/5K) copolymers depends on their hydrophobic compatibility and other physical interactions, like, hydrogen binding and π-π stacking.

TyroSpheres have been investigated for topical delivery. The rationale is that these nanoparticles can protect the drug from degradation, provide sustained/controlled release of their cargo and improve partitioning and permeation to the skin. To evaluate TyroSphere's feasibility as a skin delivery system two fluorescent dyes, Nile Red (log D= 3.10) and 5-dodecanoylaminofluorescein (DAF, LogD=7.54) were loaded in nanospheres separately and their percutaneous penetration into human cadaver skin was assessed and compared with control solution in propylene glycol using Franz diffusion cells. It was found that Nile Red and DAF delivery to skin strata was 9.0 and 2.5 times enhanced respectively when formulated into TyroSpheres relative to propylene glycol.[54] Moreover, viscous formulations of TyroSpheres —which are more suitable than liquid dispersion for topical application— were prepared using hydroxypropyl methylcellulose (HPMC) and propylene glycol. In an *ex vivo* study on human cadaver skin, the viscous formulations of Nile Red-TyroSphere resulted in similar dye deposition into SC and viable epidermis compared to TyroSphere liquid dispersion. Remarkably, in an *in vivo* study on pigs, topically applied Nile Red-loaded TyroSpheres (viscous) formulation resulted in a 40% higher dye delivery to skin than that obtained from Nile Red-TyroSpheres liquid dispersion.[55]

Among the drugs that have been loaded in TyroSpheres, a significant effort has been made to develop and characterize paclitaxel-TyroSphere formulations aiming to treat skin disorders such as psoriasis. Paclitaxel is a mitotic inhibitor drug and is marketed for cancer therapy. Paclitaxel also prevents cellular overproliferation and therefore, can potentially be used to treat psoriasis. However, the poor solubility of paclitaxel and its toxicity limits the medical applications of this drug. TyroSpheres were

able to load paclitaxel with up to 8.4% w/w loading efficiency and provided substantial enhancement of its solubility (more than 1000 fold). In a 72 h *in vitro* drug release study using dialysis cassettes, a sustained release pattern was observed with paclitaxel-TyroSpheres. In 72 h about 44 and 58% of the drug was released from the paclitaxel-TyroSpheres with 5.0 and 8.4 wt% drug loading respectively, and no burst release was observed. A viscous formulation of paclitaxel-TyroSpheres was prepared by adding 1% HPMC to the formulation, which showed similar drug release profile to TyroSphere liquid formulation. Following a skin permeation study using human cadaver skin paclitaxel-TyroSpheres in both aqueous dispersion and gel-like formulation delivered significant amounts of the drug to the epidermis and the delivery to the receptor compartment —representing the systemic circulation— was minimal.[42]

To further illustrate efficiency of TyroSpheres as topical drug delivery system for treatment of psoriasis, Nile Red loaded-TyroSpheres was applied on human cadaver skin, normal biopsy skin, and psoriatic biopsy skin to compare the permeability of the dye to different skin types. Following fluorescent analysis of skin cross sections, the penetration effect of Nile Red on psoriatic skin was 5 to 10 folds greater than that of normal biopsy skin or human cadaver skin samples. Moreover, in fluorescent images of psoriatic skin biopsies the dye was detected in the basal layer of the epidermis (where psoriasis originates) but does not appear to proceed further into the skin.[56]

Cyclosporine A (CSA) is another model drug that was studied for topical delivery using TyroSpheres. CSA is a potent immunosuppressive drug that has been found very efficient in several skin disorders, including psoriasis, atopic dermatitis, and alopecia areata. Its large molecular size (1202 Da) and low water solubility poses difficulty in

formulation and dermal penetration of this compound. Using TyroSpheres, the scientists at New Jersey Center for Biomaterials were able to obtain solubility of 8.7mg/ml and loading efficiency of up to 50%. Stability assessment of CSA-TyroSphere liquid dispersions showed that the TyroSpheres enhanced short-term stability of CSA in the formulation at 4, 25 and 37 °C temperatures compared to free CSA (not loaded in TyroSpheres). TyroSphere themselves in form of nanosuspension were stable during 6 months storage at 4°C. It is noteworthy that many other particulate systems such as PLGA nanoparticle solutions are not stable in the solution for more than a few weeks. Dermal penetration of CSA-TyroSphere in gel-like formulation was also evaluated on human cadaver skin. Following 6 h application of the formulation, the drug recovery from dermis was 22 μg per g of skin and no drug was detected in the receptor compartment (as analyzed by liquid chromatography-mass spectroscopy).[57]

Many biodegradable polymeric nanocarriers, including TyroSpheres and PLGA nanoparticles are prone to non-enzymatic hydrolytic degradation that is the cause for their instability in aqueous media in long term. Therefore, a fully reconstitutable dry formulation of TyroSpheres was developed and optimized using freeze-drying process. Sucrose was used as a lyoprotectant to provide stability of the nanoparticles during the process so that they can maintain their original properties after rehydration. With optimum concentration of sucrose, minimal increase was observed in the diameter size of paclitaxel-TyroSpheres and CSA-TyroSpheres after the freeze drying process.[56-57]

1.7. Specific aims

Previous *in vitro* and *in vivo* studies at New Jersey Center for Biomaterials, Rutgers University have lead to promising results showing TyroSpheres as an effective nanotechnology platform for loading and topical delivery of various lipophilic chemicals. The goal of this research was to further investigate the biodistribution of TyroSpheres in the skin and their applicability in treatment of dermatological disorders (e.g. acne), decreasing topical adverse effects of the therapeutic agents, and improving stability of their payload in the aqueous formulation.

To achieve this goal four specific aims were identified for this research:

Specific Aim 1. Evaluating the use of TyroSpheres for follicular drug delivery and their skin distribution.

Previous investigations have shown TyroSpheres' enhancement effect in dermal delivery of Nile Red via intercellular route. We aimed to assess TyroSpheres' role in enhancing follicular delivery by fluorescently labeling the polymer and the payload. This technique allows us to visualize nanoparticles and drug distribution in the skin and its appendages. Moreover, the potential genotoxicity of TyroSpheres was evaluated using the micronucleus test *in vitro* to assure their safety for long-term application.

Specific Aim 2. Preparation and characterization of an aqueous topical formulation of adapalene using TyroSpheres.

Adapalene was selected for this study as an anti-acne drug model with inherent fluorescent properties and was encapsulated in TyroSpheres for hair follicle delivery. The final formulation in the form of a liquid nanodispersion was characterized for drug

loading, particle size, drug crystallinity, and drug release. Acne originates in the pilosebaceous unit; thus, delivery of adapalene to the hair follicles is preferable. To assess the efficiency of our carrier system for follicular delivery of adapalene, the formulation was evaluated for sebum and SC partitioning and skin distribution of adapalene. Additionally, the nanoparticle formulation of adapalene was compared with a marketed product (Differin® gel) for skin irritation and drug delivery to the hair follicles.

Specific Aim 3. Development and characterization of a topical gel formulation of adapalene-TyroSpheres and evaluation of the formulation for acne therapy.

A semi-solid dosage form is preferred for topical products; therefore, a viscous formulation of adapalene-TyroSpheres was developed for ease of application on the skin. Two different water-soluble thickening agents were used to prepare a gel-like formulation of TyroSpheres. The formulations were characterized for particle size and rheological properties. The formulation with closer rheological characteristics to Differin® was chosen for the next series of studies. The skin irritation potential of adapalene-TyroSphere gel formulation was tested using an *in vitro* epidermal skin model and compared with that of Differin®. Next, rhino mice were used as a preclinical model for early stage of acne (microcomedones) to evaluate efficacy of the treatment with adapalene-TyroSphere gel compared to Differin® gel. Success was defined by decrease in the density and size of the utricles and increased thickness of the viable epidermis in the mouse skin.

Specific Aim 4. Evaluation of Vitamin D3-TyroSpheres for topical delivery.

Vitamin D3 (VD3) analogues have been proven to be effective in treatment of several dermatological disorders including psoriasis. We aimed to address the need of a suitable carrier system for enhancing dermal delivery of VD3 and improving its stability in the formulation. Initial work at New Jersey Center for Biomaterials has shown that VD3 is a good drug candidate to encapsulate in TyroSpheres and high drug loading is obtainable. We studied the release of VD3 from TyroSpheres through the SC at two different drug loadings. Skin distribution studies were conducted using human cadaver skin to assess VD3 delivery from TyroSpheres and compare it to a control vehicle with dermal penetration enhancement effects. Additionally, photodegradation kinetics of vitamin D3 when loaded in TyroSpheres and its stability in the formulation were studied.

1.8. References

1. Tobin, D. J., Biochemistry of human skin--our brain on the outside. *Chem Soc Rev* 2006, *35* (1), 52-67.
2. Fore-Pfliger, J., The epidermal skin barrier: implications for the wound care practitioner, part II. *Adv Skin Wound Care* 2004, *17* (9), 480-8.
3. Harding, C. R., The stratum corneum: structure and function in health and disease. *Dermatol Ther* 2004, *17 Suppl 1*, 6-15.
4. Menon, G. K.; Cleary, G. W.; Lane, M. E., The structure and function of the stratum corneum. *Int J Pharm* 2012, *435* (1), 3-9.
5. Haake, A.; Scott, G. A.; Holbrook, K. A., Structure and function of the skin: overview of the epidermis and dermis. *The biology of the skin* 2001, *2001*, 19-45.
6. Cotsarelis, G., Epithelial stem cells: a folliculocentric view. *J Invest Dermatol* 2006, *126* (7), 1459-68.
7. Zhang, Z.; Tsai, P. C.; Ramezanli, T.; Michniak-Kohn, B. B., Polymeric nanoparticles-based topical delivery systems for the treatment of dermatological diseases. *Wiley Interdisciplinary Reviews-Nanomedicine and Nanobiotechnology* 2013, *5* (3), 205-218.
8. Paudel, K. S.; Milewski, M.; Swadley, C. L.; Brogden, N. K.; Ghosh, P.; Stinchcomb, A. L., Challenges and opportunities in dermal/transdermal delivery. *Ther Deliv* 2010, *1* (1), 109-31.
9. Ramezanli Tannaz; Bozena Michniak-Kohn; Ronak Salva; Dick, L., Transdermal Delivery of Macromolecules. Catalent Applied Drug Delivery Institure: 2015.
10. Prausnitz, M. R.; Langer, R., Transdermal drug delivery. *Nat Biotechnol* 2008, *26* (11), 1261-8.
11. Barry, B. W., Drug delivery routes in skin: a novel approach. *Adv Drug Deliv Rev* 2002, *54 Suppl 1*, S31-40.
12. Escobar-Chávez, J. J.; Revilla-Vázquez, A. L.; Domínguez-Delgado, C. L.; Rodríguez-Cruz, I. M.; Aléncaster, N. C.; Díaz-Torres, R., *Nanocarrier systems for transdermal drug delivery*. INTECH Open Access Publisher: 2012.
13. Higuchi, T., Physical chemical analysis of percutaneous absorption process from creams and ointments. *J. Soc. Cosmet. Chem* 1960, *11*, 85-97.
14. Alvarez-Roman, R.; Naik, A.; Kalia, Y. N.; Guy, R. H.; Fessi, H., Skin penetration and distribution of polymeric nanoparticles. *J Control Release* 2004, *99* (1), 53-62.
15. Thong, H. Y.; Zhai, H.; Maibach, H. I., Percutaneous penetration enhancers: an overview. *Skin Pharmacol Physiol* 2007, *20* (6), 272-82.
16. Prausnitz, M. R.; Mitragotri, S.; Langer, R., Current status and future potential of transdermal drug delivery. *Nat Rev Drug Discov* 2004, *3* (2), 115-24.
17. Lauer, A. C.; Lieb, L. M.; Ramachandran, C.; Flynn, G. L.; Weiner, N. D., Transfollicular drug delivery. *Pharm Res* 1995, *12* (2), 179-86.
18. Rancan, F.; Afraz, Z.; Combadiere, B.; Blume-Peytavi, U.; Vogt, A., Hair Follicle Targeting with Nanoparticles. In *Nanotechnology in Dermatology*, Springer: 2013; pp 95-107.

19. Otberg, N.; Teichmann, A.; Rasuljev, U.; Sinkgraven, R.; Sterry, W.; Lademann, J., Follicular penetration of topically applied caffeine via a shampoo formulation. *Skin Pharmacol Physiol* 2007, *20* (4), 195-8.
20. Lademann, J.; Richter, H.; Schaefer, U. F.; Blume-Peytavi, U.; Teichmann, A.; Otberg, N.; Sterry, W., Hair follicles - a long-term reservoir for drug delivery. *Skin pharmacology and physiology* 2006, *19* (4), 232-6.
21. Meidan, V. M.; Bonner, M. C.; Michniak, B. B., Transfollicular drug delivery--is it a reality? *Int J Pharm* 2005, *306* (1-2), 1-14.
22. Makrantonaki, E.; Ganceviciene, R.; Zouboulis, C., An update on the role of the sebaceous gland in the pathogenesis of acne. *Dermatoendocrinol* 2011, *3* (1), 41-9.
23. Gelfuso, G. M.; Gratieri, T.; Delgado-Charro, M. B.; Guy, R. H.; Vianna Lopez, R. F., Iontophoresis-targeted, follicular delivery of minoxidil sulfate for the treatment of alopecia. *J Pharm Sci* 2013, *102* (5), 1488-94.
24. Jappe, U., Pathological mechanisms of acne with special emphasis on Propionibacterium acnes and related therapy. *Acta Derm Venereol* 2003, *83* (4), 241-8.
25. Well, D., Acne vulgaris: A review of causes and treatment options. *Nurse Pract* 2013, *38* (10), 22-31; quiz 32.
26. Greenman, J., Follicular pH and the development of acne. *Int J Dermatol* 1981, *20* (10), 656-8.
27. Akhavan, A.; Bershad, S., Topical acne drugs: review of clinical properties, systemic exposure, and safety. *Am J Clin Dermatol* 2003, *4* (7), 473-92.
28. Feldman, S.; Careccia, R. E.; Barham, K. L.; Hancox, J., Diagnosis and treatment of acne. *Am Fam Physician* 2004, *69* (9), 2123-30.
29. Webster, G. F., Topical tretinoin in acne therapy. *J Am Acad Dermatol* 1998, *39* (2 Pt 3), S38-44.
30. Mukherjee, S.; Date, A.; Patravale, V.; Korting, H. C.; Roeder, A.; Weindl, G., Retinoids in the treatment of skin aging: an overview of clinical efficacy and safety. *Clin Interv Aging* 2006, *1* (4), 327-48.
31. Zouboulis, C. C., Acne and sebaceous gland function. *Clin Dermatol* 2004, *22* (5), 360-6.
32. Thielitz, A.; Gollnick, H., Topical retinoids in acne vulgaris: update on efficacy and safety. *Am J Clin Dermatol* 2008, *9* (6), 369-81.
33. Panyam, J.; Labhasetwar, V., Biodegradable nanoparticles for drug and gene delivery to cells and tissue. *Adv Drug Deliv Rev* 2003, *55* (3), 329-47.
34. Papakostas, D.; Rancan, F.; Sterry, W.; Blume-Peytavi, U.; Vogt, A., Nanoparticles in dermatology. *Arch Dermatol Res* 2011, *303* (8), 533-50.
35. FDA.gov. Draft guidance: considering whether an FDA-regulated product involves the application of nanotechnology. . 2011.
36. Choi, H. S.; Frangioni, J. V., Nanoparticles for Biomedical Imaging: Fundamentals of Clinical Translation. *Mol Imaging* 2010, *9* (6), 291-310.
37. Desai, P.; Patlolla, R. R.; Singh, M., Interaction of nanoparticles and cell-penetrating peptides with skin for transdermal drug delivery. *Mol Membr Biol* 2010, *27* (7), 247-59.
38. Prow, T. W.; Grice, J. E.; Lin, L. L.; Faye, R.; Butler, M.; Becker, W.; Wurm, E. M.; Yoong, C.; Robertson, T. A.; Soyer, H. P.; Roberts, M. S., Nanoparticles and microparticles for skin drug delivery. *Adv Drug Deliv Rev* 2011, *63* (6), 470-91.

39. Fukui, T.; Kawaguchi, A. T.; Takekoshi, S.; Miyasaka, M.; Tanaka, R., Liposome-encapsulated hemoglobin accelerates skin wound healing in mice. *Artif Organs* 2012, *36* (2), 161-9.
40. Jenning, V.; Gysler, A.; Schafer-Korting, M.; Gohla, S. H., Vitamin A loaded solid lipid nanoparticles for topical use: occlusive properties and drug targeting to the upper skin. *Eur J Pharm Biopharm* 2000, *49* (3), 211-8.
41. Ridolfi, D. M.; Marcato, P. D.; Justo, G. Z.; Cordi, L.; Machado, D.; Duran, N., Chitosan-solid lipid nanoparticles as carriers for topical delivery of tretinoin. *Colloids Surf B Biointerfaces* 2012, *93*, 36-40.
42. Kilfoyle, B. E.; Sheihet, L.; Zhang, Z.; Laohoo, M.; Kohn, J.; Michniak-Kohn, B. B., Development of paclitaxel-TyroSpheres for topical skin treatment. *J Control Release* 2012, *163* (1), 18-24.
43. Bhatia, G.; Zhou, Y.; Banga, A. K., Adapalene microemulsion for transfollicular drug delivery. *J Pharm Sci* 2013, *102* (8), 2622-31.
44. de Leeuw, J.; de Vijlder, H. C.; Bjerring, P.; Neumann, H. A., Liposomes in dermatology today. *J Eur Acad Dermatol Venereol* 2009, *23* (5), 505-16.
45. Chen-yu, G.; Chun-fen, Y.; Qi-lu, L.; Qi, T.; Yan-wei, X.; Wei-na, L.; Guang-xi, Z., Development of a quercetin-loaded nanostructured lipid carrier formulation for topical delivery. *Int J Pharm* 2012, *430* (1-2), 292-8.
46. Hamishehkar, H.; Rahimpour, Y.; Kouhsoltani, M., Niosomes as a propitious carrier for topical drug delivery. *Expert Opin Drug Deliv* 2013, *10* (2), 261-72.
47. Venuganti, V. V.; Perumal, O. P., Nanosystems for dermal and transdermal drug delivery. *Drug Delivery Nanoparticles Formulation and Characterization* 2009, *191*, 126.
48. Kohn, J. B.; Yu, C., Implantable medical devices and drug delivery; tensile strength. Google Patents: 1997.
49. Nardin, C.; Bolikal, D.; Kohn, J., Nontoxic block copolymer nanospheres: Design and characterization. *Langmuir* 2004, *20* (26), 11721-11725.
50. Sheihet, L.; Dubin, R. A.; Devore, D.; Kohn, J., Hydrophobic drug delivery by self-assembling triblock copolymer-derived nanospheres. *Biomacromolecules* 2005, *6* (5), 2726-31.
51. Sheihet, L.; Piotrowska, K.; Dubin, R. A.; Kohn, J.; Devore, D., Effect of tyrosine-derived triblock copolymer compositions on nanosphere self-assembly and drug delivery. *Biomacromolecules* 2007, *8* (3), 998-1003.
52. Zhang, Z.; Ramezanli, T.; Tsai, P.-C., Drug Delivery Systems Based on Tyrosine-derived Nanospheres (TyroSpheres™). *Nanotechnology and Drug Delivery, Volume One: Nanoplatforms in Drug Delivery* 2014, *1*, 210.
53. Costache, A. D.; Sheihet, L.; Zaveri, K.; Knight, D. D.; Kohn, J., Polymer-drug interactions in tyrosine-derived triblock copolymer nanospheres: a computational modeling approach. *Mol Pharm* 2009, *6* (5), 1620-7.
54. Sheihet, L.; Chandra, P.; Batheja, P.; Devore, D.; Kohn, J.; Michniak, B., Tyrosine-derived nanospheres for enhanced topical skin penetration. *Int J Pharm* 2008, *350* (1-2), 312-9.
55. Batheja, P.; Sheihet, L.; Kohn, J.; Singer, A. J.; Michniak-Kohn, B., Topical drug delivery by a polymeric nanosphere gel: Formulation optimization and in vitro and in vivo skin distribution studies. *J Control Release* 2011, *149* (2), 159-67.

56. Kilfoyle, B. E. Tyrosine-derived nanoparticles for the topical treatment of psoriasis. Rutgers University-Graduate School-New Brunswick, 2011.
57. Goyal, R.; Macri, L.; Kohn, J., Formulation Strategy for the Delivery of Cyclosporine A: Comparison of Two Polymeric Nanospheres. *Scientific Reports* 2015, *5*.

Chapter 2. Evaluating the use of TyroSpheres for follicular drug delivery and their skin distribution

2.1. Introduction

Hair follicles are invaginations of the epidermis extending into the deeper dermis and are considered interruptions in this protective skin barrier.[1] The distribution of hair follicles varies in different skin sites. There are parts such as palm and lips, in which hair does not grow and parts such as scalp and face that follicular openings may represent up to 10% of the skin area.[2-3] Hair follicles are known to contribute significantly to the absorption of small molecules with low to intermediate octanol–water partition coefficients and (sub)micron particles.[4] They function not only as portals of entry to the viable epidermis and dermis but also serve as a reservoir for topically applied substances.[5] Recent findings have revealed that as opposed to stratum corneum (SC) that only provides a short-term reservoir function, hair follicles represent efficient long-term reservoirs (up to 10 days) for topically applied compounds and particles. That is due to slow processes of hair growth, sebum production and sebum flow rate inside the follicles.[6] Large molecules and particles with diameters of 10μm-20nm that do not normally penetrate through the epidermal lipid layers, have been found to localize in the follicular canals.[7,8] Due to this fact, hair follicles have drawn a lot of attention in the field of dermatopharmaceutics and they have been explored as an alternative pathway for both topical and transdermal drug delivery.

Nanoparticles represent important and popular dug carrier systems. In the past decade several research groups have attempted to apply nano/microcarriers for follicular delivery. There are reports in the literature where the effect of particle size on follicular penetration has been investigated.[7] The penetration depth of particles within the follicular duct was found to be size dependent. Toll et al.[9] assessed penetration of particles with diameter size of 0.75 and 6.0 μm to the follicular cavity in excised human skin. They found that 0.75 μm particles penetrated deeper into hair follicles than 6 μm particles. Other studies have shown that microparticles with less than 10 μm diameter size can accumulate in the follicular openings and particles with a few hundred-nanometer size can penetrate to the upper infundibulum. The deepest penetration to the hair follicles has been observed with nanoparticles with diameter of less than 100 nm and in some cases nanoparticles smaller than 50 nm were able to diffuse to the dermis via follicular route (Figure 2.1).[10]

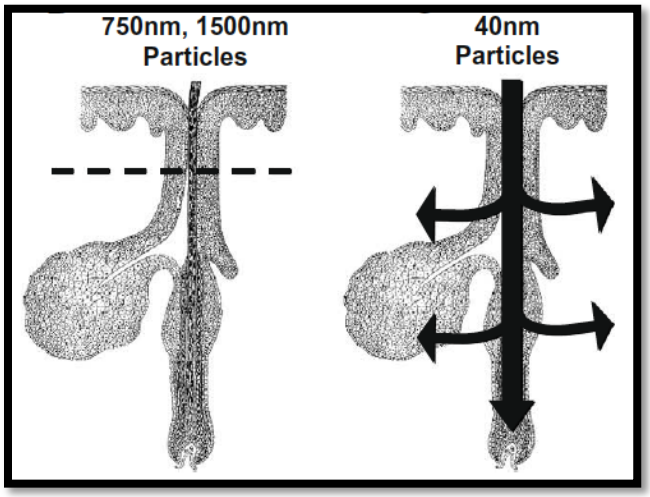

Figure 2.1. Nano/microparticles penetration to the hair follicles. Penetration depths in the follicular cavity and capacity to penetrate the epithelium depend on the particle size.[11]

One technique to evaluate follicular penetration is via cyanoacrylate skin surface biopsy. This technique has been reported in literature to assess qualitative and quantitative drug delivery to the pilosebaceous unit.[12-13] Following topical application of the formulation containing fluorescent agent on the skin and regular tape stripping, follicular cast is removed using cyanoacrylate-based glue. The samples then can be analyzed by fluorescence microscopy or dissolved in an extracting solvent to quantify the dye delivery to the hair follicles.

The expansion of nanomedicinal applications raises several health and safety issues regarding the fate of nanoparticles and their potential chronic toxicity in the human body that needs to be understood, investigated, and regulated.[14-15] Nanogenotoxicology as a discipline analyzes the potential of nanomaterials to damage DNA and impose harmful effects on genetic material. Genotoxicity assessment of drug carriers is as important as their cytotoxicity, especially if there are used for prolonged chronic treatment.[16] One common *in vitro* method to analyze potential genotoxicity of the test materials is the micronuclei test. The term "micronucleus" refers to "the small nucleus that forms whenever a chromosome or a fragment of a chromosome is not incorporated into one of the daughter nuclei during cell division." Therefore, an increase in micronuclei formation is an indication of genotoxicty.[17]

Tyrosine-derived copolymer, PEG_{5K}-*b*-oligo(desaminotyrosyl-tyrosine octyl ester suberate)-*b*-PEG_{5K} (DTO-SA/5K) has been developed at New Jersey Center for Biomaterial, Rutgers-The State University of New Jersey. This copolymer can self-assemble to polymeric micelles after addition to aqueous medium. Theses nanospheres (known as TyroSpheres) has a reproducible hydrodynamic diameter of 60-70 nm, low

polydispersity index (0.17), very low critical aggregation concentration (2.6×10^{-7} g/mL measured by Static Light Scattering), and has shown efficacy for encapsulation a wide range of hydrophobic compounds.[18-19] Initial investigations on applicability of TyroSpheres for topical delivery has shown that these nanocarriers can deliver their payload to upper skin layers. In one study, skin delivery of Nile Red (a lipophilic fluorescent drug model), which was loaded in TyroSpheres, was examined with confocal laser microscopy. The images taken down through the SC (at approximately 4 µm increments) revealed that the dye permeated through intercellular pathway (Figure 2.2).[20]

In this chapter, we aimed to assess biodistribution of TyroSpheres in the skin and find out the importance of follicular route in drug delivery via TyroSpheres. For this purpose, the DTO-SA/5k copolymer was fluorescently labeled with a coumarin derivative and Nile Red was encapsulated in TyroSpheres. The cytotoxicity of TyroSpheres was previously examined on a variety of cell lines and these nanospheres were found not toxic at concentrations up to 11.5 mg/mL.[18] However, their genotoxicity potential and safety during chronic use was still unknown. To establish TyroSpheres as a safe drug carrier, we evaluated their genotoxicity using *in vitro* micronuclei test.

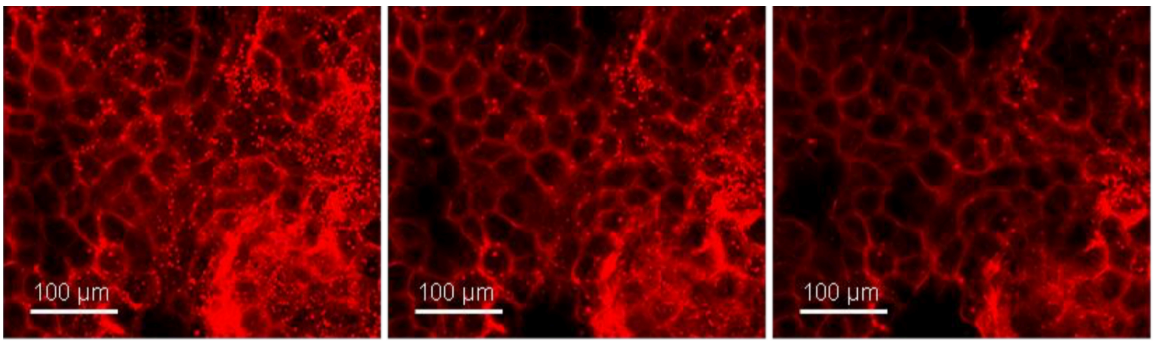

Figure 2.2. Confocal laser scanning microscopy images of human skin treated with Nile Red-TyroSpheres for 3 h showing dye penetration into SC though intercellular pathway. Images (from left to right) were taken sequentially along the z axis in increments of 4 µm.[21]

2.2. Materials and Methods

2.2.1. Materials

HPLC grade water, acetonitrile, methylene chloride, dichloromethane (DCM), methanol, and 2-propanol were purchased from Fisher Scientific, (Pittsburgh, PA). Suberic acid (SA), 4-dimethylaminopyridinium-*p*-toluene sulfate (DMPTS), poly(ethylene glycol) methyl ether (Mw 5000)-PEG5K, and cetyltrimethylammonium bromide (CTAB) were purchased from Aldrich Chemical Co. (Milwaukee, WI). Diisopropylcarbodiimide (DIPC) was purchased from Tanabe Chemicals (San Diego, CA). 5-dodecanoylaminofluorescein (DAF), and Oregon Green were obtained from Molecular Probes (Eugene, OR). Nile Red was obtained from Invitrogen (Carlsband, CA). 2- Propanol (IPA), Dulbecco's phosphate buffered saline (PBS), N,N-dimethylformamide – (DMF), and ethyl methanesulfonate (EMS) were obtained from Sigma Aldrich (St. Louis, MO). Hoechst 33258 was obtained from AnaSpec Inc. (Fremont, CA). F-12K growth medium, trypsin (0.25% Trypsin-EDTA), and fetal bovine serum (FBS) were purchased from Life Technologies (Grand Island, NY). Desaminotyrosyl-tyrosine octyl **(**DTO) and 7-amido-4-methylcoumarin were synthesized by the scientists at New Jersey Center for Biomaterials.

2.2.2. Synthesis of PEG_{5K}-*b*-oligo(desaminotyrosyl-tyrosine octyl ester suberate)-*b*-PEG_{5K} (DTO-SA/5K)

Synthesis of DTO-SA/5K copolymer was prepared as described previuosly.[20-22] Briefly, 0.9 mole equivalents of DTO, 1.0 mole equivalent of SA, and DCM were mixed until a homogeneous solution was obtained. Then, 0.5 mole equivalents of DPT was

added to the reaction mixture and was stirred continuously for 10 minutes. Next, the first portion of DIPC (2.7 mole equivalents) was added to the stirred suspension while being stirred at room temperature. Gel permeation chromatography (GPC) was applied to monitor the polymerization progress every 30 minutes to obtain the desired molecular weight (Mw) for the oligo block (~12-13 KDa). Then, 0.1 mole equivalents of PEG_{5K} were added to the polymer mixture. 5 minutes later, a second portion of DIPC was added. The PEGylation progress was also monitored by GPC while the reaction mixture was getting stirred at room temperature. After successful PEGylation, acetic acid was added to quench the un-reacted DIPC, the reaction mixture was filtered using a sintered glass funnel and the filtrate was concentrated by evaporation. The product was purified by precipitation with IPA. The precipitate was collected on a sintered glass funnel, re-dissolved and precipitated numerous times to remove excess PEG and small molecular weight polymers. The chemical structure and product purity were verified by NMR and GPC (data not shown).

2.2.3. Fabrication of fluorescently-labeled copolymer

The fluorescently-labeled tyrosine-derived copolymer (Figure 2.3) was synthesized using the similar method as described above (section 2.2.2). This time, the monomer (desaminotyrosyl tyrosine) was grafted to 7-amino-4-methylcoumarin to form desaminotyrosyl tyrosine 4-methylcoumarin-7-amide. The brief schematic of the synthesis is shown in Figure 2.4. 70% DTO and 30% fluorescent monomer were then mixed with SA. The chemical structure and product purity of the final copolymer were verified by NMR and GPC (data not shown).

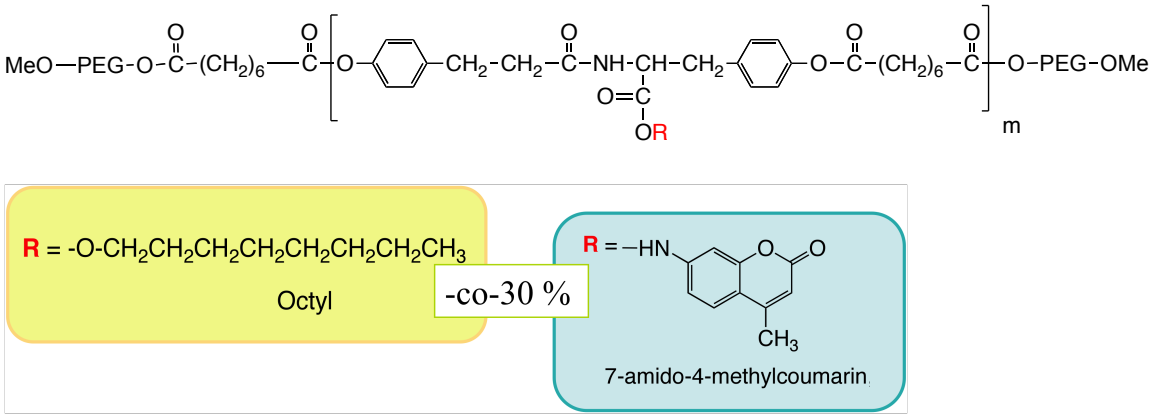

Figure 2.3. Chemical structure of the PEG_{5K}-*b*-oligo(desaminotyrosyl-tyrosine octyl ester suberate)-*b*-PEG_{5K} with and without coumarin derivative.

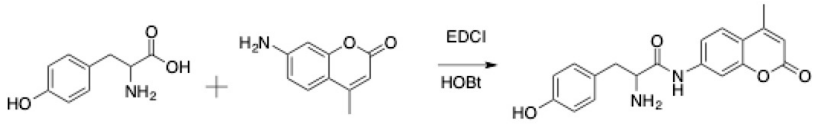

Tyrosine + 7-amino-4-methylcoumarin

L-Tyrosine 7-amido-4-methylcoumarin

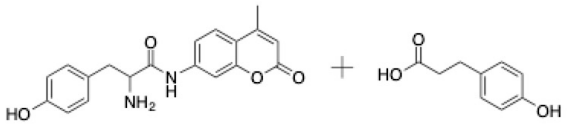

L-Tyrosine 7-amido-4-methylcoumarin + Desaminotyrosine

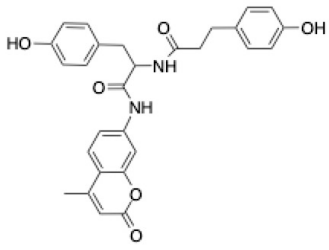

Desaminotyrosyl tyrosine
4-methylcoumarin-7-amide

Figure 2.4. Schematic synthesis of fluorescently-labeled monomer, Desaminotyrosyl tyrosine 4-methylcoumarin-7-amide. The reagents were 1-ethyl-3-(30dimethylamino propyl) carbodiimide – HCl (EDCI) and 1-HydroxyBenzoTriazole (HOBt) in tetrahydrofuran.

2.2.4. Preparation of Nile Red-TyroSphere formulations

TyroSpheres were prepared via a self-assembly technique that was reported previously. [23-24] DTO-SA/5K copolymer and Nile Red were dissolved in DMF at concentrations of 100mg/mL and 3mg/5mL respectively. Copolymer and drug solution were mixed and added drop-wise to PBS (pH 7.4) under constant stirring. The nanoparticles were formed and added slight turbidity to PBS. The nanosuspension was filtered using 0.22 μm PVDF filters (Millipore) and subjected to ultra-centrifugation (Beckman L8-70M ultracentrifuge, Beckman Coulter, Fullerton, CA) at 65,000 rpm (290,000 × g) for 3 h at 18°C. The supernatant was then decanted; the pelleted nanospheres were rinsed and re-suspended in PBS.

2.2.5. Nile Red analysis

2.2.5.1 High Performance Liquid Chromatography (HPLC) method for Nile Red analysis

Concentration of Nile Red was analyzed using an Agilent 1100 high-performance liquid chromatography (HPLC) system (Agilent Technologies, USA) using a method that was previously developed and validated for Nile Red.[23] The HPLC was equipped with a UV/Vis detector and reverse phase C18 column (Eclipse XDB-C18, 4.6 × 150 mm, 5 μm, Agilent Technologies, USA) at 25 °C. The mobile phase was a mixture of 40/60 (v/v) water/acetonitrile, which passed through the column at flow rate of 1. 5 mL/min. The UV/Vis detector was set at 550 nm.

2.2.5.2. Liquid chromatography and mass spectroscopy (LC-MS) for Nile Red

Liquid chromatography and mass spectroscopy **(**LC-MS) analysis was performed using a U3000 (Dionex) on line with linear trap quadrapole (ThermoFisher). In general, sample was injected in full loop mode and separated by a reversed-phase column (Discovery BIO Wide Pore C18, 3 μm, 5 cm × 2.1 mm, Supelco analytical) with 80% acetonitrile:0.2% formic acid (80:20) as mobile phase at a flow rate of 200 μL/min for 20 minutes. Mass spectroscopy data was acquired with full MS from 150 to 1000 (positive mode) followed by targeted MSMS of 319.3 (mono-protonated ion of Nile Red). MSMS detailed parameters include: isolation width - 7 Da; normalized collision energy - 35%; activation Q - 0.15, activation time - 16 milliseconds. Full MS and MSMS data were both acquired in centroid mode. Quantification of Nile Red was by peak integration and peak area calculation of the mono-protonated ion of Nile Red (m/z 319.3) or of the MSMS fragments (275). Linearity for molecular weight 319 Da (corresponding to mono-protonated Nile Red) was established in test matrix over the range of 5.0 to 500 ng/mL. For standard curve and tuning of the mass spectroscopy, a calibration curve of methanolic solution of Nile Red was prepared from 0.5 ng/mL to 5 μg/mL.

2.2.6. Evaluation of Cutaneous uptake of Nile Red from Nile Red-TyroSpheres applied on human cadaver skin

Dermatomed human skin samples (300-600 μm) of a Caucasian male donor were obtained from New York Firefighters Skin Bank (New York, NY). The permeation study was carried out using vertical Franz diffusion cells with donor area of 0.64 cm^2 (PermeGear Inc., Hellertown PA) according to previously described methods.[20] PBS pH 7.4 containing 1% Tween 80 was added to the receptor compartment. The skin samples

were treated with 500 μL of Nile Red-TyroSpheres (0.05 wt% drug loading) liquid dispersion formulations for 1, 2, and 3 h. The temperature of the Franz cells was maintained at 37°C. At the end of the study, the skin pieces were washed and removed from the Franz cells. Epidermal and dermal layers were manually separated using tweezers. Receptor medium was collected in separate tubes. Nile Red was extracted in methanol from skin layers with aid of homogenization (Polytron® PT10/35 - Kinematica, Switzerland). The Nile Red content in epidermis, dermis, and receptor medium were determined by LC-MS.

2.2.7. Biodistribution of TyroSpheres in human skin

Dermatomed human skin samples (300-600 μm) of a Caucasian male donor were obtained from New York Firefighters Skin Bank (New York, NY). Vertical Franz diffusion cells with donor/receptor area of 0.64 cm^2 (PermeGear Inc., Hellertown PA) were used for this study. Nile Red-TyroSpheres liquid dispersion that was made from fluorescently-labeled tyrosine-derived copolymer shown in Figure 2.3 (Nile Red-fluor-TyroSpheres) was applied on the skin for 12 h. At the end of the permeation study, excess formulation was removed from the skin, the surface was rinsed with PBS and dried with a cotton stick.

2.2.7.1. Fluorescence microscopy

To visualize skin distribution of TyroSpheres and Nile Red, dried ice was used to freeze the skin pieces, which were then cut into smaller strips and embedded in Optimal Cutting Temperature (OCT) medium. The samples were stored at -80°C until use. Vertical cross-sections (15 μm) of the skin were prepared with a cryostat (Leica Cryostat

CM 3050S, Wetzlar, Germany) and collected on glass slides. The samples were then subjected to fluorescent and phase-contrast microscopy (Zeiss microscope).

2.2.8. Skin destitution study of Nile Red-TyroSpheres in pig ear skin

A pig ear was isolated from a Yorkshire pig (3 month old, 38 kg, purchased from Barton's West End Farms, Oxford, NJ) and stored in RPMI media at 4°C for a few days until use. On the day of study the porcine skin connected to the cartilage was cut into small pieces (around 4 cm^2), rinsed with PBS, and mounted on vertical Franz diffusion cells with donor/receptor diffusion area of 3.14 cm2. Nile Red-TyroSpheres (0.1% w/w), or Nile Red solution in propylene glycol (0.1% w/w) was applied on the skin area. The formulations were gently massaged for 3 minutes on the skin using a glass rod. The donor compartment remained uncovered for the duration of the study. The skin from the same donor was used as control.

2.2.8.1. Fluorescence microscopy of the skin

To visualize depth of drug penetration, vertical cross-sections (15 μm thick) of the skin specimens were prepared by embedding in Optimal Cutting Temperature (OCT) medium and sectioned with the Leica cryostat. The samples were then subjected to fluorescence and phase-contrast microscopy.

2.2.8.2. Differential tape stripping

Differential tape stripping of the skin samples was done according to a procedure described by Teichmann et al.[13] After termination of the permeation study and removing the excess formulation from the skin, the effective area was subjected to tape stripping. A total of 25 rounds of tape stripping were applied to remove the SC layers using adhesive

3M-Scotch® tapes (St. Paul, MN). Briefly, pieces of tape were applied on the skin. A roller was used to stretch the skin gently to avoid generation of wrinkles. The tape strips were removed with forceps and pooled together in a 50 mL centrifuge tube. Following SC removal, cyanoacrylate skin biopsies were collected using superglue (Loctite, Henkel Corporation, Ohio). Cyanoacrylate skin biopsies containing follicular casts were analyzed with fluorescent microscopy.

2.2.9. Genotoxicity assessment of TyroSpheres

Genotoxicity of TyroSpheres (with no drug loading) was assessed based on an established method using Chinese Hamster Ovary (CHO-K1) cells.[16]

2.2.9.1. Cytotoxicity of TyroSpheres on CHO-K1 cells

First, the maximal tolerated concentration of TyroSpheres for CHO-K1 cells was determined. Briefly, CHO-K1 cells were seeded in 96-well plates at 5,000 cells/well seeding density in F-12K growth medium containing 10% FBS and gentamycin (50µg/mL). The cells were incubated for 24 hours to ensure sufficient attachment (37°C, 10% CO_2, RH 95%). Next, the growth medium was replaced with F-12K containing various amounts of TyroSpheres. The wells were incubated for additional 24 h. AlamarBlue® metabolic assay was performed to evaluate the cytotoxicity of TyroSpheres according to the method described by Kilfoyle et al.[25] Briefly, after rinsing the cells couple of times with PBS, cell culture medium containing 10% AlamarBlue® reagent was added and the cells were incubated until the negative controls started to turn pink. The fluorescence intensity was measured (560nm/590nm; manual gain 97%) using a Tecan

Infinite 200M fluorescent plate reader. Plain cell culture medium treatment was used as 100% cell viability.

2.2.9.2. One-day and three-day genotoxicity study

The highest concentration of TyroSpheres that was found nontoxic to CHO-K1 cells was used for genotoxicity study. For one-day and three-day genotoxicity studies, CHO-K1 cells were seeded on 6-well plates at 25,000 cells/well and 10,000 cells/well respectively. The wells were incubated overnight at 37°C, 10% CO_2, and RH 95%. The next day, TyroSphere dispersions in growth medium at concentrations determined previously were added to the wells. 3 mL of F-12K medium containing 5µL of EMS was applied on the wells as a positive control. The plates were incubated for 24 or 72 h. Then, the cells were stained with the fluorescent dye, Hoechst 33258, according to the procedure described by Dayan et al.[17] Then, the cells were analyzed under a fluorescent microscope (Olympus, New York, NY) for presence of micronuclei. 1,000 cells were counted at random and the number of micronuclei observed was recorded. The study was done in triplicate.

2.2.10. Statistical analysis

Statistical analysis was performed using Prism Version 6 (GraphPad software, La Jolla California). One-way analysis of variance ANOVA followed by Tukey's post hoc or Wilcoxon signed-rank test (in case the normal distribution assumption did not exist) were applied to determine the difference among the groups in every study.

2.3. Results and discussion

2.3.1. Cutaneous uptake of Nile Red from TyroSphere formulations

Nile Red-TyroSpheres with presence of different thickening agents and chemical enhancer have been previously tested *in vitro* and *in vivo*.[23-24] In this study we aimed to examine delivery of the dye from TyroSphere formulations in short-time application. Figure 2.5 provides the results of the permeation study. Nile Red delivery to epidermis was significantly higher than dermis in all three time points ($p< 0.01$). The dye recovery from receptor compartment was minimal, which was expected due to lipophilicity of the drug model. No significant difference in Nile Red skin permeation among the three time points was observed.

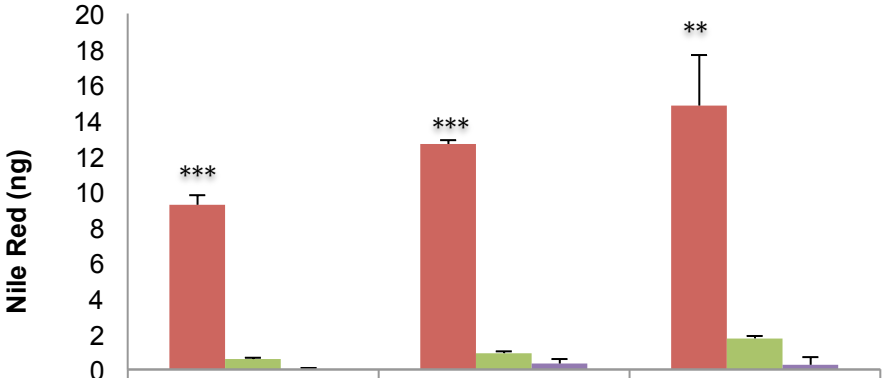

Figure 2.5. Nile Red distribution in epidermis, dermis and receptor compartment following, 1, 2, and 3 h application of Nile Red-TyroSpheres (NR-NP) on human cadaver skin. The data are shown as mean ± SE. ***(p<0.001) and **(p<0.01) show significant difference in Nile Red recovery between epidermis and dermis, from column analysis and Wilcoxon signed-rank test.

The results of this study were in agreement with other permeation studies done with Nile Red-Tyrosphere formulations, where TyroSpheres were able to deliver the dye to upper layers of skin and enhanced the permeation compared to some dermal penetration enhancers, such as propylene glycol.[24]

2.3.2. Biodistribution of TyroSpheres in human skin

One of the common techniques to examine biodistribution of the particulate systems in skin is to covalently bind a fluorescent moiety to their structure. Coumarin derivatives in pH 7 emit at about 450 nm, which can be visualized by fluorescence microscope in DAPI channel. Nile Red emits at 636 nm in the red region, where the epidermis and hair follicles minimally autofluoresce and thus, it is a good lipophilic model drug to study dermal delivery. Following application of Nile Red-fluor-TyroSpheres on human skin, nanoparticles were not detected in skin layers while, Nile Red delivery to the epidermis was clear from the red fluorescent signal observed in the skin samples (Figure 2.6) This dual-fluorescent tag technique revealed that TyroSpheres delivered their payload into the skin but the nanoparticles and/or the polymer that makes up the TyroSpheres were left behind at the surface of the skin and were washed off during removal of the remaining formulation.

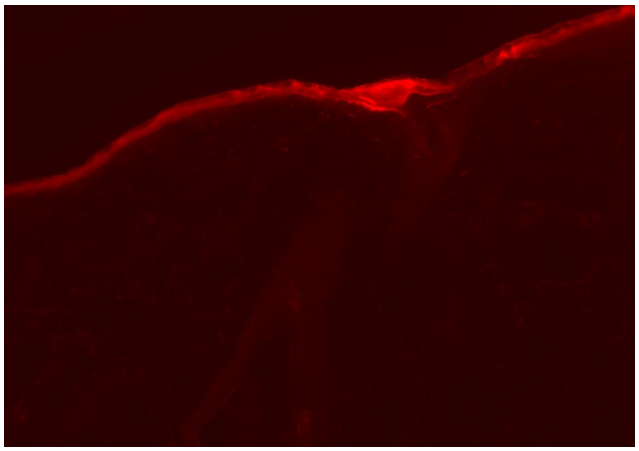

Figure 2.6. Nile Red delivery to the epidermis. Fluorescent image was taken at 10x magnification from vertical cross-section of human skin treated with Nile Red-TyroSpheres.

Remarkably, TyroSpheres were detected in the hair follicles, where high red fluorescent signal was also observed. Figure 2.7 shows Nile Red-fluor-TyroSpheres accumulation in the follicular cavity that resulted in delivery of the dye to the follicular epithelium. Therefore, TyroSpheres did not penetrate to the epidermis but were able to use the appendageal route and accumulated in the hair follicles. This can be very advantageous for topical delivery because hair follicles are considered as long-term reservoir for topically applied compounds. Nanoparticles with sustained release profile can remain in the hair follicles for a few days and provide a gradual delivery of their cargo to the skin.[21] This part of the work was performed by Dr. Zheng Zhang at New Jersey Center for Biomaterials.

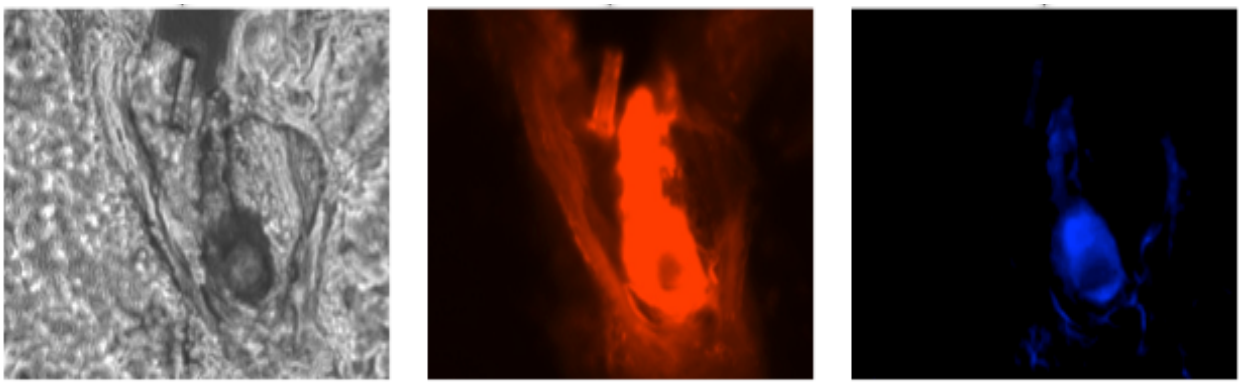

Figure 2.7. Bright phase and fluorescent images taken from vertical cross section of the skin treated with fluorescently-labeled TyroSpheres loaded with Nile Red (Nile Red-fluor-TyroSphere). The red and blue colors inside a hair follicle are from Nile Red and TyroSpheres respectively.

2.3.3. Skin distribution of Nile Red-TyroSpheres in pig ear skin

In order to investigate applicability of TyroSpheres for follicular delivery, Nile Red-loaded TyroSphere formulation was applied on pig ear skin. Pig ear skin has similar follicular structures to human skin[26] with higher follicular density than many areas in human skin that makes it more practical to be used for *ex vivo* follicular penetration studies. As opposed to excised human skin, excised porcine ear tissue connected to the cartilage does not contract; therefore, its hair follicles better resemble the *in vivo* conditions.[27] In a study by Raber et al.[28] porcine ear skin was found to be a suitable surrogate for *in vivo* conditions in humans when assessing nanoparticle accumulation in hair follicles. Figure 2.8.B depicts a vertical cross section of skin treated with Nile Red-TyroSpheres. Red color observed in follicular epithelium and hair shaft surroundings revealed that TyroSpheres are able to penetrate into the hair follicles to a depth of more than 600 μm.

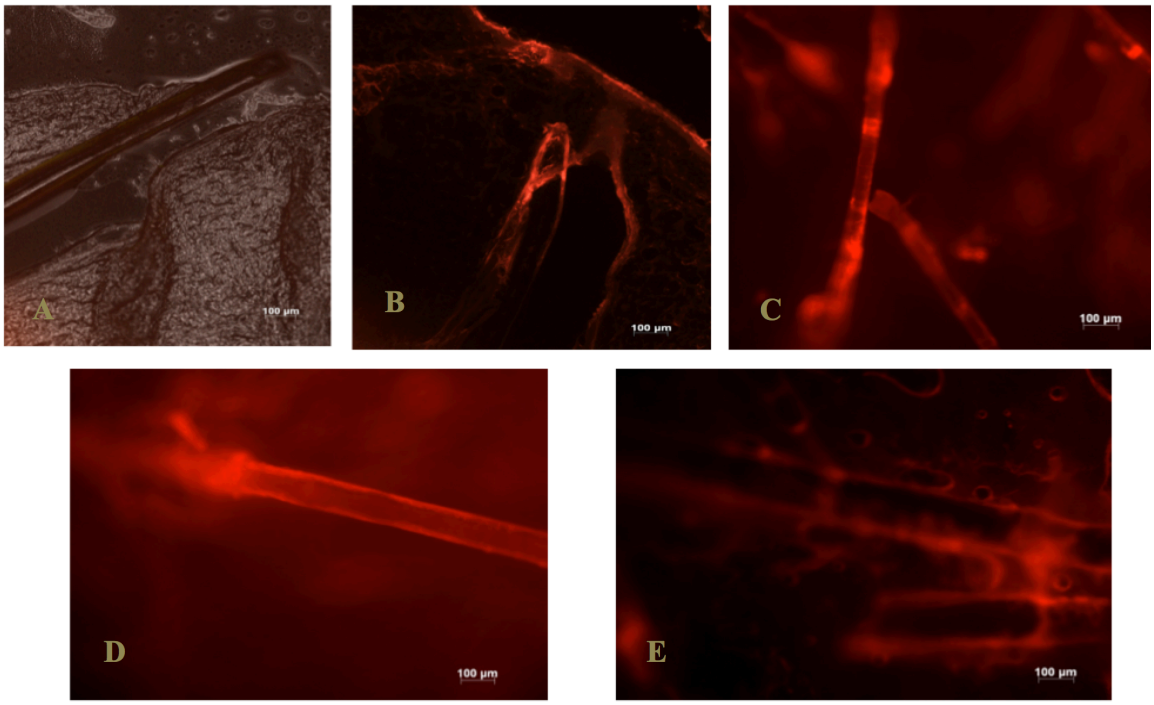

Figure 2.8. Nile Red localization within the hair follicles and epidermis. A) Fluorescent and bright phase image taken from control skin without treatment, fluorescent images taken from B) vertical cross-section C and D) cyanoacrylate surface biopsies of porcine ear skin treated with Nile Red-TyroSpheres, and E) cyanoacrylate surface biopsy of porcine ear skin treated with Nile Red solution in propylene glycol. Scale bar = 100 µm.

Another approach to study follicular penetration is via cyanoacrylate surface biopsy. This technique has been reported in literature to assess qualitative and quantitative drug delivery to the pilosebaceous unit.[13, 29] Following topical application of the fluorescent agent in the TyroSphere formulation on pig skin and regular tape stripping, follicular cast was removed and subsequently analyzed by fluorescence microscopy for presence of Nile Red. The micrographs in Figure 2.7.C and 2.7.D confirm dye delivery to the hair follicles and penetration depth of nearly 1 mm by means of TyroSpheres. Application of Nile Red solution resulted in significant lower delivery of the dye in the follicular cavity (Figure 2.7.E).

The role of TyroSpheres in follicular delivery is attributed to their small particle size and flexible structure. The mechanism of nanoparticles penetration into hair follicles has been explained via the "geared pump" effect of hair shaft.[30] The cuticular layers — produced by keratinocyte desquamation —have a zigzag structure along the hair shaft with 500-800 nm thickness. The nanoparticles are entrapped underneath the cuticular cells and the moving hair shaft can pump them deeper into the hair follicle.[31] On the other hand, the non-particulate substances that cannot be trapped in hair surface structure are quickly moved out of the follicular opening by the sebum that is being produced. Massaging the formulation following topical application on the skin has been proposed to mimic hair movement and geared pump effect in *ex vivo* conditions.[32] Thus, we included mechanical massaging in our experimental protocol.

2.3.4. Genotoxicity study of TyroSpheres

Micronuclei test was conducted to assess genotoxicity potential of TyroSpheres. TyroSpheres showed over 90% cell viability at concentrations as high as 1 and 2.5 mg/mL (the maximal tolerated concentrations). Thus, these concentrations were used for the micronuclei test. Results of genotoxicity study are provided in Figures 2.9 and 2.10 Figure 2.9 shows representative images of stained cells incubated with TyroSpheres and micronuclei formation in the cells treated with positive control (EMS). Quantitative analysis of one day and three-day genotoxicity are presented in Figure 2.10 The number of micronuclei in the cells treated with TyroSpheres was not significantly different than that of the negative control (cells incubated with growth medium) but was significantly lower than the cells treated with EMS ($p< 0.01$). Shah et al.[16] examined genotoxicity potential of various types of nanocarriers on CHO-K1 cells. They found that nanocarriers

with positive surface charges induce the formation of additional micronuclei when compared with spontaneous micronucleus formation in negative control, while neutral and negatively charged nanocarriers did not elicit genotoxicity. Since TyroSpheres have neutral surface charge, we did not expect to find them genotoxic and our results are in agreement with findings from Shah et al. This finding confirms safety of TyroSpheres for drug delivery in treatment of chronic diseases. The exact mechanisms behind genotoxic effects of nanomaterials are still unknown. However, it has been suggested that there is a positive correlation between micronuclei formation and surface charge of nanoparticles.[16]

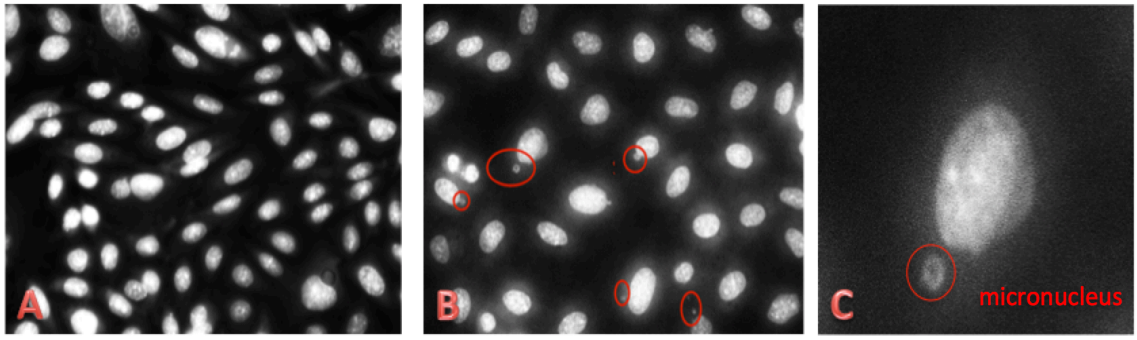

Figure 2.9. Genotoxicity (formation of micronuclei) test of TyroSpheres. Representative fluorescence microscopy images of stained nuclei of CHO-K1 cells incubated for 24 hours with A) TyroSpheres (1mg/mL) and B) ethyl methanesulfonate (EMS, positive control). The micronuclei are circled in red. C) Example of micronucleus formation in higher magnification.

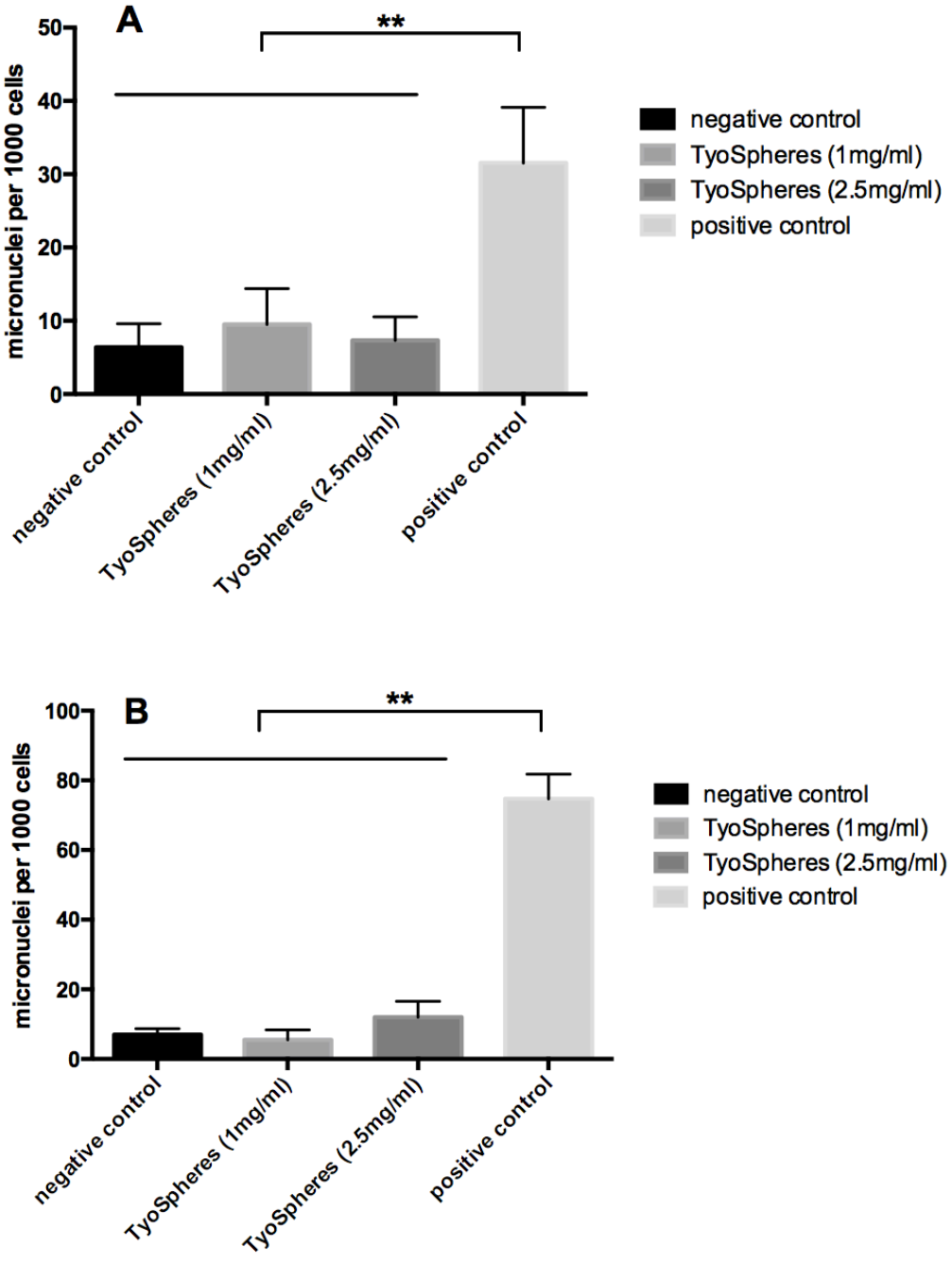

Figure 2.10. Results of A) one-day and B) three-day genotoxicity study with Chinese Hamster Ovary cells. The TyroSphere-treated groups showed no significant genotoxicity as compared to negative control (growth medium) but were significantly less genotoxic when compared with the Ethyl methanesulfonamide (EMS)-treated group, **(p<0.01) from one-way ANOVA and Tukey's post hoc test. Results are reported as number of micronuclei per 1000 cells counted (mean±SD).

2.4. Conclusions

TyroSpheres are polymeric nanocarriers capable of encapsulating hydrophobic agents. These nanoparticles have been developed and tested as topical delivery systems at New Jersey Center for Biomaterials. We evaluated the potential of TyroSpheres for topical drug delivery to the hair follicles and their safety for long-term application. Skin distribution studies on human cadaver skin and pig ear skin revealed that the nanospheres can be localized in the follicular duct and deliver the model drug to pilosebaceous unit and the surrounding epithelium. By analyzing cyanoacrylate skin surface biopsies with fluorescence microscope, we determined penetration depth of over 1 mm for Nile Red that was delivered by TyroSpheres. This high depth of delivery is attributed to small particle size of TyroSpheres. Additionally the *in vitro* micronuclei test was performed and TyroSpheres were found not to be genotoxic. Hence, TyroSpheres offer a promising platform for the safe and effective topical delivery of hydrophobic drugs as required for treatment of skin disorders.

2.5. References

1. Agarwal, R.; Katare, O. P.; Vyas, S. P., The pilosebaceous unit: a pivotal route for topical drug delivery. *Methods and findings in experimental and clinical pharmacology* 2000, *22* (2), 129-33.
2. Otberg, N.; Richter, H.; Schaefer, H.; Blume-Peytavi, U.; Sterry, W.; Lademann, J., Variations of hair follicle size and distribution in different body sites. *The Journal of investigative dermatology* 2004, *122* (1), 14-9.
3. Meidan, V. M.; Bonner, M. C.; Michniak, B. B., Transfollicular drug delivery--is it a reality? *Int J Pharm* 2005, *306* (1-2), 1-14.
4. Frum, Y.; Eccleston, G. M.; Meidan, V. M., In-vitro permeation of drugs into porcine hair follicles: is it quantitatively equivalent to permeation into human hair follicles? *Journal of Pharmacy and Pharmacology* 2008, *60* (2), 145-151.
5. Rancan, F.; Afraz, Z.; Combadiere, B.; Blume-Peytavi, U.; Vogt, A., Hair Follicle Targeting with Nanoparticles. In *Nanotechnology in Dermatology*, Springer: 2013; pp 95-107.
6. Lademann, J.; Richter, H.; Schaefer, U. F.; Blume-Peytavi, U.; Teichmann, A.; Otberg, N.; Sterry, W., Hair follicles - a long-term reservoir for drug delivery. *Skin pharmacology and physiology* 2006, *19* (4), 232-6.
7. Vogt, A.; Combadiere, B.; Hadam, S.; Stieler, K. M.; Lademann, J.; Schaefer, H.; Autran, B.; Sterry, W.; Blume-Peytavi, U., 40 nm, but not 750 or 1,500 nm, nanoparticles enter epidermal CD1a+ cells after transcutaneous application on human skin. *J Invest Dermatol* 2006, *126* (6), 1316-22.
8. Prow, T. W.; Grice, J. E.; Lin, L. L.; Faye, R.; Butler, M.; Becker, W.; Wurm, E. M.; Yoong, C.; Robertson, T. A.; Soyer, H. P.; Roberts, M. S., Nanoparticles and microparticles for skin drug delivery. *Adv Drug Deliv Rev* 2011, *63* (6), 470-91.
9. Toll, R.; Jacobi, U.; Richter, H.; Lademann, J.; Schaefer, H.; Blume-Peytavi, U., Penetration profile of microspheres in follicular targeting of terminal hair follicles. *J Invest Dermatol* 2004, *123* (1), 168-76.
10. Papakostas, D.; Rancan, F.; Sterry, W.; Blume-Peytavi, U.; Vogt, A., Nanoparticles in dermatology. *Archives of dermatological research* 2011, *303* (8), 533-50.
11. Knorr, F.; Lademann, J.; Patzelt, A.; Sterry, W.; Blume-Peytavi, U.; Vogt, A., Follicular transport route--research progress and future perspectives. *Eur J Pharm Biopharm* 2009, *71* (2), 173-80.
12. Bhatia, G.; Zhou, Y.; Banga, A. K., Adapalene microemulsion for transfollicular drug delivery. *Journal of pharmaceutical sciences* 2013, *102* (8), 2622-31.
13. Teichmann, A.; Jacobi, U.; Ossadnik, M.; Richter, H.; Koch, S.; Sterry, W.; Lademann, J., Differential stripping: determination of the amount of topically applied substances penetrated into the hair follicles. *J Invest Dermatol* 2005, *125* (2), 264-9.
14. Vega-Villa, K. R.; Takemoto, J. K.; Yanez, J. A.; Remsberg, C. M.; Forrest, M. L.; Davies, N. M., Clinical toxicities of nanocarrier systems. *Adv Drug Deliv Rev* 2008, *60* (8), 929-38.
15. Warheit, D. B.; Donner, E. M., Rationale of genotoxicity testing of nanomaterials: regulatory requirements and appropriateness of available OECD test guidelines. *Nanotoxicology* 2010, *4*, 409-13.

16. Shah, V.; Taratula, O.; Garbuzenko, O. B.; Patil, M. L.; Savla, R.; Zhang, M.; Minko, T., Genotoxicity of different nanocarriers: possible modifications for the delivery of nucleic acids. *Curr Drug Discov Technol* 2013, *10* (1), 8-15.
17. Dayan, N.; Shah, V.; Minko, T., Genotoxic potential evaluation of a cosmetic insoluble substance by the micronuclei assay. *J Cosmet Sci* 2011, *62* (1), 29-39.
18. (a) Sheihet, L.; Piotrowska, K.; Dubin, R. A.; Kohn, J.; Devore, D., Effect of tyrosine-derived triblock copolymer compositions on nanosphere self-assembly and drug delivery. *Biomacromolecules* 2007, *8* (3), 998-1003; (b) Sheihet, L.; Dubin, R. A.; Devore, D.; Kohn, J., Hydrophobic drug delivery by self-assembling triblock copolymer-derived nanospheres. *Biomacromolecules* 2005, *6* (5), 2726-31.
19. Zhang, Z.; Ramezanli, T.; Tsai, P.-C., Drug Delivery Systems Based on Tyrosine-derived Nanospheres (TyroSpheres™). *Nanotechnology and Drug Delivery, Volume One: Nanoplatforms in Drug Delivery* 2014, *1*, 210.
20. Kilfoyle, B. E. Tyrosine-derived nanoparticles for the topical treatment of psoriasis. Rutgers University-Graduate School-New Brunswick, 2011.
21. Otberg, N.; Teichmann, A.; Rasuljev, U.; Sinkgraven, R.; Sterry, W.; Lademann, J., Follicular penetration of topically applied caffeine via a shampoo formulation. *Skin Pharmacol Physiol* 2007, *20* (4), 195-8.
22. Nardin, C.; Bolikal, D.; Kohn, J., Nontoxic block copolymer nanospheres: Design and characterization. *Langmuir* 2004, *20* (26), 11721-11725.
23. Sheihet, L.; Chandra, P.; Batheja, P.; Devore, D.; Kohn, J.; Michniak, B., Tyrosine-derived nanospheres for enhanced topical skin penetration. *Int J Pharm* 2008, *350* (1-2), 312-9.
24. Batheja, P.; Sheihet, L.; Kohn, J.; Singer, A. J.; Michniak-Kohn, B., Topical drug delivery by a polymeric nanosphere gel: Formulation optimization and in vitro and in vivo skin distribution studies. *J Control Release* 2011, *149* (2), 159-67.
25. Kilfoyle, B. E.; Sheihet, L.; Zhang, Z.; Laohoo, M.; Kohn, J.; Michniak-Kohn, B. B., Development of paclitaxel-TyroSpheres for topical skin treatment. *J Control Release* 2012, *163* (1), 18-24.
26. Jacobi, U.; Kaiser, M.; Toll, R.; Mangelsdorf, S.; Audring, H.; Otberg, N.; Sterry, W.; Lademann, J., Porcine ear skin: an in vitro model for human skin. *Skin Res Technol* 2007, *13* (1), 19-24.
27. Lademann, J.; Richter, H.; Meinke, M.; Sterry, W.; Patzelt, A., Which skin model is the most appropriate for the investigation of topically applied substances into the hair follicles? *Skin Pharmacol Physiol* 2010, *23* (1), 47-52.
28. Raber, A. S.; Mittal, A.; Schafer, J.; Bakowsky, U.; Reichrath, J.; Vogt, T.; Schaefer, U. F.; Hansen, S.; Lehr, C. M., Quantification of nanoparticle uptake into hair follicles in pig ear and human forearm. *J Control Release* 2014, *179*, 25-32.
29. Ossadnik, M.; Czaika, V.; Teichmann, A.; Sterry, W.; Tietz, H. J.; Lademann, J.; Koch, S., Differential stripping: introduction of a method to show the penetration of topically applied antifungal substances into the hair follicles. *Mycoses* 2007, *50* (6), 457-62.
30. Lademann, J.; Richter, H.; Schaefer, U. F.; Blume-Peytavi, U.; Teichmann, A.; Otberg, N.; Sterry, W., Hair follicles - a long-term reservoir for drug delivery. *Skin Pharmacol Physiol* 2006, *19* (4), 232-6.

31. Lademann, J.; Patzelt, A.; Richter, H.; Antoniou, C.; Sterry, W.; Knorr, F., Determination of the cuticula thickness of human and porcine hairs and their potential influence on the penetration of nanoparticles into the hair follicles. *Journal of biomedical optics* 2009, *14* (2), 021014.
32. Lademann, J.; Richter, H.; Teichmann, A.; Otberg, N.; Blume-Peytavi, U.; Luengo, J.; Weiss, B.; Schaefer, U. F.; Lehr, C. M.; Wepf, R.; Sterry, W., Nanoparticles--an efficient carrier for drug delivery into the hair follicles. *Eur J Pharm Biopharm* 2007, *66* (2), 159-64.

Chapter 3: Development and characterization of a polymeric nanoparticle-based formulation of adapalene for topical acne therapy

3.1. Introduction

Skin, the most accessible organ of the body, possesses significant barrier properties that inhibit the passive transport of many topically applied compounds. This barrier is mostly due to the presence of keratin-rich corneocytes and intercellular lipid compositions in the uppermost layer of the skin, the stratum corneum (SC).[1] Hair follicles are invaginations of the epidermis extending into the deeper dermis and are considered interruptions in this protective skin barrier.[2] Due to this fact, hair follicles have been explored as an alternative pathway for both topical and transdermal drug delivery. Large molecules and particles that do not normally penetrate into viable skin layers can localize at hair follicles.[3,4]

The nanotechnology platform has drawn attention for potential use in the field of topical delivery. Actives loaded in the carrier systems are exemplified by antimicrobial agents (e.g. roxithromycin[5]), retinoids (e.g. tretinoin[6]), and anti inflammatory agents (e.g. flufenamic acid[7]). Nanoparticles based on biocompatible polymers, such as poly(lactide-co-glycolide) (PLGA), chitosan, poly(ε-caprolactone), and tyrosine-derived amphiphilic copolymers can improve drug stability in the formulation, provide readily-tunable drug release profiles,[8] and enhance dermal delivery.[9] Recently, some groups have shown applicability of nanocarriers for follicular and transfollicular drug delivery.[10-11] This is especially beneficial for skin disorders such as acne and alopecia, where the hair follicle itself is the therapeutic target site.

Acne is a chronic inflammatory disorder involving the pilosebaceous unit, where altered keratinization, increased sebum production, inflammation, and bacterial colonization lead to progression of acne lesions. The early and non-inflammatory stage of acne usually features comedones, where the abnormal desquamation of follicular epithelium occurs and the pilosebaceous canal is partially or completely clogged with excess keratin and dead cells.[12] Retinoids are vitamin A derivatives that are used as first-line therapy for comedonal and inflammatory acne. They bind to the retinoic acid nuclear receptor (RAR) and activate genes responsible for cellular differentiation. They have anti-proliferative effects on the sebocytes and as a result decrease sebum production and microcomedone formation.[13,14]

Adapalene is a third generation retinoid with anti-inflammatory, keratolytic and anti-seborrheic effects. However, adapalene's physicochemical properties (pKa = 4.23, logP = 8.04, from SciFinder database-https://scifinder.cas.org) limit its local bioavailability in skin strata and hair follicles. Figure 3.1 depicts the chemical structure of adapalene. Although adapalene is known to have higher patient compliance than the first generation retinoids, some topical adverse effects such as erythema, dryness, and scaling have been reported with its commercial formulation.[15] These topical adverse effects may be elected from retinoid as well as vehicle-related irritation. Encapsulation of retinoids with nano/microparticles in an alcohol-free formulation has been suggested as one main way of circumventing the topical side effects and enhancing follicular delivery.[16,17] Very few reported nanotechnology approaches for adapalene topical delivery can be found in literature, where mostly the lipid-based formulations were used for enhancing its follicular delivery.[18,19] Nevertheless, the authors neither compared their nanoparticle

formulation with the adapalene marketed product nor examined its skin irritancy properties.

In vitro monolayers of epidermal keratinocytes or dermal fibroblasts have been used in various *in vitro* assays to predict the irritation potential of topically applied compounds. Although cell culture models lack barrier properties of intact skin and may overestimate the irritancy of the chemicals, they can be used as a tool to compare irritation potential of different formulations/compounds.[20] The European Center for the Validation of Alternative Methods (ECVAM) has endorsed the use of reconstituted human epidermis models (EPISKIN- Episkin SNC and EpiDerm™- MatTek Corp.) for prediction of acute skin irritation.[21] The irritation evaluation includes cell viability assessment by MTT reduction assay and measurement of pro-inflammatory cytokines, such as IL-1α release. Theses three dimensional(3D) *in vitro* models can serve as an alternative to animals in skin irritation testing of chemicals.

In this chapter we aimed to explore the applicability of biocompatible tyrosine-derived polymeric nanoparticles (TyroSpheres) for topical hair follicle delivery of adapalene. In this study, adapalene was used as an anti-acne drug. Adapalene-loaded TyroSpheres (adapalene-TyroSpheres) were fabricated and characterized for size, binding efficiency, and crystallinity. Detailed drug release, partitioning, and biodistribution studies were carried out and skin irritancy was assessed using 2D and 3D *in vitro* models. These studies provided additional evidence for the potential of TyroSpheres as an effective topical delivery system for acne therapy that does not result in skin irritation.

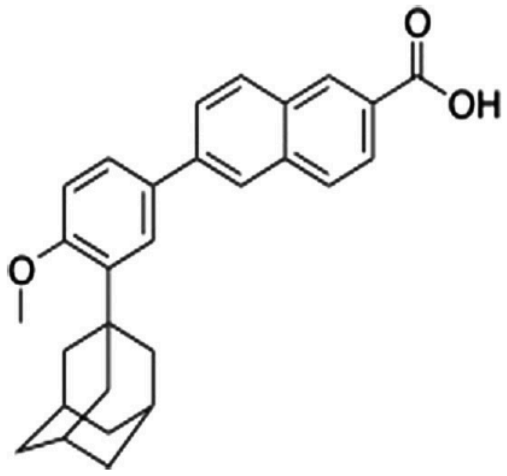

Figure 3.1. Chemical structure of adapalene.

3.2. Materials and Methods

3.2.1. Materials

Suberic acid (SA), poly(ethylene glycol) monomethyl ether MW 5000 (PEG_{5K}), trifluoroacetic acid (TFA), Tween-80, dimethylformamide (DMF), stearic acid, oleic acid, cholesteryl oleate, and Dulbecco's Phosphate Buffered Saline (PBS) were purchased from Sigma Aldrich (St. Louis, MO). Dulbecco's Modified Eagle Medium, high glucose (DMEM), gentamycin (50 mg/mL), RPMI-1640 medium, trypsin (0.25% Trypsin-EDTA), Nile Red, fetal bovine serum (FBS), and Dulbecco's Phosphate Buffered Saline without calcium chloride and magnesium chloride (DPBS) were purchased from Life Technologies (Grand Island, NY). HPLC grade water, acetonitrile, and methanol were obtained from Fisher Scientific (Pittsburgh, PA). Adapalene was purchased from BOC Sciences (Shirley, NY). Squalene and cholesterol were obtained from Alpha Acer (Ward

Hill, MA). Cetyl ester wax was obtained from PCCA (Houston, TX). Coconut oil, cottonseed oil and olive oil were obtained from Acros Organics (Morris Plains, NJ). Uranyl acetate was obtained from Electron Microscopy Sciences (Hatfield, PA). AlamarBlue® reagent was obtained from AbD Serotec (Raleigh, NC). HaCaT cells were received as a generous gift from Dr. Qing Ren (Department of Radiation Oncology at Thomas Jefferson University). EpiDerm™ skin kit, EpiDerm™ culture medium, and MTT assay kit were purchased from MatTek Corporation (Ashland, MA). ABA triblock copolymer PEG_{5K}-*b*-oligo(desaminotyrosyl-tyrosine octyl ester suberate)-*b*-PEG_{5K} (M_n = 22.9 kDa, Mw = 31.9 kDa, PD = 1.39 obtained from gel permeation chromatography) was synthesized according to previously published and established procedures from the New Jersey Center for Biomaterials, Rutgers University and their chemical structure and purity were confirmed by ^{1}H NMR.[22,23] All reagents were used as received.

3.2.2. HPLC method development and validation for adapalene

3.2.2.1. Method characteristics

An Agilent 1100 HPLC system (Agilent Technologies, USA) equipped with a UV/Vis detector and reversed phase column (Promonax Luna 5 μm C18(2), 4.6 × 150 mm) was used for chromatographic separations at 25°C. A mixture of acetonitrile: water (0.1% TFA) 87:13 (v/v) was applied as the mobile phase at a flow rate of 1 mL/min. The detection wavelength was set at 309 nm and injection volume was 20 μL.

3.2.2.2. Standard solutions and calibration curve

Adapalene standard solutions were prepared by dissolving 25 mg of drug in 25 mL DMF in a volumetric flask (stock solution) with aid of bath sonication. Next, standard solutions were made by serial dilution from the stock solution. Standard calibration curves were prepared at adapalene concentrations ranging from 0.1 to 500 µg/mL.

3.2.2.3. Method validation

Precision is a measure of the reproducibility of the analytical method and is determined by multiple sampling of several standard concentrations in one HPLC run. The precision can be expressed as the relative standard deviation (RSD).

$$\%RSD=(SD/mean)\times 100$$

The method was also validated for linearity of the calibration curve and intra and inter-day variability by running HPLC for the standard solutions 3 times per day and on 3 different days respectively. Limit of detection (is the lowest concentration of a sample that can be detected) and limit of quantification (the lowest concentration of the analyte in a sample that can be determined with acceptable precision and accuracy) were determined.

3.2.3. Preparation of adapalene loaded-TyroSphere formulations

ABA triblock copolymer PEG_{5K}-*b*-oligo(desaminotyrosyl-tyrosine octyl ester suberate)-*b*-PEG_{5K} was used for the preparation of TyroSpheres. Adapalene-TyroSpheres and empty TyroSpheres (without drug) were prepared via self-assembly technique as described previously.[23-24] Briefly, adapalene and DTO/SA copolymer were dissolved in DMF separately and then were mixed at ratios shown in Table 3.3 The combination of

drug and polymer solution was added dropwise to PBS, pH 7.4 (at ratio of 0.6:14.4, v:v) under constant stirring. The nanoparticles were formed and added slight turbidity to PBS. The nanosuspension was filtered using 0.22 μm PVDF filters (Millipore) and subjected for ultra-centrifugation (Beckman L8-70M ultracentrifuge, Beckman Coulter, Fullerton, CA) at 65,000 rpm (290,000 × g) for 3 h at 18°C. The supernatant was then discarded, the pelleted nanospheres were rinsed and re-suspended in PBS overnight.

3.2.4. Characterization of adapalene-TyroSphere formulations

3.2.4.1. Adapalene solubility in different aqueous media

The solubility of adapalene in PBS media with and without presence of various amounts of Tween 80 (0.1, 1, and 10% w/w) was measured to allow comparison with the adapalene-TyroSphere formulation. Super-saturated solutions of adapalene were prepared by adding excess drug to each medium. Samples were vortexed and placed in a shaking water bath (100 rpm) at 37 °C for 24 h. The samples were then centrifuged and filtered through 0.45 μm PVDF filters (Whatman, Clifton, NJ), lyophilized, and re-dissolved in DMF. Adapalene concentrations in each medium was determined using HPLC.

3.2.4.2. Particle size and size distribution

Particle size and polydispersity index (PDI) of the TyroSphere formulations were measured using DLS technique (Beckman Coulter Delsa™ Nano) at 25 °C in triplicate. TyroSphere liquid dispersions were diluted 10 times for size measurement and were examined by normalized intensity distribution using the CONTIN method for cumulants, size distribution, and polydispersity. An average of 50 measurements were recorded per replicate (n = 4).

3.2.4.3. Particle morphology

Particle morphology was studied with transmission electron microscopy (TEM). For sample preparation, small aliquot of 10 times diluted adapalene-TyroSpheres was deposited on Formvar/Carbon-coated grid and 1% uranyl acetate aqueous solution was used for background staining. Electron micrographs were taken using JEM 100 CX TEM (JEOL Ltd, Japan).

3.2.4.4. Adapalene-TyroSpheres encapsulation efficiency

Drug concentration in the final purified nano-dispersion was measured by HPLC (as described above) after dissolving freeze-dried aliquots of the adapalene-TyroSphere formulation in DMF. Binding efficiency and loading efficiency were calculated as described below:

$$\%Binding\ Efficiency\ = \frac{drug\ amount\ in\ TyroSpheres}{initial\ amount\ in\ the\ feed} \times 100$$

$$\%\ Loading\ Efficiency = \frac{drug\ amount\ in\ TyroSpheres}{mass\ of\ TyroSPheres} \times 100$$

3.2.5. Wide angle X-ray diffraction (WAXD)

The X-ray diffraction (XRD) analysis of adapalene, TyroSpheres, adapalene-TyroSpheres and adapalene physically mixed with TyroSpheres was carried out to study the crystallinity of adapalene. A PANalytical PW3040/60 X'Pert PRO instrument (Almelo, The Netherlands) was used with the following settings: scanning range from 5 to 50° (2θ) and scanning speed 4°/min with a step size of 0.026°. Jade software (version 9) was used for data processing.

3.2.6. Adapalene partitioning in artificial human sebum and in stratum corneum

3.2.6.1. Preparation of artificial human sebum

Sebum is a mixture of lipids produced by sebaceous glands in the skin. The main components of the sebum are squalene, wax esters, triglycerides, fatty acids, cholesterol and cholesterol esters.[25] The chemical composition of the artificial sebum used in our study is shown in Table 3.1. The sebum components were selected from commercially available products, based on human sebum chemical composition reported in the literature.[26] Artificial human sebum was prepared according to method described by Valiveti et al.[27] Briefly, the ingredients were weighed and transferred to a glass beaker, heated up to 60°C with stirring for a few minutes to melt. After formation of a homogenous mixture, the artificial sebum was kept at 4°C until use. The heated artificial sebum in liquid form was applied for artificial sebum/water partitioning study (see Figure 3.2) and it solidified in a few seconds after application at temperatures below 40°C.

Table 3.1. Chemical composition of artificial human sebum used in our study.

Ingredient	**% (w/w)**
Squalene	15
Paraffin wax	10
Cetyl ester	15
Olive oil	10
Cottonseed oil	25
Coconut oil	10
Oleic acid	1.4
Palmitic acid	5
Palmitoleic acid	5
Cholesterol	1.2
Cholesterol oleate	2.4

3.2.6.2. Isolation of stratum corneum

Dermatomed human cadaver skin samples (thickness 300-600 μm) from the posterior torso of a male Caucasian donor were obtained from New York Firefighters Skin Bank (New York, NY). The frozen skin was thawed in room temperature and the epidermis was separated by immersing the skin pieces in deionized water and heating up to 60°C.[28] Next, the epidermal layer was transferred to a Petri dish containing 0.025% trypsin solution and incubated at room temperature for 4 h. Then the viable layers of epidermis was removed by a cotton swap and the remaining SC membranes were rinsed with PBS (pH 7.4), dried in in a desiccator overnight and stored at -20°C until use.

3.2.6.3. Adapalene partition coefficient for sebum and stratum corneum

Partitioning of adapalene in artificial sebum and in SC was assessed following standard procedure.[27] For partitioning of adapalene, one drop of heated artificial sebum (10-15 mg) or a piece of SC (4-5 mg) was added to adapalene-TyroSphere aqueous dispersion (0.015% drug content), and the mixture was kept in a shaking water bath (100 rpm) at 37°C for 15 h (see Figure 3.2). The vials were centrifuged at 4000 rpm at 25°C for 6 min using a benchtop centrifuge (Allegra 6, Beckman Coulter) and the adapalene content in supernatant and pellet (sebum or SC) was determined separately by HPLC. The partition coefficient values were calculated from the following equation.[27]

$$Partition\ Coefficient = \frac{drug\ concentration\ \ in\ 1\ g\ of\ sebum/SC}{drug\ concentration\ in\ 1\ g\ of\ aqueous\ suspension}$$

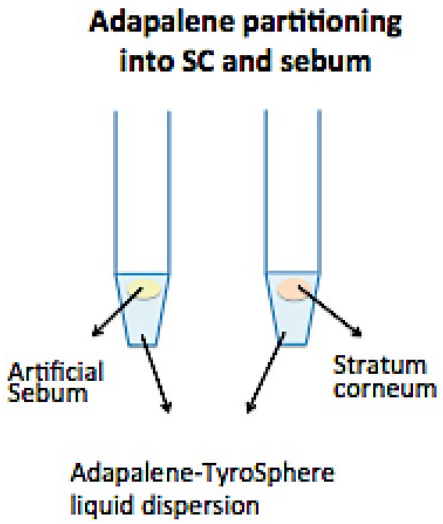

Figure 3.2 Schematic illustration of adapalene partitioning study.

3.2.7. Adapalene release through stratum corneum via Franz diffusion cells

SC separated from human cadaver skin was mounted on vertical Franz diffusion cells with receptor volume of 5 mL and effective diffusion area (donor/receptor contacting area) of 0.64 cm^2 (PermeGear, Hellertown, PA). 20% v/v DMF in PBS (pH 7.4) was used as the releasing medium, which was stirred with a magnetic bar at 600 rpm during the experiment at 37 °C. 200 µL of adapalene-TyroSpheres (0.02% w/w) was added to the donor chamber, which was occluded with parafilm to prevent water evaporation. At pre-determined time-points, aliquots of 400 µL were collected from the receptor compartment and replaced with the equivalent amount of the fresh releasing medium. Following lyophilization of the samples and re-dissolving adapalene in DMF, the drug content was analyzed by HPLC (Figure 3.3).

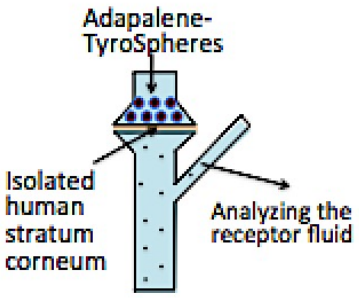

Figure 3.3 Schematic illustration of adapalene release study.

3.2.8. Skin permeation study of adapalene-TyroSpheres and the adapalene commercial product

3.2.8.1. *Ex vivo* skin distribution study using human cadaver skin

Dermatomed human skin samples (400-600 µm) from the posterior torso of a Caucasian male donor obtained from New York Firefighters Skin Bank (New York, NY) were used for this experiment. The permeation studies were carried out at 37 °C using vertical Franz diffusion cells. PBS pH 7.4 containing 1% Tween 80 was added to the receptor compartment. The skin samples were treated with either 100 µL Differin® lotion 0.1% (w/w) or 500 µL of adapalene-TyroSphere liquid dispersion (0.02% w/w) for 12 h. Then, the skin pieces were washed and removed from the Franz cells. Epidermal and dermal layers were manually separated using tweezers. Adapalene was extracted in DMF from skin layers with aid of homogenization (Polytron® PT10/35 - Kinematica, Switzerland). The adapalene content in epidermis, dermis, receptor media and donor compartment was determined by HPLC.

3.2.8.2 *Ex vivo* skin distribution study using porcine ear skin

An ear was isolated from a Yorkshire pig (3 month old, 38 kg, purchased from Barton's West End Farms, Oxford, NJ) and stored in RPMI-1640 medium (Invitrogen) at 4°C for a few days until use. On the day of study the porcine ear skin connected to the cartilage was cut into smaller pieces (around 4 cm^2), rinsed with PBS, and mounted on vertical Franz diffusion cells with effective diffusion area of 3.14 cm^2. The receptor solution consisted of 1% w/w Tween 80 in PBS (pH 7.4). Adapalene-TyroSphere formulation (0.025% w/w), and Differin® gel (0.1% w/w), were applied on the pig ear skin topically. The formulations were gently massaged for 3 minutes on the skin using a glass rod. The skin distribution study was carried out for 12 h and 24 h, respectively. The skin specimens that were applied on Franz diffusion cells without treatment were used as control. At the end of the permeation experiment, excess formulation was removed from the pig ear skin, the surface was rinsed with PBS, dried with a cotton stick and subsequently subjected to the treatments described as following:

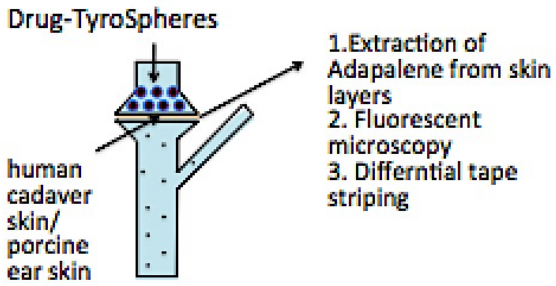

Figure 3.4. Schematic illustration of adapalene-TyroSpheres skin distribution study.

3.2.8.2.1. Fluorescence imaging of the skin

Fluorescent images were taken from surface of the skin and hair follicle openings using Olympus CK40 microscope equipped with a UV source and filters for fluorescence measurement. To visualize depth of drug penetration, skin pieces were frozen over dry ice, and then cut into smaller strips and embedded in Optimal Cutting Temperature (OCT) medium. Vertical cross-sections (15 μm) of the skin were prepared with a cryostat (Leica Cryostat CM 3050S, Wetzlar, Germany) and collected on glass slides. The samples were then subjected to fluorescence and phase-contrast microscopy.

3.2.8.2.2. Differential tape stripping of the skin

Differential tape stripping of the skin samples was done according to a procedure described by Teichmann et al.[29] After termination of the permeation study and removing the excess formulation from the skin, the effective area was subjected to tape stripping. A total of 25 rounds of tape stripping were applied to remove the SC layer using adhesive 3M-Scotch® tapes (St. Paul, MN). A roller was used to stretch the skin gently to avoid generation of wrinkles. The tape strips were collected with forceps and pooled together in a 50 mL centrifuge tube. Following SC removal, cyanoacrylate skin biopsies were performed by applying superglue (Loctite, Henkel Corporation, Ohio) to remove the whole follicular cast. To quantify adapalene delivery to SC, hair follicles, and remaining skin biopsies, drug was extracted from the tapes, cyanoacrylate skin biopsies, and the remaining skin respectively using DMF and 1 h bath sonication. Then samples were analyzed by HPLC.

3.2.9. Skin irritation studies of adapalene-TyroSpheres and the adapalene commercial product

3.2.9.1. *In vitro* skin irritation analysis on a 2D cell-based model

3.2.9.1.1 HaCaT culture

HaCaTs (a cell line of human keratinocytes) with passage number below 20 was utilized in the study. The cells were cultured in Dulbecco's Modified Eagle Medium (DMEM) supplemented with 10% fetal bovine serum (FBS) and 50 mg/mL gentamycin (37°C, 10% CO_2, RH 95%). When 90% confluency was reached, the cells were rinsed with DPBS, and trypsinized. The cell concentration was measured with a Cellometer Auto A4, Nexcelom (Bioscience, MA).

3.2.9.1.2. *In vitro* irritation study on HaCaT monolayers

HaCaT cells were seeded in 96-well plates at 5,000 cells/well seeding density. The cells were incubated for 24 hours to ensure sufficient attachment. Next, the medium was replaced with DMEM medium (without serum) containing the following: Differin®, adapalene solution, and adapalene-TyroSpheres. The concentration of adapalene in the wells was 0.5-10 µg/mL (0.05-1 µg/well). The HaCaTs were incubated with media containing adapalene formulations or their vehicles for 1 h. Next the media was replaced with fresh DMEM containing serum and the wells were placed in an incubator (37°C, 10% CO_2, RH 95%) for 42 h. The irritation potential of adapalene formulations, vehicles and solvents used to make the TyroSphere formulation and adapalene solution was analyzed by AlamarBlue® metabolic assay.

3.2.9.1.3. AlamarBlue® metabolic assay

Cell culture medium containing 10% AlamarBlue® reagent was added and the cells were incubated until the negative controls started to turn pink. The fluorescence intensity was measured (560nm/590nm; manual gain 97%) using a Tecan Infinite 200M fluorescent plate reader. Plain cell culture medium treatment was used as 100% cell viability.

3.2.9.2. *In vitro* skin irritation analysis on a three-dimensional (3D) skin model

Fully differentiated human epidermis (EpiDerm™) specimens were purchased from MatTek Corporation (Ashland, MA). The *in vitro* irritation study was conducted according to a protocol provided by the manufacturer. Upon arrival, the tissues were transferred to 6-well plates and incubated at 37°C overnight in 0.9 mL assay medium (EPI-100-ASY, MatTek) at the air-liquid interface. The next day, the surface of EpiDerm™ was treated with Differin® gel or adapalene-TyroSphere liquid dispersion at drug concentration of 40 μg/cm^2 in triplicate. The tissues were fed from the bottom with the fresh assay medium and incubated at 37°C and 5% CO_2 for 3 h or 24 h. EpiDerm™ samples treated with PBS pH 7.4 were used as negative control. The irritation potential of adapalene formulations was evaluated by MTT cell viability assay and inflammatory mediators/cytokine analysis (to determine IL-1α and IL-8 content in the media), after the dosing period was completed.

3.2.9.2.1. MTT assay

In the *in vitro* skin irritation analysis using three-dimensional (3D) epidermal skin model, the viability of the tissues after dosing was analyzed by MTT. The tissue specimens were rinsed with PBS and transferred to 24-well plates containing 300µL MTT solution (provided by MatTek Corp.) and incubated for 3 h. Next, the tissues were immersed in a 24-well plate containing 2 mL extracting solution per well. The plate was sealed and incubated at room temperature overnight. The optical density (OD) of the extracted samples was measured at 570 nm. Percent tissue viability was calculated using the following formula:

$$\%\, Viability = 100 \times \frac{\text{OD (sample)}}{\text{OD (negative control)}}$$

3.2.9.2.2. ELISA assay

Release of IL-1α and IL-8 in the EpiDerm™ culture medium was quantified using ELISA kits from BioLegend (San Diego, CA) according to the assay protocol provided by the manufacturer. UV–Vis spectrophotometric measurements were performed with a Biotek PowerWave X microplate reader.

3.2.10. Statistical analysis

For particle size, drug binding and loading efficiencies, solubility, and drug release the results are reported as mean ± standard deviation (SD). For skin distribution studies and irritation assays, the results are reported as mean ± standard error (SE). For particle size analysis and irritation study, the differences were determined by one-way ANOVA followed by Tukey's post hoc test using Prism version 6 (GraphPad software,

La Jolla California). Student t-test (unpaired) in the Excel program was used to compare adapalene penetration into epidermis, SC and hair follicles between adapalene-TyroSpheres and Differin® treated samples. For all analysis, a *P* value of less than 0.05 derived from a two-tailed test was considered significant unless specified.

3.3 Results and Discussion

3.3.1. HPLC method validation

Figure 3.5 depicts the adapalene chromatogram peak obtained from the current HPLC method and appeared around 10.8 min. The peak's shape passed the requirement for symmetry and sharpness.

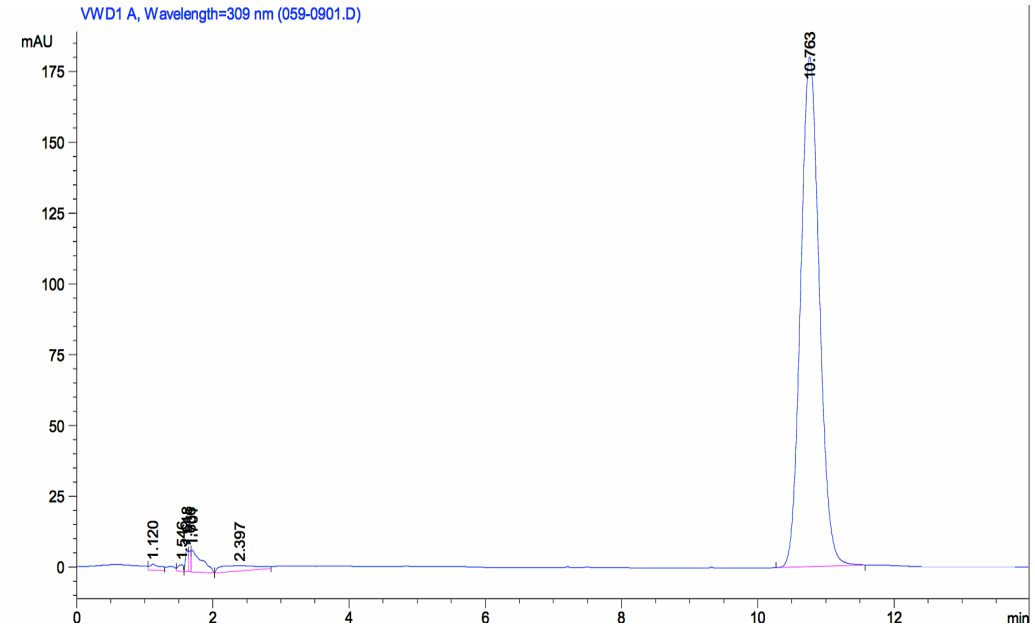

Figure 3.5. Chromatogram peak of adapalene at retention time of 10.8 min.

Figure 3.6 shows the standard calibration curve obtained from three separate HPLC runs for adapalene solutions ranging from 0.25-500 µg/mL. Linearity of the current method was confirmed with an R^2 value of 0.9999. Limit of quantification and limit of detection were found to be 0.1 and 0.01 µg/mL respectively.

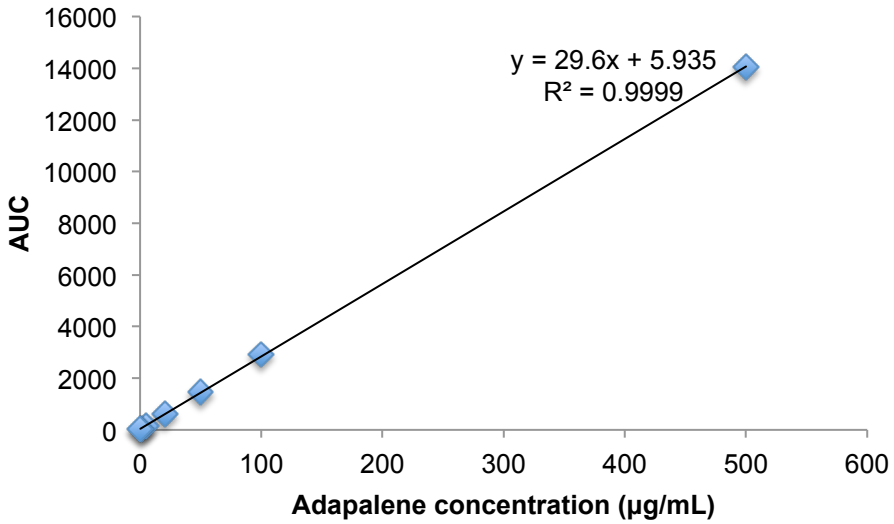

Figure 3.6. Adapalene standard curve for HPLC assay.

The results of inter-day and intra-day variability assessment are provided in Table 3.2 and 3.3 respectively. The %RSD for the slope of the best fit line was calculated as 0.98% and 1.02% for inter-day and intra-day precision respectively. These values are lower than the requirement %RSD value of 2%.

Table 3.2. Adapalene standard concentrations with average chromatogram peak area, standard deviation (SD), and relative standard deviation (RSD) of three separate runs in three days.

Concentration (µg/mL)	Average AUC	SD	%RSD
500	14167.7	350.4	2.47
200	5709.3	62.9	1.10
100	2932.6	63.7	2.17
50	1471.6	26.8	1.82
25	732.7	6.8	0.93
20	596.0	11.3	1.90
5	152.6	2.7	1.77
1	33.3	0.8	2.27
0.25	11.0	1.2	10.71

Table 3.3. Adapalene standard concentrations with average chromatogram peak area, standard deviation (SD), and relative standard deviation (RSD) of three separate runs in one day.

Concentration (µg/mL)	Average AUC	SD	%RSD
200	5760	43.6	0.76
100	2894	19.4	0.67
50	1493	30	2
25	736	1.52	0.21
5	155	2	1.29
1	32.7	0.6	1.8

The current method also passed the test for repeatability expressed by % RSD of five replicates at concentrations of 100.0, 50, and 25 µg/mL (see Table 3.4).

Table 3.4. Precision analysis of adapalene HPLC method. The average AUC was calculated from 5 consecutive injections of each concentration during one run.

Concentration (µg/mL)	Average AUC	SD	%RSD
100	2920	22.4	0.77
50	1493.8	5.17	0.35
25	745.4	2.41	0.32

3.3.2. Adapalene-TyroSpheres: Characterization of the liquid formulation

Due to its amphiphilic nature, PEG_{5K}-*b*-oligo(DTO-SA)-*b*-PEG_{5K} can self-assemble to form micellar-like spherical-shaped drug carriers (TyroSpheres) in aqueous media and encapsulate hydrophobic drugs. Previous studies reported that TyroSpheres were able to encapsulate a wide range of hydrophobic agents and significantly enhance their solubility.[24,9] Table 3.5 provides the solubility of adapalene in PBS either as loaded in the TyroSpheres or supplemented with various concentrations of Polysorbate 80 (Tween 80). Adapalene aqueous solubility in plain PBS, pH 7.4 was below HPLC detection limit (10 ng/mL). The maximum solubility in 3% TyroSphere dispersion was significantly higher than that in 10% Polysorbate 80 solution ($P<0.05$).

In a previous study a computational modeling approach was employed to study interaction between PEG_{5K}-*b*-oligo(DTO-SA)-*b*-PEG_{5K} copolymer and several hydrophobic model compounds.[30] The results indicate that the PEG_{5K}-*b*-oligo(DTO-SA)-*b*-PEG_{5K} copolymer system interacts with drugs via hydrophobic interactions, hydrogen binding and/or π−π stacking, causing drug entrapment inside the hydrophobic core of the TyroSphere. We propose the same mechanism for adapalene-TyroSphere interactions. The aromatic rings in the adapalene structure are presumed to form π stacking with aromatic rings in the DTO-SA segment. The formation of the hydrogen bonds between the carboxyl group in adapalene and amide group in the TyroSphere is also highly possible. The hydrophobic interactions, the π stacking, and the hydrogen binding, can jointly contribute to the enhanced solubility of adapalene in TyroSphere formulation.

Table 3.5. Solubility of adapalene in several aqueous media at room temperature, and that of adapalene loaded in TyroSpheres (3 wt% in PBS). The results are shown as mean ± SD (n=3).

Sample content	**Concentration of adapalene (µg/mL)**
Adapalene in PBS, pH 7.4	< 10 ng/mL
Adapalene in 0.1% (w/w) Tween 80	3.7±0.8
Adapalene in 0.5% (w/w) Tween 80	15.4±3.9
Adapalene in 1.0% (w/w) Tween 80	37.6 ±7.7
Adapalene in 10% (w/w) Tween 80	219.8±26.0
Adapalene in 3 wt% TyroSpheres	**265±35.3**

Adapalene binding and loading efficiencies in TyroSpheres (with two different initial drug and polymer inputs) are presented in Table 3.6 The initial drug-to-polymer ratio highly influences the drug loading and encapsulation efficiency. The drug to copolymer ratio of 1.3 wt% resulted in the highest drug binding efficiency. Beyond this level, binding efficiency markedly reduced. The binding efficiencies for formulations with 1 wt% drug/polymer ratio were around 70%. By increasing initial drug input, the available binding sites inside TyroSpheres are occupied and the remaining unbound adapalene precipitates in the aqueous medium. Therefore, 1.3 wt% is the maximum loading efficiency obtained with TyroSpheres.

Table 3.6. Composition of different adapalene-TyroSphere formulations (Ada-Np) and TyroSpheres without drug (empty-Np) and their characteristics: particle size, polydispersity index (PDI), and binding and loading efficiencies. The results are shown as mean ± SD (n = 3).

Formulation	Adapalene	DTO-SA/5k polymer	PDI	%Binding efficiency	% Loading efficiency
Ada-Np-1	0.6 mg	60 mg	0.14±0.03	68.5±5.2	1.25±0.06
Ada-Np-2	0.8 mg	60 mg	0.18±0.02	58.6±6.0	1.31±0.12
Ada-Np-3	1.0 mg	60 mg	0.15±0.04	27.9±4.2	0.67±0.18
Ada-Np-4	0.8 mg	80 mg	0.19±0.03	69.3±6.6	1.28±0.15
Ada-Np-5	1.0 mg	80 mg	0.19±0.03	61.1±8.2	1.44±0.27
Empty-Np-1	-	60 mg	0.13±0.03	-	-
Empty-Np-2	-	80 mg	0.19±0.01	-	-

TyroSpheres had an average diameter of about 70 nm (based on DLS technique). As demonstrated in Figure 3.7, adapalene encapsulation in TyroSpheres did not have a significant effect on the particle size. Adapalene-TyroSpheres demonstrated a neutral surface charge (as determined by zeta potential, data not shown). Increasing the polymer input from 60 mg to 80 mg resulted in larger nanoparticles ($p<0.05$), while the polydispersity index (PDI) in all cases was below 0.2. Filtration of TyroSphere liquid dispersion with PVDF syringe filters (0.22 μm Merck Millipore) in the last step of their preparation did not have a significant effect on the particle sizes.

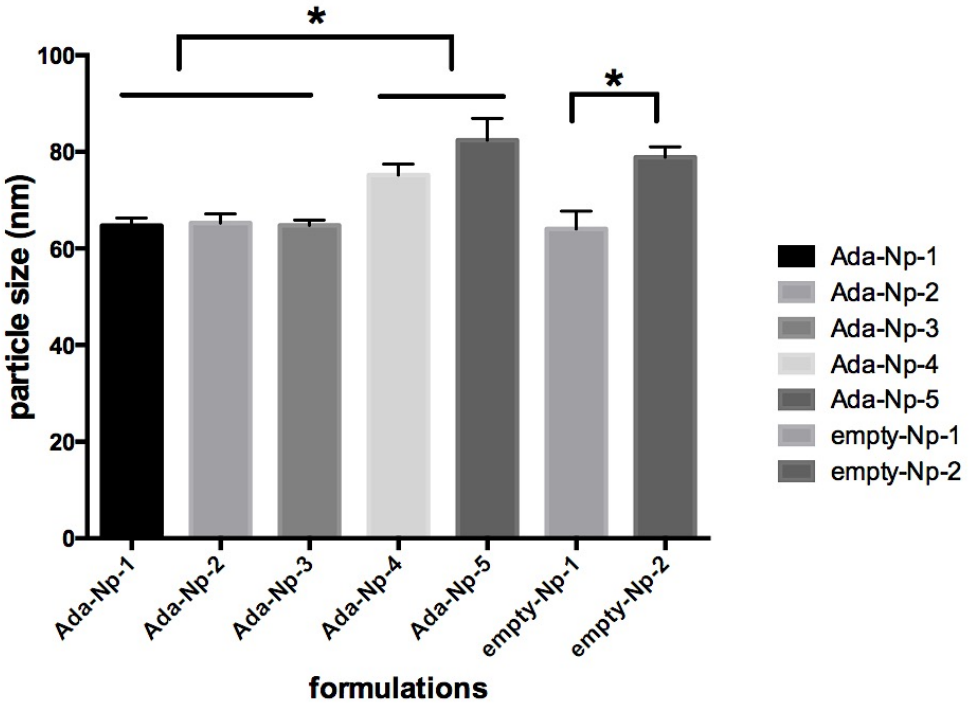

Figure 3.7. Average diameter of nanoparticles in different adapalene-TyroSphere formulations (Ada-Np) and TyroSpheres without drug (empty-Np). The results are presented as mean ± SD. * $p< 0.05$ (determined by one-way ANOVA followed by Tukey's post hoc test) is considered to be statistically significant between the particle size of TyroSpheres prepared with two different copolymer concentrations.

Figure 3.8 depicts the spherical morphology and 30-50 nm diameter size of TyroSpheres obtained by TEM. The diameter size of TyroSpheres appears to be smaller than what was observed by light scattering analysis. This difference in the size distribution may be due to dehydration of nanoparticles and outer PEG layer during specimen preparation, which causes shrinkage of nanoparticles.

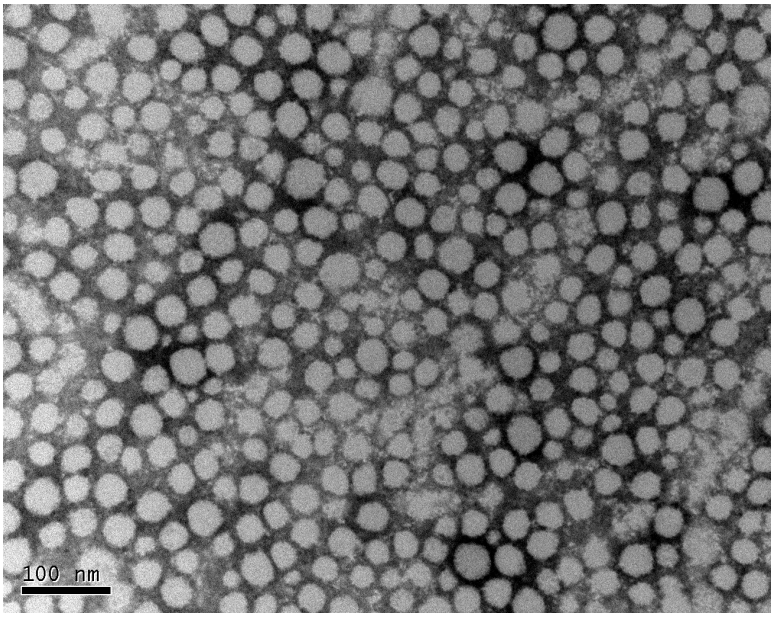

Figure 3.8. Transmission electron micrograph of adapalene-TyroSphere liquid dispersion.

3.3.3. XRD analysis

The XRD spectra of adapalene, TyroSpheres, and adapalene- TyroSpheres are provided in Figure 3.9. The sharp and intense peaks from 10 to 30° (2θ) confirm the crystalline nature of adapalene.[16,31] These peaks are absent in the XRD pattern of empty TyroSpheres and adapalene-TyroSpheres. The appearance of sharp peak at 27.5° (2θ) in TyroSphere samples is due to the presence of sodium chloride in the buffer. The two weak intensity peaks at 19 and 23° (2θ) were resulted from the copolymer. In order to ensure that the crystalline diffraction peaks of adapalene can be detected at concentrations as low as 0.75-1 % w/w in adapalene-TyroSphere formulations, adapalene was physically mixed with freeze dried nanoparticles at a ratio of 1 to 100. As it is shown in Figure 3.9 the characteristic peaks of crystalline adapalene at 15, 16.5, 22.5, and 25

(2θ), which are absent in adapalene-TyroSpheres XRD pattern, can be observed in the physical mixture of adapalene and TyroSpheres.

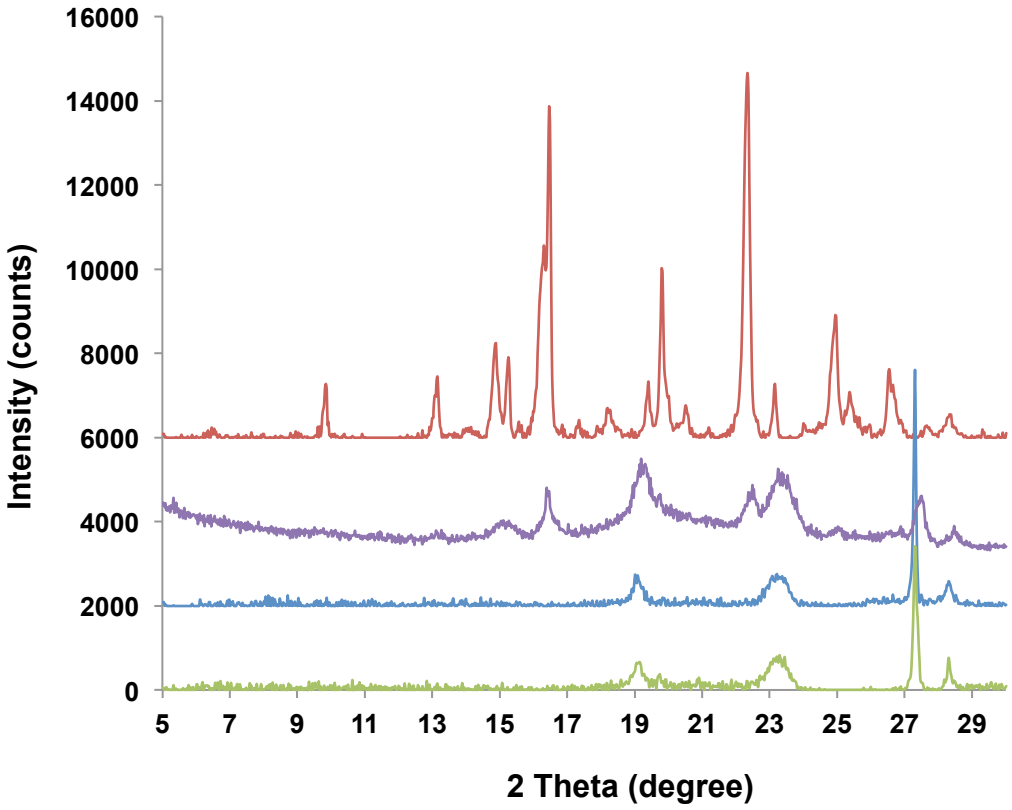

Figure 3.9. X-Ray diffraction analysis of adapalene (red), adapalene physically mixed with TyroSpheres (purple), adapalene loaded in TyroSpheres (blue), and TyroSpheres without drug (green).

In XRD analysis, the disappearance of characteristic diffraction peaks of adapalene confirms its encapsulation in TyroSpheres. A similar phenomenon has been reported in the literature with adapalene or other actives entrapped in nanoparticles.[16, 32] This could be due to the formation of an amorphous complex of API in polymeric nanocarrier matrix. Another possible scenario explaining this observation is that

encapsulated API exists as very small nanocrystals and does not scatter X-rays efficiently.[33]

3.3.4. Evaluation of adapalene-TyroSpheres for topical delivery

3.3.4.1. Adapalene partitioning into stratum corneum and sebum

To evaluate TyroSpheres' applicability as a drug carrier in acne therapy, adapalene partitioning, release and distribution in the skin compartments were studied. Drug transport through the skin is assumed to occur via two independent pathways: transepidermal and transappendagal (mainly hair follicles). Therefore, total flux (J_{total}) is the sum of flux through SC (J_{SC}) and through hair follicles (J_{sebum}).[34] In the following equation, A_{sebum} and A_{sc} are the actual areas of follicular and transepidermal routes; D_{sebum} and D_{sc} are the drug's diffusion coefficients through sebum and SC; K_{sebum} and K_{sc} are the partition coefficient values of the drug in sebum/water and SC/water; C is concentration of the drug in the formulation; while h_{sebum} and h_{sc}, are thicknesses of sebum and SC, respectively.

$$J_{total} = [A_{sebum} \frac{D_{sebum}\, K_{sebum}\, C}{h_{sebum}} + A_{SC} \frac{D_{SC}\, K_{SC}\, C}{h_{SC}}]$$

According to Valiveti et al.[27], the greatest variability among compounds' flux transport is generated from differences in partition coefficients. When $K_{sebum} \gg K_{sc}$, then $J_{sebum} \gg J_{SC}$ and the compound is more likely to transport through pilosebaceous unit. In our study, we analyzed adapalene partitioning from TyroSphere aqueous dispersion into

SC and artificial human sebum, respectively. Following 15 h incubation, K_{sebum} and K_{SC} were calculated as 39.5± 7.1 and 18.6±1.5, respectively. Since adapalene has a very high logP, it tends to partition between the lipophilic cores of nanoparticles and the lipophilic medium (SC or sebum). As the follicular cavity is filled with sebum, it is essential for a successful follicular delivery that the drug is able to adequately partition from the vehicle into sebum. This significantly higher value for K_{sebum} than K_{SC} ($p<0.01$) indicates that our system is an appropriate candidate for follicular delivery. On the other hand, the density of hair follicles varies in different parts of human skin. The scalp and face have the highest occupancy of hair follicles (up to 10% of the total skin area).[35] For an anti-comedolytic agent like adapalene, the face is the main application site; thus, the follicular pathway can play an important role in the topical delivery of this drug.

3.3.4.2. Adapalene release from TyroSpheres and diffusion through stratum corneum

The ability of a carrier to release the drug is very important and is usually measured *in vitro* using a semi-permeable membrane in an aqueous environment. However, this method for drug release studies cannot predict the behavior of nanocarriers in contact with human sebum and SC. The rate of drug release can drastically change due to the increased lipophilicity of the surrounding environment. In case of a hydrophobic drug, faster drug release can be expected when nanocarriers contact a lipophilic environment (SC or sebum). In our case, since adapalene is highly lipophilic, analyzing the drug release in aqueous environments was not useful. During the 72 h study, we realized that adapalene is released from TyroSpheres and precipitates on the cellulose

membrane. No drug was detected in the release compartment (1% or 10% Tween in PBS). Adapalene micron-sized crystals, which do not normally exist in adapalene-TyroSphere formulations, were observed on the dialysis membrane and visualized by fluorescence microscopy. (Figure 3.10)

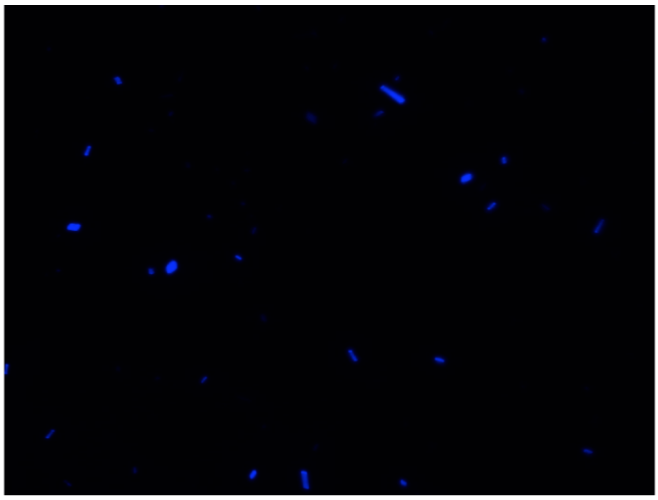

Figure 3.10. Fluorescent image taken from the dialysis membrane following 72 h release study. The blue particles are adapalene crystals that are formed from the portion of the drug released from TyroSpheres.

For a better understanding of the release behavior of adapalene from TyroSpheres while mimicking cutaneous conditions, we studied drug release and diffusion through SC. DMF was added to the receptor compartment (20 vol% in PBS) to provide a sink condition and also an adequate driving force for the released drug to diffuse across the SC. Minimal change in particle size of TyroSphere dispersion —applied in the donor compartment— after the majority of the loaded drug was released, assured that DMF diffusion to the donor compartment was negligible. Therefore, the drug release did not occur due to dissociation and degradation of the nanoparticles and adapalene detected in the receptor compartment is the portion of drug released from TyroSpheres and diffused

across the SC. Sustained release of adapalene through SC was recorded. The data was fit to Higuchi square root model, where the cumulative drug release has a linear correlation with root of time (R^2=0.99) (Figure 3.11). This indicates that the drug release from TyroSpheres is diffusion controlled. The diffusion flux across SC was determined as 1.4 μg/cm^2/h.

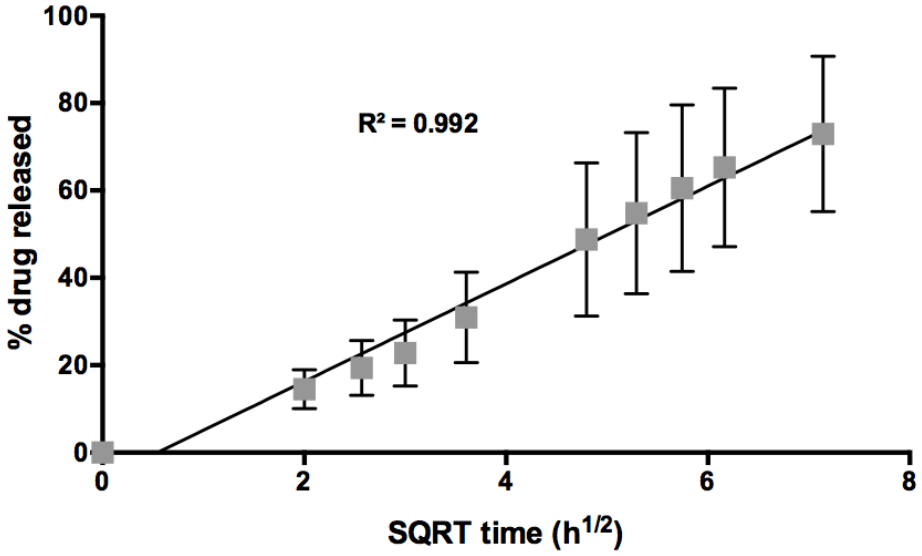

Figure 3.11. Release of adapalene from TyroSpheres and diffusion across stratum corneum as a function of square root (SQRT) of time. Results are shown as mean ± SD (n=5).

3.3.4.3. Skin distribution study on human cadaver skin

The ability of TyroSpheres to deliver adapalene to human cadaver skin was evaluated and compared with the adapalene marketed product (Differin®). The permeation results are provided in Figure 3.12. TyroSpheres could deliver higher amounts of adapalene to the epidermis compared to Differin® (p<0.05). Delivery to the dermis was minimal and the drug was not detected in the receptor compartment; this

outcome was expected due to high octanol/water partition coefficient of adapalene. The mass balance recovery was 85-95%.

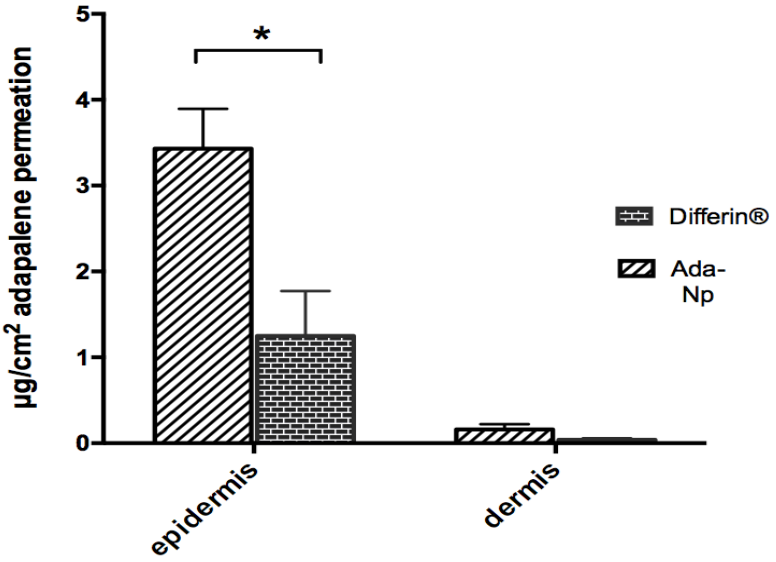

Figure 3.12. Skin distribution of adapalene-TyroSpheres Ada-NP-1 (see Table 3.6) and Differin® in human cadaver skin. The statistical data is expressed as mean ± SE (n = 6), * $P<0.05$ from Student t-test.

3.3.4.4. Skin distribution study on pig ear skin (evaluating the follicular delivery of adapalene)

In order to investigate applicability of TyroSpheres for follicular delivery, adapalene-TyroSphere formulation was applied on pig ear skin. Pig ear skin has similar follicular structures to human skin[36], but with higher follicular density than many areas in human. This makes it more practical to use pig ear skin for *ex vivo* follicular penetration studies. As opposed to excised human skin, excised porcine ear tissue connected to the cartilage does not contract; therefore, its hair follicles better resemble the *in vivo* conditions.[37] In a study by Raber et al.[38] porcine ear skin was found to be a suitable

surrogate for *in vivo* conditions in humans when assessing nanoparticle accumulation in hair follicles. Adapalene inherent fluorescent properties (emission wavelength = 428 nm) allowed visualization of the drug distribution in the pig ear skin layers including the hair follicles. Images taken from surface of the skin clearly showed accumulation of adapalene in the hair follicle openings (Figure 3.13.A). Fluorescent images from cross sections of pig skin samples treated with adapalene-TyroSpheres confirmed the presence of the drug in the hair follicles, as well as upper epidermal layers 12 h after skin application (Figure 3.13.B).

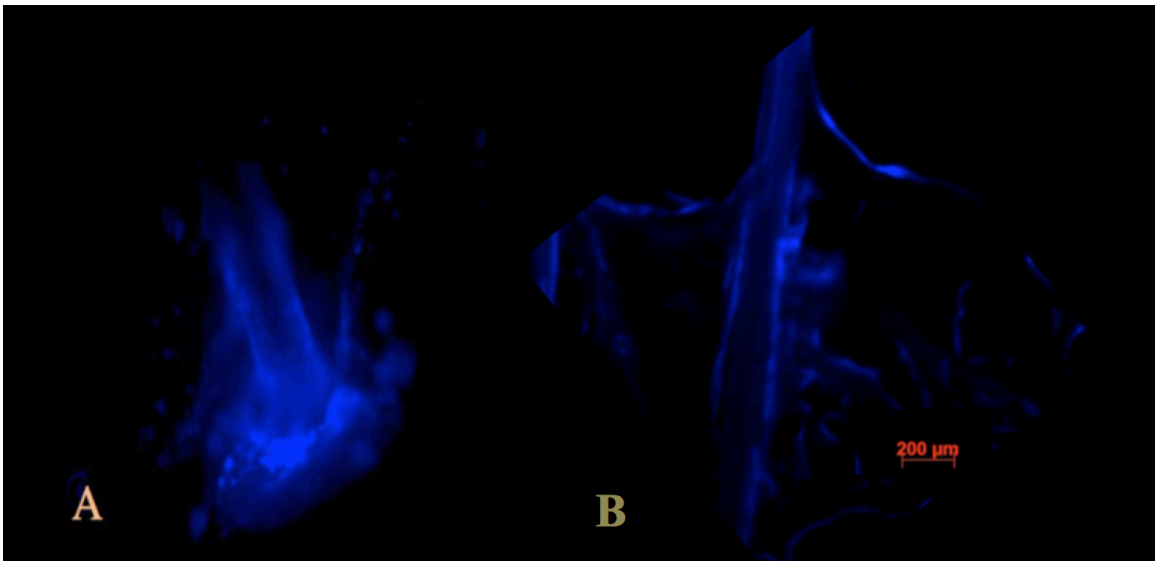

Figure 3.13. Adapalene localization within the hair follicles and epidermis. Fluorescent images taken from A) the surface, B) vertical section of porcine ear skin treated with adapalene-TyroSpheres. Adapalene, showing blue fluorescence, is distributed in follicular epithelium, hair follicle and stratum corneum.

Another approach to study follicular penetration is via cyanoacrylate surface biopsy. This technique has been reported in literature to assess qualitative and quantitative drug delivery to the pilosebaceous unit.[18,29] Following 12 h application of the adapalene formulations on porcine ear skin, adapalene extracted from combined 25 tape

stripped per samples were considered as drug delivered to SC. Adapalene extracted from cyanoacrylate skin biopsies represented drug delivery to follicular cavity, and drug extracted from the remaining skin shows drug permeation to viable epidermis and lower layers of skin (Figure 3.14). As shown in Figure 3.10, adapalene accumulation in the hair follicles during 12 h exposure was 288±60 and 185±66 ng/cm^2, for skin specimens treated with adapalene-TyroSphere and Differin®, respectively. In literature, various values are reported for hair follicle density in the pig ear. Hair follicle density varies based on the breed and age of the pigs. Following microscopic evaluation of the porcine ear skin used in our experiment, the average hair follicle density and follicular diameter was found to be 40/cm^2 and 150 μm respectively. As a result, adapalene delivery to the hair follicles by TyroSphere and Differin® was calculated as 51.5±10.8 and 33.0±11.8 μg/mm^2 follicular area. Thus, TyroSphere formulation significantly enhanced drug delivery to the follicular cast, which is in agreement with our findings from fluorescent analysis.

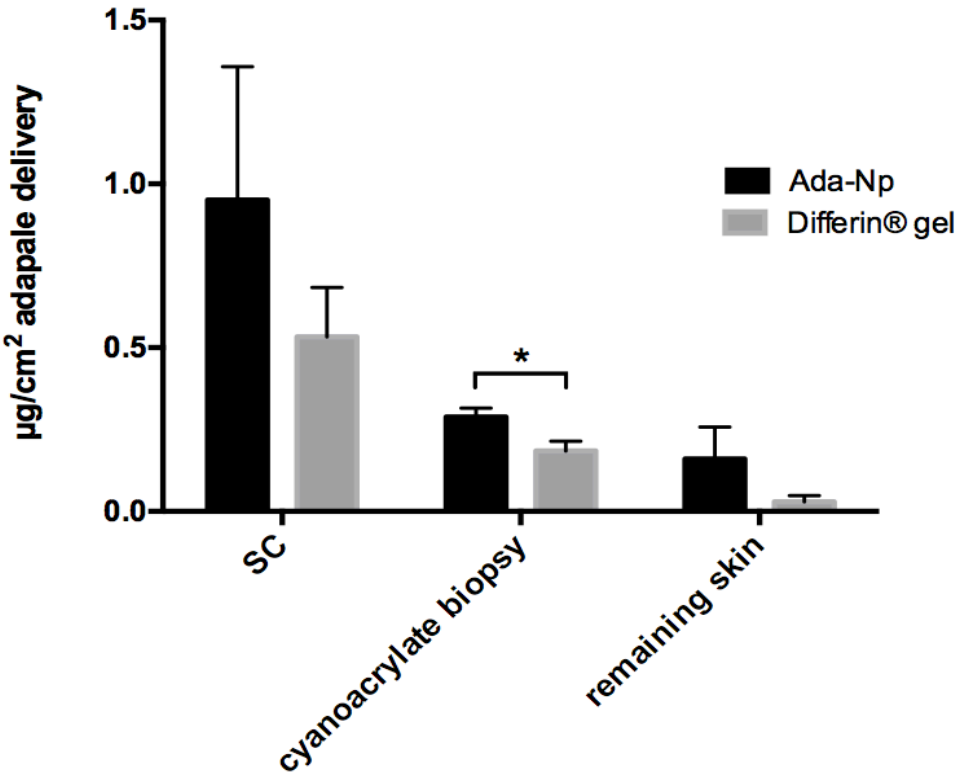

Figure 3.14. Distribution of adapalene from Differin® and adapalene-TyroSphere (Ada-Np) formulations in stratum corneum (SC), hair follicles and the remaining skin after differential tape stripping. Results are shown as mean ± SE (n = 5), * $P<0.05$ from Wilcoxon signed-rank test.

The role of TyroSpheres in follicular delivery is attributed to their small particle size. The mechanism of nanoparticles penetration into hair follicles has been explained via the "geared pump" effect of hair shaft.[39] Massaging the formulation following topical application on the skin has been proposed to mimic hair movement and geared pump effect in *ex vivo* conditions.[40] Thus, we included mechanical massaging in our experimental protocol. Generally, the mechanism for penetration enhancement of intact polymeric nanoparticles is their ability to penetrate into the superficial layers of the SC, where the encapsulated drug will be released into the deeper skin layers.[41] We believe that this mechanism and the accumulation of TyroSpheres in the hair follicles are the

main reasons for enhancing topical delivery of adapalene as compared to the commercial product.

3.3.5. Irritation study of adapalene formulation

The most frequent side effect of topical retinoids is known as the "retinoid reaction", which is characterized by pruritus, peeling, burning, and redness in the site of application and peaks within the first few weeks of the treatment. This phenomenon is due to the free carboxylic acid in the structure of retinoids and occurs more with application of tretinoin and tazarotene than with adapalene. Release of pro-inflammatory cytokines such as IL-1α, IL-6, TNF-α, and IL-8 in is known to initiate this retinoid reaction.[14, 42]

We first tested the *in vitro* irritation of adapalene formulations using 2D irritation model based on an immortalized human keratinocyte line, HaCaT. Figure 3.15.A shows the metabolic activity of HaCaTs (obtained from AlamarBlue® assay) that were exposed to 0.5-10 μg/mL adapalene in different formulations.

Clearly, the metabolic activity of HaCaTs decreased when the cells were treated with a higher dose of adapalene in all the formulations. It is noteworthy that under the same adapalene content, the cells treated with adapalene-TyroSpheres had significantly higher metabolic activity than groups treated with the formulations based on adapalene solution and the Differin® ($p<0.05$). The vehicles and solvent used to prepare adapalene-TyroSpheres and adapalene solution were also tested separately and they did not affect cell metabolic activity (Figure 3.15.B). The results on this 2D model demonstrated that

adapalene encapsulation in TyroSpheres significantly decreased the drug's irritation potential.

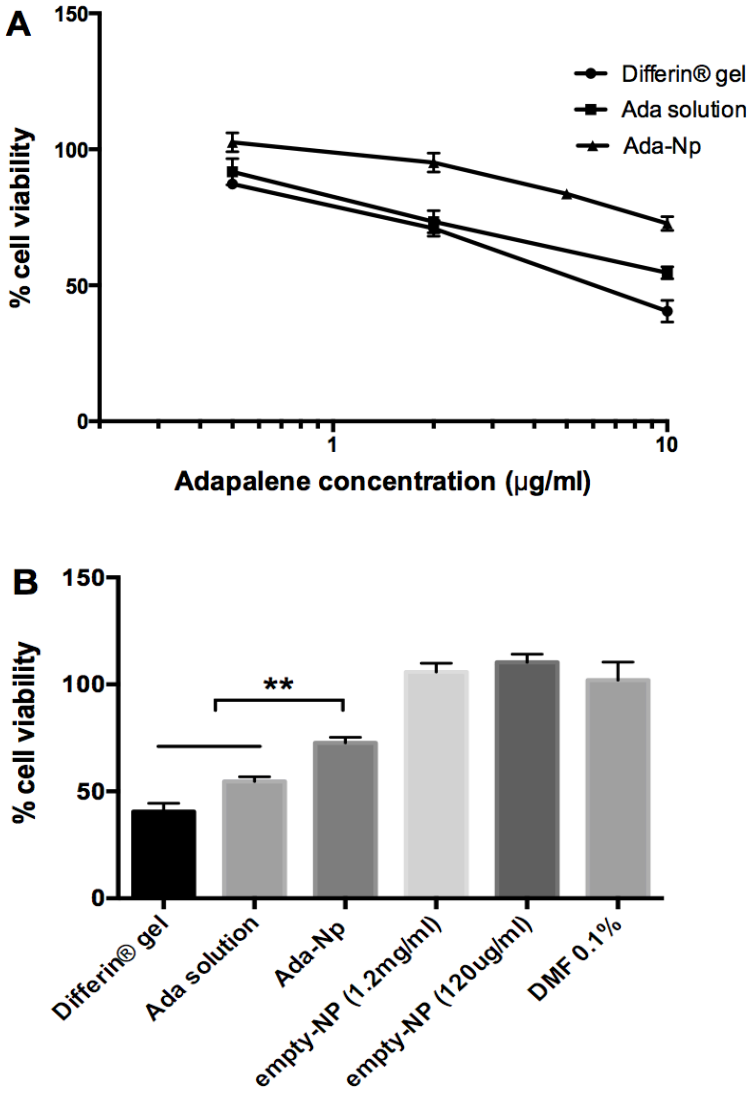

Figure 3.15. Results of skin irritation study on HaCaTs**.**
A) % Cell viability of HaCaTs treated with different content of adapalene in TyroSpheres (Ada-Np), Differin® and solution form. Under the same adapalene concentrations, the cells treated with adapalene-TyroSpheres had highest cell viability comparing to the ones treated with Differin® ($P<0.05$).
B) % Cell viability of HaCaTs treated with 10 µg/mL adapalene in different vehicles, TyroSpheres without drug (empty-Np), and 0.1% DMF in PBS. Data are shown as mean ± SE (n = 8), ** $P<0.01$ determined by one-way ANOVA followed by Tukey's post hoc test.

We also employed a 3D model to evaluate the irritation potential of adapalene formulations. Based on MTT tissue viability assay performed on EpiDerm™ treated with the adapalene formulations, both Differin® and TyroSphere formulations were found to be not irritant. Remarkably, 24 h application of adapalene-TyroSpheres resulted in higher tissue viability (Figure 3.16) and less secretion of IL-1α (Figure 3.17) and IL-8 (Figure 3.18) compared to treatment with Differin®. There was no significant difference in release of pro-inflammatory cytokines from EpiDerm™ treated with adapalene-TyroSphere and negative control (PBS). Therefore, TyroSphere formulation of adapalene was associated with less dermal irritation compared to the commercial gel. This can be attributed to controlled release of the drug from nanoparticles, which prevents direct contact of all dose of adapalene with the skin cells. Moreover, potentially irritant ingredients, such as alcohol and chemical penetration enhancers, which exist in Differin® are not present in adapalene-TyroSpheres. Similar observations have been reported in the literature, where irritation-inducing drugs such as retinoic acid were encapsulated in particulate systems.[43,44]

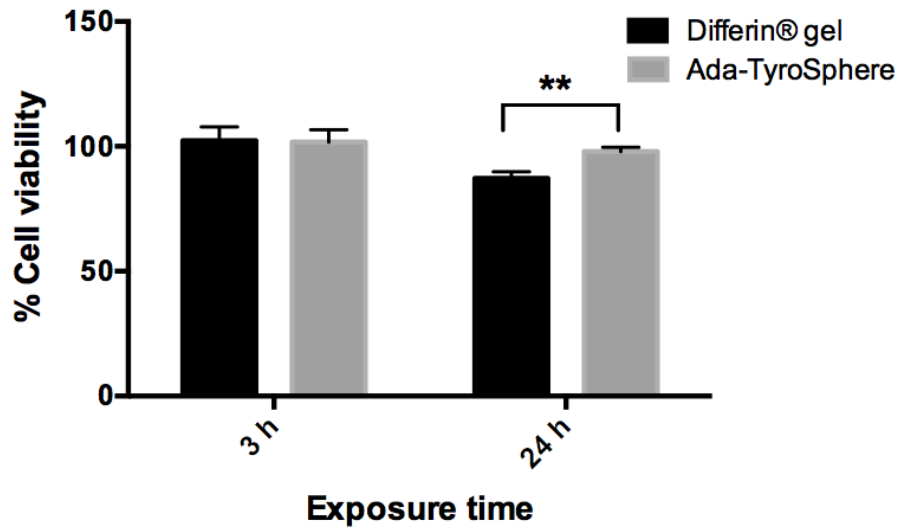

Figure 3.16. Percentage tissue viability of EpiDerm™, treated with adapalene-TyroSpheres, and Differin® for 3 and 24 h obtained from MTT assay. Data are shown as mean ± SE, ** P<0.01 from Student t-test.

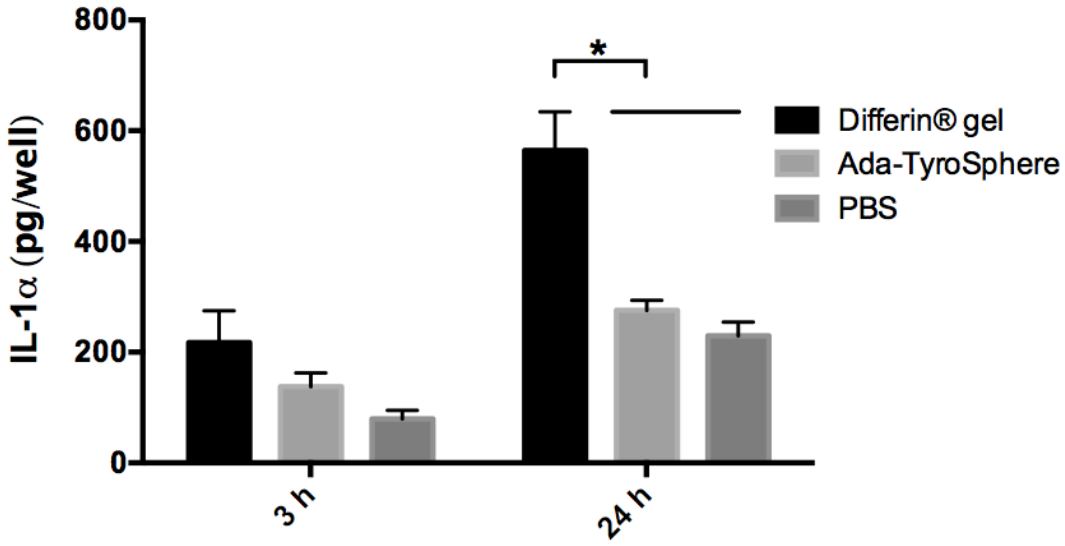

Figure 3.17. Release of IL-1α from EpiDerm™ treated with adapalene-TyroSpheres, Differin®, and phosphate buffered saline (PBS) for 3 and 24 h. Data are shown as mean ± SE, * P<0.05 determined by one-way ANOVA followed by Tukey's post hoc test. The data on interleukin release are representative of two independent ELISA assays for each cytokine.

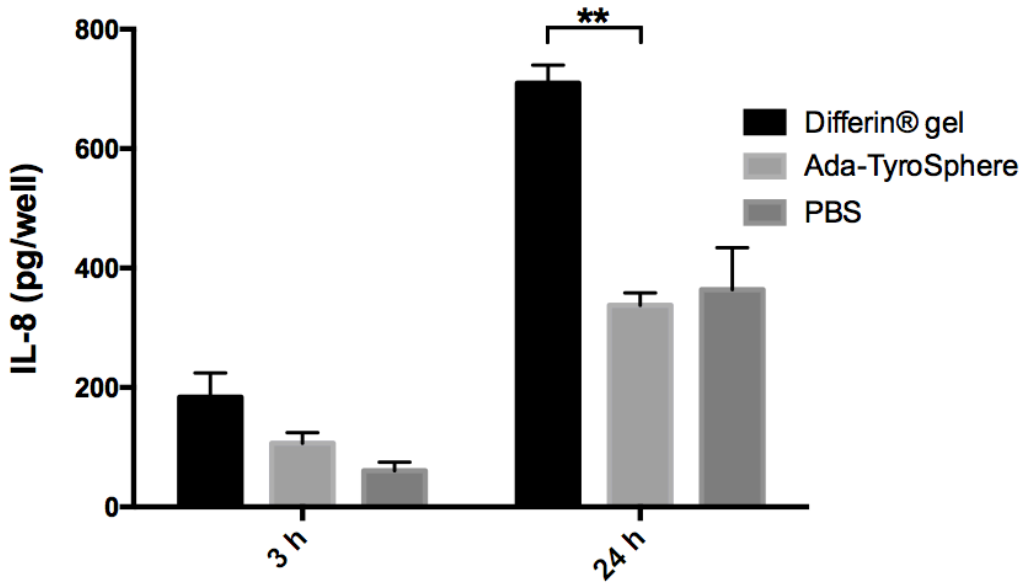

Figure 3.18. Release of IL-8 from EpiDerm™ treated with adapalene-TyroSpheres, Differin®, and phosphate buffered saline (PBS) for 3 and 24 h. Data are shown as mean ± SE, ** $P<0.01$ determined by one-way ANOVA followed by Tukey's post hoc test. The data on interleukin release are representative of two independent ELISA assays for each cytokine.

3.4. Conclusions

TyroSphere formulations with less drug content than the marketed product were able to deliver comparable amount of adapalene to the epidermis and hair follicles. There are several possible reasons for the cutaneous penetration enhancement effect that was observed with TyroSpheres: accumulation of nanoparticles in skin appendages, decreased crystallinity of the active in TyroSphere formulation, and/or providing higher concentration gradient by increasing apparent solubility and thermodynamic activity of the drug molecules loaded in nanoparticles. Small particle size and deformability of TyroSpheres in addition to good partitioning of adapalene in human sebum contribute to the targeted adapalene delivery to the hair follicles, where acne originates. These nanocarriers were also found to decrease irritation potential of the retinoid in *In vitro*

models. Therefore, adapalene-TyroSpheres represent an innovative alternative approach for topical treatment of early stages of acne. Nevertheless, further studies are needed to examine therapeutic efficacy of this formulation in clinical acne models.

3.5. References

1. Schaefer, H.; Zesch, A.; Stättgen, G., *Skin permeability*. Springer: 1982.
2. Agarwal, R.; Katare, O. P.; Vyas, S. P., The pilosebaceous unit: a pivotal route for topical drug delivery. *Methods and findings in experimental and clinical pharmacology* 2000, *22* (2), 129-33.
3. Vogt, A.; Combadiere, B.; Hadam, S.; Stieler, K. M.; Lademann, J.; Schaefer, H.; Autran, B.; Sterry, W.; Blume-Peytavi, U., 40 nm, but not 750 or 1,500 nm, nanoparticles enter epidermal CD1a+ cells after transcutaneous application on human skin. *The Journal of investigative dermatology* 2006, *126* (6), 1316-22.
4. Prow, T. W.; Grice, J. E.; Lin, L. L.; Faye, R.; Butler, M.; Becker, W.; Wurm, E. M.; Yoong, C.; Robertson, T. A.; Soyer, H. P.; Roberts, M. S., Nanoparticles and microparticles for skin drug delivery. *Adv Drug Deliv Rev* 2011, *63* (6), 470-91.
5. Glowka, E.; Wosicka-Frackowiak, H.; Hyla, K.; Stefanowska, J.; Jastrzebska, K.; Klapiszewski, L.; Jesionowski, T.; Cal, K., Polymeric nanoparticles-embedded organogel for roxithromycin delivery to hair follicles. *European journal of pharmaceutics and biopharmaceutics : official journal of Arbeitsgemeinschaft fur Pharmazeutische Verfahrenstechnik e.V* 2014, *88* (1), 75-84.
6. Ourique, A. F.; Pohlmann, A. R.; Guterres, S. S.; Beck, R. C., Tretinoin-loaded nanocapsules: Preparation, physicochemical characterization, and photostability study. *International journal of pharmaceutics* 2008, *352* (1-2), 1-4.
7. Luengo, J.; Weiss, B.; Schneider, M.; Ehlers, A.; Stracke, F.; Konig, K.; Kostka, K. H.; Lehr, C. M.; Schaefer, U. F., Influence of nanoencapsulation on human skin transport of flufenamic acid. *Skin pharmacology and physiology* 2006, *19* (4), 190-7.
8. Wang, W.; Cheng, D.; Gong, F.; Miao, X.; Shuai, X., Design of multifunctional micelle for tumor-targeted intracellular drug release and fluorescent imaging. *Advanced materials* 2012, *24* (1), 115-20.
9. Kilfoyle, B. E.; Sheihet, L.; Zhang, Z.; Laohoo, M.; Kohn, J.; Michniak-Kohn, B. B., Development of paclitaxel-TyroSpheres for topical skin treatment. *J Control Release* 2012, *163* (1), 18-24.
10. Alvarez-Roman, R.; Naik, A.; Kalia, Y. N.; Guy, R. H.; Fessi, H., Skin penetration and distribution of polymeric nanoparticles. *J Control Release* 2004, *99* (1), 53-62.
11. Mittal, A.; Schulze, K.; Ebensen, T.; Weissmann, S.; Hansen, S.; Guzman, C. A.; Lehr, C. M., Inverse micellar sugar glass (IMSG) nanoparticles for transfollicular vaccination. *Journal of controlled release : official journal of the Controlled Release Society* 2015, *206*, 140-152.

12. Greenman, J., Follicular pH and the development of acne. *Int J Dermatol* 1981, *20* (10), 656-8.
13. Zouboulis, C. C., Acne and sebaceous gland function. *Clin Dermatol* 2004, *22* (5), 360-6.
14. Mukherjee, S.; Date, A.; Patravale, V.; Korting, H. C.; Roeder, A.; Weindl, G., Retinoids in the treatment of skin aging: an overview of clinical efficacy and safety. *Clin Interv Aging* 2006, *1* (4), 327-48.
15. Waugh, J.; Noble, S.; Scott, L. J., Adapalene: a review of its use in the treatment of acne vulgaris. *Drugs* 2004, *64* (13), 1465-78.
16. Guo, C.; Khengar, R. H.; Sun, M.; Wang, Z.; Fan, A.; Zhao, Y., Acid-responsive polymeric nanocarriers for topical adapalene delivery. *Pharmaceutical research* 2014, *31* (11), 3051-9.
17. Rao, G. R.; Ghosh, S.; Dhurat, R.; Sharma, A.; Dongre, P.; Baliga, V. P., Efficacy, safety, and tolerability of microsphere adapalene vs. conventional adapalene for acne vulgaris. *International journal of dermatology* 2009, *48* (12), 1360-5.
18. Bhatia, G.; Zhou, Y.; Banga, A. K., Adapalene microemulsion for transfollicular drug delivery. *J Pharm Sci* 2013, *102* (8), 2622-31.
19. Harde, H.; Agrawal, A. K.; Katariya, M.; Kale, D.; Jain, S., Development of a topical adapalene-solid lipid nanoparticle loaded gel with enhanced efficacy and improved skin tolerability. *Rsc Adv* 2015, *5* (55), 43917-43929.
20. Van de Sandt, J.; Roguet, R.; Cohen, C.; Esdaile, D.; Ponec, M.; Corsini, E.; Barker, C.; Fusenig, N.; Liebsch, M.; Benford, D., The use of human keratinocytes and human skin models for predicting skin irritation. *ATLA-NOTTINGHAM-* 1999, *27*, 723-744.
21. Spielmann, H.; Hoffmann, S.; Liebsch, M.; Botham, P.; Fentem, J. H.; Eskes, C.; Roguet, R.; Cotovio, J.; Cole, T.; Worth, A.; Heylings, J.; Jones, P.; Robles, C.; Kandarova, H.; Gamer, A.; Remmele, M.; Curren, R.; Raabe, H.; Cockshott, A.; Gerner, I.; Zuang, V., The ECVAM international validation study on in vitro tests for acute skin irritation: report on the validity of the EPISKIN and EpiDerm assays and on the Skin Integrity Function Test. *Alternatives to laboratory animals : ATLA* 2007, *35* (6), 559-601.
22. Sheihet, L.; Dubin, R. A.; Devore, D.; Kohn, J., Hydrophobic drug delivery by self-assembling triblock copolymer-derived nanospheres. *Biomacromolecules* 2005, *6* (5), 2726-31.
23. Sheihet, L.; Piotrowska, K.; Dubin, R. A.; Kohn, J.; Devore, D., Effect of tyrosine-derived triblock copolymer compositions on nanosphere self-assembly and drug delivery. *Biomacromolecules* 2007, *8* (3), 998-1003.
24. Batheja, P.; Sheihet, L.; Kohn, J.; Singer, A. J.; Michniak-Kohn, B., Topical drug delivery by a polymeric nanosphere gel: Formulation optimization and in vitro and in vivo skin distribution studies. *J Control Release* 2011, *149* (2), 159-67.
25. Pochi, P. E.; Strauss, J. S., Sebaceous gland inhibition from combined glucocorticoid-estrogen treatment. *Archives of dermatology* 1976, *112* (8), 1108-9.
26. Nordstrom, K. M.; Labows, J. N.; McGinley, K. J.; Leyden, J. J., Characterization of wax esters, triglycerides, and free fatty acids of follicular casts. *Journal of investigative dermatology* 1986, *86* (6), 700-705.
27. Valiveti, S.; Wesley, J.; Lu, G. W., Investigation of drug partition property in artificial sebum. *International journal of pharmaceutics* 2008, *346* (1-2), 10-6.

28. Kligman, A. M.; Christophers, E., Preparation of isolated sheets of human stratum corneum. *Archives of dermatology* 1963, *88* (6), 702-705.
29. Teichmann, A.; Jacobi, U.; Ossadnik, M.; Richter, H.; Koch, S.; Sterry, W.; Lademann, J., Differential stripping: determination of the amount of topically applied substances penetrated into the hair follicles. *The Journal of investigative dermatology* 2005, *125* (2), 264-9.
30. Costache, A. D.; Sheihet, L.; Zaveri, K.; Knight, D. D.; Kohn, J., Polymer-drug interactions in tyrosine-derived triblock copolymer nanospheres: a computational modeling approach. *Mol Pharm* 2009, *6* (5), 1620-7.
31. Lauterbach, A.; Mueller-Goymann, C. C., Development, formulation, and characterization of an adapalene-loaded solid lipid microparticle dispersion for follicular penetration. *Int J Pharm* 2014, *466* (1-2), 122-32.
32. Shaikh, J.; Ankola, D. D.; Beniwal, V.; Singh, D.; Kumar, M. N., Nanoparticle encapsulation improves oral bioavailability of curcumin by at least 9-fold when compared to curcumin administered with piperine as absorption enhancer. *European journal of pharmaceutical sciences : official journal of the European Federation for Pharmaceutical Sciences* 2009, *37* (3-4), 223-30.
33. Goyal, R.; Macri, L.; Kohn, J., Formulation Strategy for the Delivery of Cyclosporine A: Comparison of Two Polymeric Nanospheres. *Scientific Reports* 2015, *5*.
34. Roy, S. D.; Flynn, G. L., Transdermal delivery of narcotic analgesics: pH, anatomical, and subject influences on cutaneous permeability of fentanyl and sufentanil. *Pharmaceutical research* 1990, *7* (8), 842-7.
35. Rancan, F.; Afraz, Z.; Combadiere, B.; Blume-Peytavi, U.; Vogt, A., Hair Follicle Targeting with Nanoparticles. In *Nanotechnology in Dermatology*, Springer: 2013; pp 95-107.
36. Jacobi, U.; Kaiser, M.; Toll, R.; Mangelsdorf, S.; Audring, H.; Otberg, N.; Sterry, W.; Lademann, J., Porcine ear skin: an in vitro model for human skin. *Skin research and technology : official journal of International Society for Bioengineering and the Skin* 2007, *13* (1), 19-24.
37. Lademann, J.; Richter, H.; Meinke, M.; Sterry, W.; Patzelt, A., Which skin model is the most appropriate for the investigation of topically applied substances into the hair follicles? *Skin pharmacology and physiology* 2010, *23* (1), 47-52.
38. Raber, A. S.; Mittal, A.; Schafer, J.; Bakowsky, U.; Reichrath, J.; Vogt, T.; Schaefer, U. F.; Hansen, S.; Lehr, C. M., Quantification of nanoparticle uptake into hair follicles in pig ear and human forearm. *Journal of controlled release : official journal of the Controlled Release Society* 2014, *179*, 25-32.
39. Lademann, J.; Richter, H.; Schaefer, U. F.; Blume-Peytavi, U.; Teichmann, A.; Otberg, N.; Sterry, W., Hair follicles - a long-term reservoir for drug delivery. *Skin pharmacology and physiology* 2006, *19* (4), 232-6.
40. Lademann, J.; Richter, H.; Teichmann, A.; Otberg, N.; Blume-Peytavi, U.; Luengo, J.; Weiss, B.; Schaefer, U. F.; Lehr, C. M.; Wepf, R.; Sterry, W., Nanoparticles--an efficient carrier for drug delivery into the hair follicles. *European journal of pharmaceutics and biopharmaceutics : official journal of Arbeitsgemeinschaft fur Pharmazeutische Verfahrenstechnik e.V* 2007, *66* (2), 159-64.

41. Desai, P.; Patlolla, R. R.; Singh, M., Interaction of nanoparticles and cell-penetrating peptides with skin for transdermal drug delivery. *Mol Membr Biol* 2010, *27* (7), 247-59.
42. Orfanos, C. E.; Zouboulis, C. C.; Almond-Roesler, B.; Geilen, C. C., Current use and future potential role of retinoids in dermatology. *Drugs* 1997, *53* (3), 358-88.
43. Castro, G. A.; Oliveira, C. A.; Mahecha, G. A.; Ferreira, L. A., Comedolytic effect and reduced skin irritation of a new formulation of all-trans retinoic acid-loaded solid lipid nanoparticles for topical treatment of acne. *Archives of dermatological research* 2011, *303* (7), 513-20.
44. Castro, G. A.; Coelho, A. L.; Oliveira, C. A.; Mahecha, G. A.; Orefice, R. L.; Ferreira, L. A., Formation of ion pairing as an alternative to improve encapsulation and stability and to reduce skin irritation of retinoic acid loaded in solid lipid nanoparticles. *International journal of pharmaceutics* 2009, *381* (1), 77-83.

Chapter 4: Development and characterization of a topical gel formulation of adapalene-TyroSpheres and its clinical efficacy assessment

4.1. Introduction

Acne is a chronic inflammatory disorder involving the pilosebaceous unit and it is one of the most common skin diseases in the young population. It is associated with altered keratinization, increased sebum production, inflammation, bacterial colonization in the hair follicles, and immunological host reactions. The early and non-inflammatory stage of the acne usually features comedones, where the abnormal desquamation of follicular epithelium, increased cohesiveness of corneocytes, and androgen-driven activation of sebum secretion can occur. As a result the follicular orifice is partially or completely clogged with excess keratin and dead cells and the drainage of sebum to the surface of the skin is obstructed.[1-2]

Topical medications are preferred in the treatment of mild to moderate acne.[3] Retinoids are vitamin A derivatives and are used in first-line topical therapy of the comedonal acne.[3] They influence keratinocyte differentiation through their interaction with retinoic acid nuclear receptors (RARs) that activate genes responsible for cellular differentiation, which results in decreased microcomedone formation.[4] Adapalene is a third generation retinoid with anti-inflammatory, keratolytic and anti-seborrheic effects. Adapalene's challenging properties (pKa=4.23, logP=8.04, from SciFinder database) limit its local bioavailability. Erythema, dryness, and scaling have been reported with

commercial adapalene formulations.[5] These topical adverse effects may be derived from the active ingredient as well as other ingredients in the formulation (e.g. alcohol or chemical penetration enhancers).

In the previous chapter, we showed that TyroSpheres effectively encapsulated adapalene and substantially enhanced its aqueous solubility, while decreasing the crystallinity of the drug in the formulation. Skin distribution of adapalene via TyroSphere formulation was evaluated *ex vivo* using human cadaver and porcine ear skin and this was compared with the commercial adapalene formulation, Differin®. Sustained drug release across stratum corneum in 51 h was observed from the TyroSphere liquid dispersion. Additionally, *in vitro* skin irritation studies demonstrated that encapsulation of adapalene in TyroSpheres significantly reduced the irritancy of the drug to monolayer HaCaTs and reconstituted human epidermis (EpiDerm™, MatTek Corp.). Adapalene-TyroSphere aqueous suspension, have the flow properties and viscosity very similar to that of water and thus it is not ideal for topical administration. This has been addressed in the previous studies and several pharmaceutically acceptable thickening agents, such as Carbopol and hydroxypropyl methylcellulose (HPMC) were used to prepare viscous formulations for TyroSpheres.[6-7] The gel system not only can serve as a stabilizer, but can also form a uniform dispersion of the carriers in the matrix and increase the contact time of the nanoparticles on the skin resulting in enhanced skin penetration of the payload.[6] There are several studies in literature, where hydrophilic gels have been used as an effective and inert environment for drug-loaded nanocarriers including nanospheres[7], nanocapsules[8], liposomes[9], and solid lipid nanoparticles[10].

Two different water-soluble thickening agents that are commonly used in many topical formulations were chosen for this study. Cellulose ether derivatives, such as HPMC and hydroxyethyl cellulose are not only popular in the pharmaceutical industry to make sustained release oral dosage forms (tablets), but are also widely used for thickening topical products and adjusting their rheology.[11-12] Poloxamer 407 is an amphiphilic synthetic copolymer that consists of hydrophobic poly(oxypropylene) block between two hydrophilic poly(oxyethylene) blocks.[13] The aqueous solution of poloxamer 407 shows thermoreversible properties: it is in a fluid state at room temperature and transitions to a gel at temperatures above 30°C (The sol-gel transition temperature decreases with increase in polymer concentration). In Food and Drug Administration (FDA) guidelines, poloxamer 407 is presented as an "inactive" ingredient for the preparation of various dosage forms, including ophthalmic and topical formulations. This copolymer has been shown to stabilize proteins and micro/nanoparticle-based formulations.[14]

The rhino mouse (RH J/LeJ) is a strain of hairless mouse that carries the rh gene (recessive allele of the hairless gene). At around 4 weeks, the coat hair of the mice is irreversibly lost and the upper part of the follicular unit forms epidermal pseudocomedone known as an utriculus or utricle.[15] These utricles (utriculi) become filled with solid impactions of horny cells and sebum and enlarge as the animal ages.[16] At 7-8 weeks, these sebaceous follicles progressively distended due to accumulation of horny material and histologically resemble human microcomedones.[15] Therefore, utriculi reduction assay using the rhino mouse is a well-characterized preclinical model for

evaluation of comedolysis and epithelial differentation[16-17] and can be predictive of retinoid efficacy.[18]

In this chapter we report on the development and characterization of topical gel formulations of adapalene-TyroSpheres. The rheological behavior of the TyroSphere gels was assessed and their potential skin irritation and comedolytic efficacy in comparison with the commercial adapalene gel (Differin®) were studied using the well-established *in vitro* and *in vivo* models.

4.2. Materials and Methods

4.2.1. Materials

Suberic acid (SA), poly(ethylene glycol) monomethyl ether MW 5000 (PEG5K), trifluoroacetic acid (TFA), Tween-80, dimethylformamide (DMF), neutral buffered formalin solution, high viscosity hydroxypropyl methyl cellulose (HV HMPC) viscosity 2,600-5,600 cP, 2% in H2O (20°C), 10% neutral buffered formalin solution, adapalene, and Dulbecco's phosphate buffered saline (PBS) were purchased from Sigma Aldrich (St. Louis, MO). Dulbecco's modified Eagle medium, high glucose (DMEM), gentamycin (50mg/mL), trypsin (0.25% Trypsin-EDTA), fetal bovine serum (FBS), trypsin-EDTA solution, and Dulbecco's phosphate buffered saline without calcium chloride and magnesium chloride (DPBS) were purchased from Life Technologies (Grand Island, NY). HPLC grade water, acetonitrile, and methanol, and the reagents used for tissue dehydration were obtained from Fisher Scientific (Pittsburgh, PA). Uranyl acetate was purchased from Electron Microscopy Sciences (Hatfield, PA). Micronized poloxamer

407 (MP407) was a generous gift from BASF (Florham Park, NJ). EpiDerm™ skin kit, EpiDerm™ culture medium, and MTT assay kit were purchased from MatTek Corporation (Ashland, MA). Rhino mice (male Homozygous, 5-6 weeks old) were obtained from Jackson Laboratory (Bar Harbor, ME). The reagents used for tissue staining were purchased from Biosystems (Buffalo Grove, IL). PEG_{5K}-*b*-oligo(desaminotyrosyl-tyrosine octyl ester suberate)-*b*-PEG_{5K} ((DTO-SA/5K) M_n = 22.9 kDa, Mw = 31.9 kDa, PD = 1.39 obtained from gel permeation chromatography) was synthesized according to previously published and established procedures in the New Jersey Center for Biomaterials and their chemical structure and purity were confirmed by ^{1}H NMR.[19,20]

4.2.2. Preparation of adapalene-TyroSphere gel formulation

ABA triblock copolymers composed of hydrophilic A blocks of poly(ethylene glycol) and hydrophobic B blocks of desaminotyrosyl-tyrosine octyl ester and subaric acid were used for preparation of TyroSpheres. Adapalene loaded-TyroSpheres were prepared by dissolving adapalene and DTO/SA-5K copolymer in DMF. The combination of drug and polymer solution was added dropwise to PBS, pH 7.4 under constant stirring. The nanoparticles were formed and added slight turbidity to PBS. The nanosuspension was filtered using 0.22 μm PVDF filters (Millipore, Ireland) and subjected for ultra-centrifugation (Beckman L8-70M ultracentrifuge, Beckman Coulter, Fullerton, CA) at 65000 rpm (290 000 × g) for 3 h at 18°C. The supernatant was then discarded; the pelleted nanospheres were rinsed and re-suspended in PBS overnight. The viscous formulations were prepared by dissolving the thickening agent in TyroSphere liquid dispersion under constant stirring overnight. The polymers used to form gel-like

formulations of TyroSphere were HV HPMC (at 1.5 and 2% w/w), and MP407 (at 15 and 20% w/w). In case of MP407, the TyroSphere dispersion was cooled down to 4°C before addition of the thickening agent.

4.2.3. Size and morphology of TyroSpheres in the gel formulation

The hydrodynamic diameter and morphology of nanoparticles in gel formulations were determined by transmission electron microscopy (TEM). For sample preparation, small aliquots of 10 times diluted TyroSphere formulations were deposited onto Formvar/Carbon-coated grid and 1% uranyl acetate (Electron Microscopy Sciences, Hatfield, PA) aqueous solution was used for background staining. Electron micrographs were taken on a model JEM 100CX TEM (JEOL Ltd).

4.2.4. Homogeneity analysis

To analyse the content uniformity of adapalene in TyroSphere gel formulations, five samples were taken from each gel. The samples were weighed and then lyophilized. Adapalene in dried samples was extracted with DMF and the amount of drug in each sample (w/w) was quantified using HPLC. The variability of adapalene content in TyroSphere gels were reported as % RSD, % RSD = (mean drug content/standard deviation)×100.

4.2.4.1 Adapalene quantification using an HPLC method

An Agilent 1100 high-performance liquid chromatography (HPLC) system (Agilent Technologies, USA) equipped with a UV/Vis detector and reverse phase column (Promonax Luna 5µm C18(2) ,4.6 × 150 mm) was used for chromatographic separations at 25 °C. A mixture of acetonitrile: water (0.1% TFA) 87:13 (v/v) was applied as the mobile phase with flow rate of 1 mL/min. The detection wavelength was set at 309 nm and injection volume was 20 µL. Standard calibration curve was prepared at adapalene concentrations ranging from 0.1 to 100 µg/mL.

4.2.5. *Ex vivo* skin distribution study using porcine ear skin

An ear was isolated from a Yorkshire pig (3 month old, 38 kg purchased from Barton's West End Farms, Oxford, NJ) and stored in RPMI-1640 medium at 4°C for a few days until use. On the day of study the porcine ear skin connected to the cartilage was cut into smaller pieces (around 4 cm^2), rinsed with PBS, and mounted on vertical Franz diffusion cells with effective diffusion area of 3.14 cm^2. The receptor solution consisted of 1% w/w Tween 80 in PBS (pH 7.4). 250 µL of adapalene-TyroSphere gel formulation made with 15% MP407 or 2% HV HPMC (0.025% w/w), and 100µL of Differin® gel (0.1% w/w), were applied on the pig ear skin topically. The formulations were gently massaged for 3 minutes on the skin using a glass rod. The skin distribution study was carried out for 12 h. The skin specimens that were applied on Franz diffusion cells without treatment were used as control. At the end of the permeation experiment, excess formulation was removed from the pig ear skin, the surface was rinsed with PBS,

dried with a cotton swab and subsequently subjected to fluorescence imaging or tape stripping.

4.2.5.1. Fluorescent imaging of skin

To visualize depth of drug penetration, skin pieces were frozen over dry ice, and then cut into smaller strips and embedded in Optimal Cutting Temperature (OCT) medium. Vertical cross-sections (15 μm) of the skin were prepared with a cryostat (Leica Cryostat CM 3050S, Wetzlar, Germany) and collected on glass slides. The samples were then subjected to fluorescence and phase-contrast microscopy using a Zeiss microscope.

4.2.5.2. Tape stripping of the skin

Following termination of the permeation study and rinsing the surface of the skin, the effective area was subjected to tape stripping. A total of 25 rounds of tape stripping were applied to remove the SC layer using adhesive 3M-Scotch® tapes (St. Paul, MN). A roller was used to stretch the skin gently to avoid generation of wrinkles. The tape strips were collected with forceps and pooled together in a 50 ml centrifuge tube. To quantify adapalene delivery to SC, drug was extracted from the tapes using DMF and 1 h bath sonication. Then all samples were analyzed using HPLC.

4.2.6. Rheological Characteristics

Rheological measurements were performed on the TyroSphere gel formulations and Differin® gel using a Kinexus rheometer (Malvern, Worcestershire, UK) equipped

with a parallel plate temperature control geometry (diameter: 40 mm, gap: 1 mm). TyroSphere viscous formulations were prepared from HV HPMC (1.5 and 2 wt%) and MP407 (15 and 20 wt%) and stored at room temperature for 24-48 h before the study. The samples were equilibrated on the plate for 5 min to reach the running temperature before each measurement. All the rheological studies were performed in triplicate.

4.2.6.1. Oscillation test

The frequency sweep test was performed with constant shear stress of 0.1 at 25 and 32 °C (temperature of the surface of the skin). Rheological test parameters, including storage/elasticity (G') and loss/viscosity (G'') moduli, were obtained over non-destructive frequency range of 0.628-62.8 rad/s.

4.2.6.2. Strain sweep test

The strain sweep test was conducted to determine linear viscoelastic regime of the formulations. The test was run at a constant frequency of 1 rad/s with % shear stress ranging from 0.01 to 10.

4.2.6.3. Temperature sweep test

Shear viscosity was measured as a function of temperature under constant frequency of 1 rad/s and 0.1% shear strain. The test was performed for a range of 4-40°C. The sol-gel transition temperature was determined for MP407.

4.2.7. Further adapalene-TyroSphere MP407 gel characterization

4.2.7.1. Fluorescence microscopy

A small aliquot of adapalene-TyroSpheres in 15 wt% MP407 gel and Differin® gel was added on the glass slide and covered with cover slid. Fluorescent images were taken from the slides using Zeiss fluorescent microscope in the Dapi channel equipped with AxioCam MRm camera.

4.2.7.2. Field emission scanning electron microscopy (FE SEM)

TyroSpheres in 15 wt% MP407 gel medium with and without adapalene were dispersed lightly on a double-sided sticky tapes mounted to aluminum stubs (sample grid) and air-dried for 2 days. Then, the samples were sputter-coated with 15nm of gold using an Electron Microscopy Sciences EMS150T ES coater and imaged with a field emission scanning electron microscope (Zeiss Sigma).

4.2.7.3. Adapalene release from TyroSphere MP407 gel

Release of adapalene from TyroSphere in 15 wt% MP407 formulation was studied using SC. SC separated from human cadaver skin was mounted on the vertical Franz diffusion cells with receiving volume of 5 ml and 0.64cm^2 area (PermeGear, Hellertown, PA). 20% DMF in PBS (pH 7.4) was used as the releasing media. The release study was conducted at 37 °C under constant stirring of the releasing media. At pre-determined time points, aliquots of 400 µL were collected from the receptor compartment and were replaced with the equivalent amount of the releasing media.

Following lyophilization of the samples and adapalene extraction, the drug content was analyzed by HPLC.

4.2.8. Skin irritation studies of adapalene-TyroSphere gel and the adapalene commercial product

4.2.8.1. *In vitro* skin irritation analysis using two-dimensional model (keratinocyte monolayers)

4.2.8.1.1. HaCaT culture

HaCaTs (a cell line of human keratinocytes) with passage number below 20 was utilized in the study. The cells were cultured in Dulbecco's Modified Eagle Medium (DMEM) supplemented with 10% fetal bovine serum (FBS) and 50 mg/ml gentamycin (37°C, 10% CO_2, RH 95%). When 90% confluency was reached, the cells were rinsed with DPBS and trypsinized. The cell concentration was measured with a Cellometer Auto A4, Nexcelom (Bioscience, MA).

4.2.8.1.2. *In vitro* irritation study using HaCaT monolayers

HaCaT cells were seeded in 96-well plates at 5,000 cells/well seeding density. The cells were incubated for 24 hours to ensure sufficient attachment. Next, the medium was replaced with DMEM medium (without serum) containing the following: Differin®, adapalene solution, and adapalene-TyroSpheres in 15% MP407 gel system. The concentration of adapalene in the wells was 0.5-10 μg/ml (0.05-1 μg/well). The HaCaTs were incubated with media containing adapalene formulations or their vehicles for 1 h. Next the media was replaced with fresh DMEM containing serum and the wells were

placed in an incubator (37°C, 10% CO_2, RH 95%) for 42 h. The irritation potential of adapalene formulations was analyzed by AlamarBlue® metabolic assay.

3.2.8.1.3. AlamarBlue® metabolic assay

Cell culture medium containing 10% AlamarBlue® reagent was added and the cells were incubated until the negative controls started to turn pink. The fluorescence intensity was measured (560nm/590nm; manual gain 97%) using a Tecan Infinite 200M fluorescent plate reader. Plain cell culture medium treatment was used as 100% cell viability.

4.2.8.2. *In vitro* skin irritation analysis on a three-dimensional (3D) epidermal skin model

Fully differentiated human epidermis (EpiDerm™) specimens were purchased from MatTek Corporation (Ashland, MA). The *in vitro* irritation study was conducted according to a protocol provided by the manufacturer. Upon arrival, the tissues were transferred to 6-well plates and incubated at 37°C overnight in 0.9 ml assay medium (EPI-100-ASY, MatTek) at the air-liquid interface. The next day, the surface of EpiDerm™ was treated with Differin® gel or adapalene-TyroSphere MP407 gel at drug concentration of 40 μg/cm^2 in triplicate. The tissues were fed from the bottom with the fresh assay medium and incubated at 37°C and 5% CO_2 for 3 h or 24 h. EpiDerm™ samples treated with PBS pH 7.4 were used as a negative control. The irritation potential of adapalene formulations was evaluated by MTT cell viability assay and inflammatory

mediators/cytokine analysis (to determine IL-1α and IL-8 content in the medium), after the dosing period was completed.

4.2.8.2.1. MTT assay on the 3D epidermal skin model

In the *in vitro* skin irritation analysis using three-dimensional (3D) epidermal skin model, the viability of the tissues after dosing was analyzed by MTT. The tissue specimens were rinsed with PBS and transferred to 24-well plates containing 300 µL MTT solution (provided by MatTek Corp.) and incubated for 3 h. Next, the tissues were immersed in a 24-well plate containing 2 ml extracting solution per well. The plate was sealed and incubated at room temperature overnight. The optical density (OD) of the extracted samples was measured at 570 nm. Percent tissue viability was calculated using the following formula:

$$\%\, Viability = 100 \times \frac{\text{OD (sample)}}{\text{OD (negative control)}}$$

4.2.8.2.2 ELISA assay

Release of IL-1α and IL-8 in the EpiDerm™ culture medium was quantified using ELISA kits from BioLegend (San Diego, CA) according to the assay protocol provided by the manufacturer. UV/Vis spectrophotometric measurements were performed with a Biotek PowerWave X microplate reader.

4.2.9. Rhino mouse study

4.2.9.1. Animals

Male Homozygous rhino mice (RH J/LeJ) were purchased from The Jackson Laboratory (Bar Harbor, ME). The mice were 6-8 weeks old and weighed 18-22 g at the beginning of the study. The animals were housed in groups of four in autoclaved individually ventilated cages at an AAALAC-accredited facility. All animal handling was conducted at the Nelson animal facility (Rutgers University). The mice were fed with PicoLab® Rodent diet 20 (LabDiet, St Louis, MO) and received autoclaved house water. The experimental protocol was reviewed and approved by the IACUC at Rutgers-The State University of New Jersey.

4.2.9.2. Experimental design and treatments

The total 15 rhino mice were used for this study and were divided in 3 groups: Differin® gel (0.1% w/w), adapalene-TyroSphere 15% MP407 gel-1 (0.05% w/w) and adapalene-TyroSphere 15% MP407 gel-2 (0.03% w/w). The mice treated with similar formulations were caged together.

The mice were anesthetized by inhalation of isoflurane (2-4% in 100% O2). The dorsal skin of animals were treated topically with the following adapalene formulations: Differin® (35 μg/cm^2) or adapalene-TyroSphere MP407-1 (35 μg/cm^2) and adapalene-TyroSphere MP407-2 (20 μg/cm^2). The treated area was covered with Tegaderm™ dressing (3M Health Care, St. Paul, MN) after dosing to prevent rub-off and oral ingestion of the formulations. After covering with Tegaderm™ the gels were massaged on the skin for about 30 s using a cotton swap. The dosing was done once daily for 14

days. The mice were examined for signs of skin irritation every day before receiving adapalene treatment.

4.2.9.3. Skin biopsies and epidermis mounting technique

On day 15 of the study the mice were euthanized by CO_2 inhalation. Next, the skin was cleaned and the treated dorsal skin was removed, cut into smaller fragments (about 1 cm^2), and stored in 10% neutral buffered formalin to be used for histological analyses. The untreated dorsal skin areas were also collected and stored in formalin to be used as negative control.

In order to prepare the epidermal sheets, first the skin specimens were placed into 1% acetic acid solution at 4°C overnight. The next day, the dermal layer was gently peeled using a forceps and the epidermis pieces were dehydrated with ethanol (70, 95 and 100% v/v) and cleared with xylene. The cleared epidermis was placed on a glass slide with the dermal side facing up and subjected to microscopic evaluation.[21-22]

4.2.9.4. Histological analyses of the mouse skin biopsies

Following fixation in formalin solution overnight, the tissues were dehydrated with ethanol (70, 95 and 100% v/v) and xylene respectively following the routine procedure. The skin samples were then embedded in paraffin. The samples were sectioned at 5 μm using a microtome (Microm HM 3555). For each animal skin fragment, three sections were made 3-5 mm apart and were collected on one glass slide. Next the samples were deparaffinized by xylene, rehydrated in a gradient of ethanol solutions, and stained with haematoxylin and eosin (H&E).

4.2.9.5. Quantitative analysis of the utricles

The H&E stained samples were analyzed with Zeiss optical microscope equipped with Axiocam ERc 5s camera. The depth and diameter of the utricles were measured using AxioVision microscope software. Utricles were quantitatively assessed in 3 ways: i) density of the utricles, which was done by counting number of utricles per 6 millimeters length of the skin from vertical cross sections; ii) diameter of the utricle opening that was measured for all the utricles in 6 millimeters length of skin from the vertical cross sections; and iii) the depth of the utricles that was measured for 6 millimeters length of skin in the vertical cross sections (see Figure 4.1).

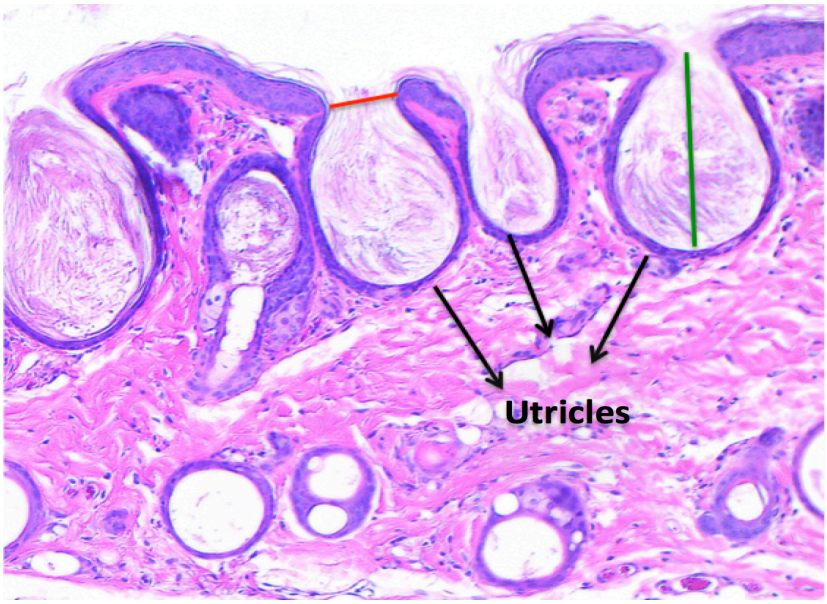

Figure 4.1. Rhino mouse skin cross section stained with haematoxylin and eosin. The arrows are showing keratin-containing utricles in a 9-week old rhino mouse. The diameter of utricle opening and the utricle depth is shown by red and green line respectively.

The efficacy of TyroSphere gel treatment relative to Differin® was evaluated by comparing the % reduction in size of utricles, calculated as following:

$$\%reduction\ in\ size = \frac{(average\ utricle\ size\ in\ untreated\ skin - average\ utricle\ size\ after\ treatment)}{average\ utricle\ size\ in\ untreated\ skin} \times 100$$

4.2.10. Statistical analysis

The results of skin distribution studies, irritation assays, and animal studies are reported as mean ± standard error (SE). Statistical analysis was performed using Prism Version 6 (GraphPad software, La Jolla California). Student t-test and one-way analysis of variance ANOVA followed by Tukey's post hoc or Wilcoxon signed-rank test (in case the normal distribution assumption did not exist) were applied to determine the difference among the groups in every study. For all analysis, a *P* value of less than 0.05 derived from a two-tailed test was considered significant unless specified.

4.3. Results and Discussion

4.3.1. Adapalene-TyroSphere viscous formulations

DTO-SA copolymers are composed of hydrophilic PEG side chains and hydrophobic desaminotyrosyl alkyl ester backbone. Because of its amphiphilic nature, this copolymer system can self-assemble to nanomicelles (TyroSpheres) in aqueous media and encapsulate a wide range of hydrophobic molecules like adapalene in its

hydrophobic core. Gel formulations of adapalene-TyroSphere were developed for a more convenient topical dosage form that has less flow properties and could maintain on the skin. Figure 4.2 shows gel/viscous formulations made with HV HPMC and MP 407. The presence of nanoparticles results in slight turbidity of the gel formulations. The MP407 TyroSpheres form a clearer gel than that using HV HPMC TyroSpheres.

Figure 4.2. Viscous formulations of TyroSpheres.
Left image: 1.5% high viscosity hydroxypropyl methylcellulose (left: in adapalene-TyroSphere suspension Right: in phosphate buffered saline)
Right image: 15% micronized poloxamer 407 (left: in adapalene-TyroSphere suspension, Right: in phosphate buffered saline)

4.3.1.1. Particle size analysis

TEM was used to study particle size of adapalene-TyroSphere viscous formulations. TEM images of final adapalene-TyroSphere gel-like formulations (Figure 4.3) show particle diameters similar to what observed with adapalene-TyroSphere liquid dispersion, a narrow particle size distribution, and lack of particle agglomeration in the presence of thickening agents.

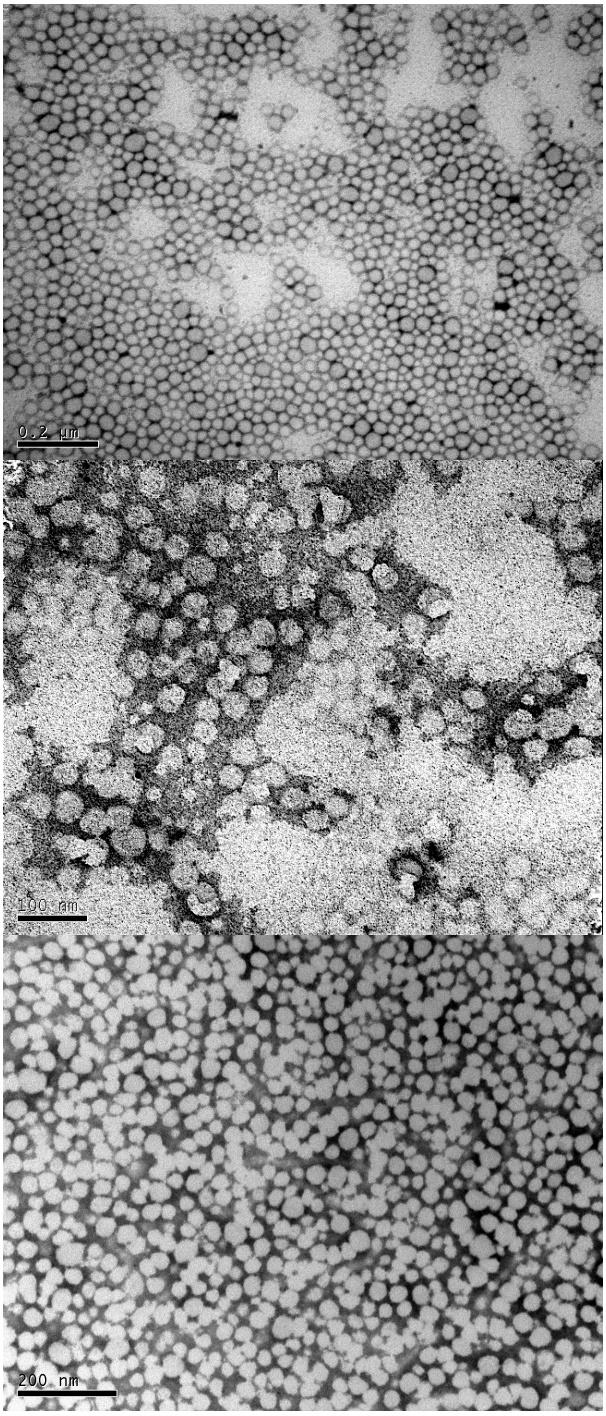

Figure 4.3. Transmission electron micrographs of adapalene-TyroSpheres from the top to bottom: in liquid suspension, 2% HV HPMC, and 15% MP407.

4.3.1.2. Content uniformity

Homogeneity of the gel-like adapalene-TyroSphere formulations (0.025% w/w) was studied by measuring drug content in the gel samples. The relative standard deviation (RSD) was calculated as 4.5, and 2.9% for 2% HV HPMC and 15% MP 407 Adapalene-TyroSphere gels respectively, which are in acceptable range for the pharmaceutical semi-solid dosage forms.

4.3.2. Adapalene distribution in skin from TyroSpheres viscous formulation

In the last two chapters we demonstrated TyroSpheres applicability for drug delivery to pilosebaceous unit. Adapalene-TyroSphere gels were also applied on pig ear skin and the drug delivery to the hair follicles and upper epidermis was assessed by fluorescence microscopy. Figure 4.4 depicts fluorescent images taken from the pig skin treated with adapalene-TyroSphere gels (0.025 wt% drug content) and Differin® (0.1 wt% drug content). With all three treatments adapalene was distributed in the upper epidermis layers and hair follicles. Despite lower drug concentration, the fluorescent intensity of the samples treated with adapalene-TyroSphere gels appears to be more than that of Differin®, suggesting enhancement of drug delivery from TyroSphere formulations.

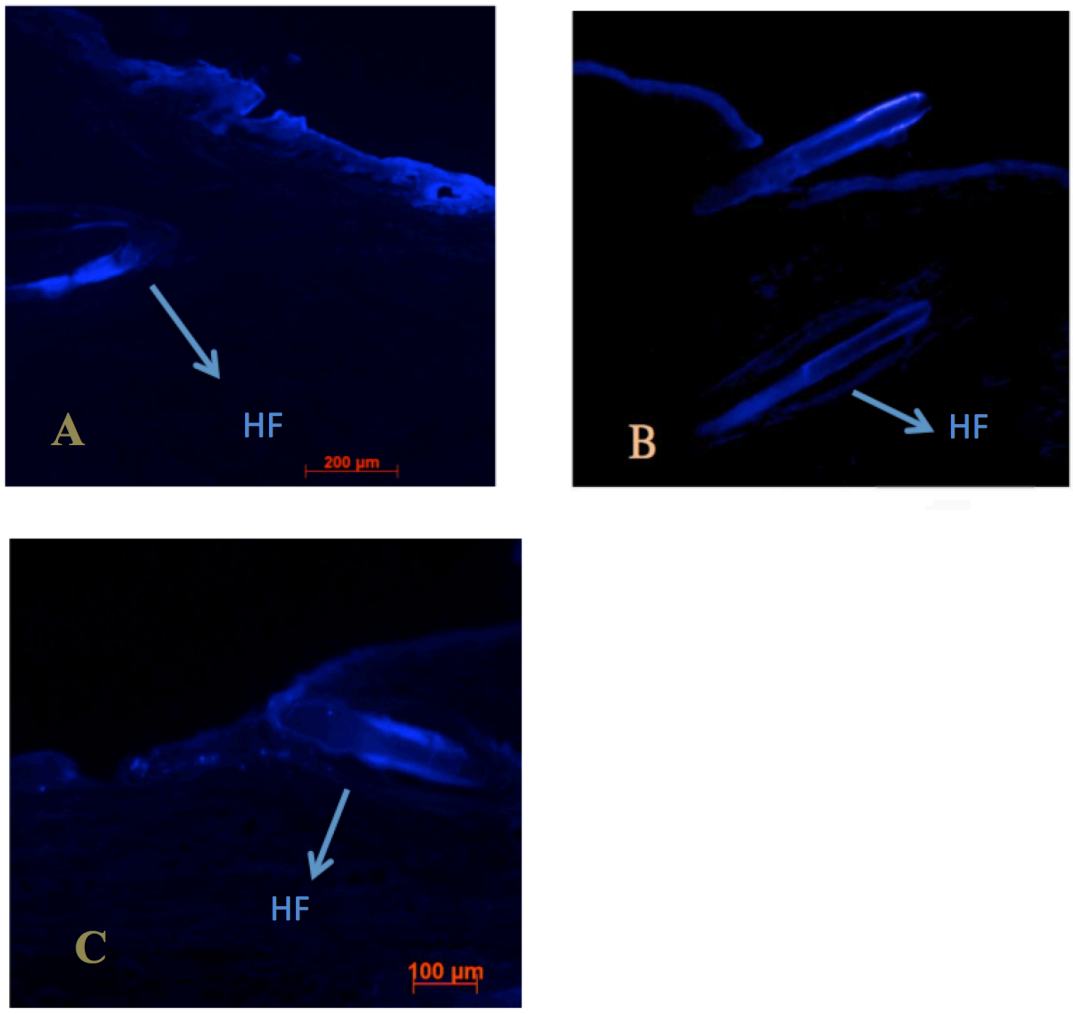

Figure 4.4. Adapalene distribution within the hair follicle (HF) and upper epidermis. Fluorescent images were taken from vertical section of porcine ear skin treated with A) adapalene-TyroSpheres in 15% MP407, B) adapalene-TyroSpheres in 2% HV HPMC, and C) Differin® gel. Adapalene, showing blue fluorescence, is distributed in hair follicles, hair shaft and stratum corneum.

Adapalene delivery to SC was also quantified and the TyroSphere gel formulations were compared with the marketed gel, Differin®. Figure 4.5 demonstrates adapalene extracted from SC following 12 h permeation study on pig ear skin. There was no significant difference among the TyroSphere gel formulations (15% MP407 and 2% HV HPMC) and Differin® gel. It is noteworthy that the drug content in TyroSphere

formulations was 0.025 wt% while Differin® contains 0.1wt% adapalene. This observation is due to penetration enhancement effect of TyroSpheres on drug delivery through intercellular pathway.

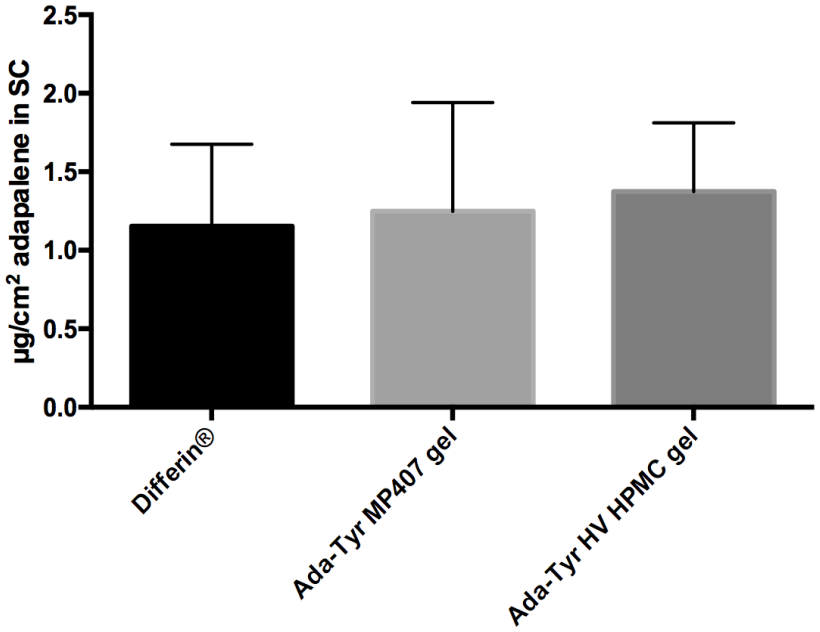

Figure 4.5. Adapalene delivery to the SC following 12 h application of the gel formulations on the pig skin. Adapalene-TyroSphere (Ada-Tyr) gel formulations (with 0.025% drug content were able to deliver similar amounts of drug to the SC, compared to Differin® with 0.1% drug content.

4.3.3. Rheological analysis

The mechanical strength and viscoelastic properties of adapalene-TyroSphere viscous formulations were studied to analyze rheological behavior of these topical formulations and compare them with Differin® gel as a reference standard.

4.3.3.1. Frequency sweep test

Rheological behavior of topical/transdermal formulations has a profound effect on their spreadability, retention and contact time on the skin surface.[6] Oscillatory measurements are one of the most recommended methods for rheological studies.[23] The results of oscillation study are illustrated in Figures 4.6-4.8, where storage (G') and loss (G'') moduli were measured as a function of frequency.

Figure 4.6 depicts the frequency sweep test on adapalene-TyroSpheres in 2% and 1.5% HV HPMC. At both concentrations, the HPMC formulations behaved as viscous solutions and both G' and G'' showed relative strong dependency on the frequency. The values obtained for G' were lower than G'' at similar oscillation rate, showing the system is primarily viscous rather than elastic. This trend was observed at both 25 and 32 °C. Additionally, presence of adapalene-TyroSpheres did not significantly affect the shear moduli.

In Figure 4.7 the G' and G'' of MP407 gels are plotted logarithmically against frequency. At both 15 and 20 wt% of MP407, the oscillation rate did not affect G' and G'' and the G' was much higher than G'' indicating the system is elastic. Similar trend was observed with the gels at 32°C with higher values for both of the shear moduli The results of frequency sweep test showed that the gels made with MP407 are well-structured system and sedimentation of particles are unlikely to occur. Presence of TyroSpheres slightly increased the viscosity but did not change the behavior of the system.

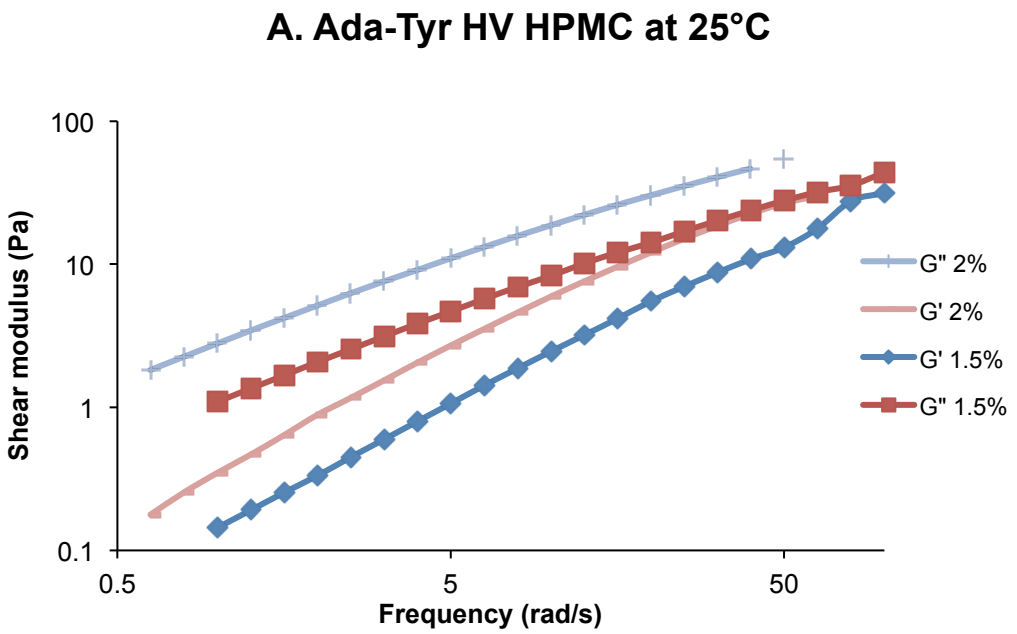

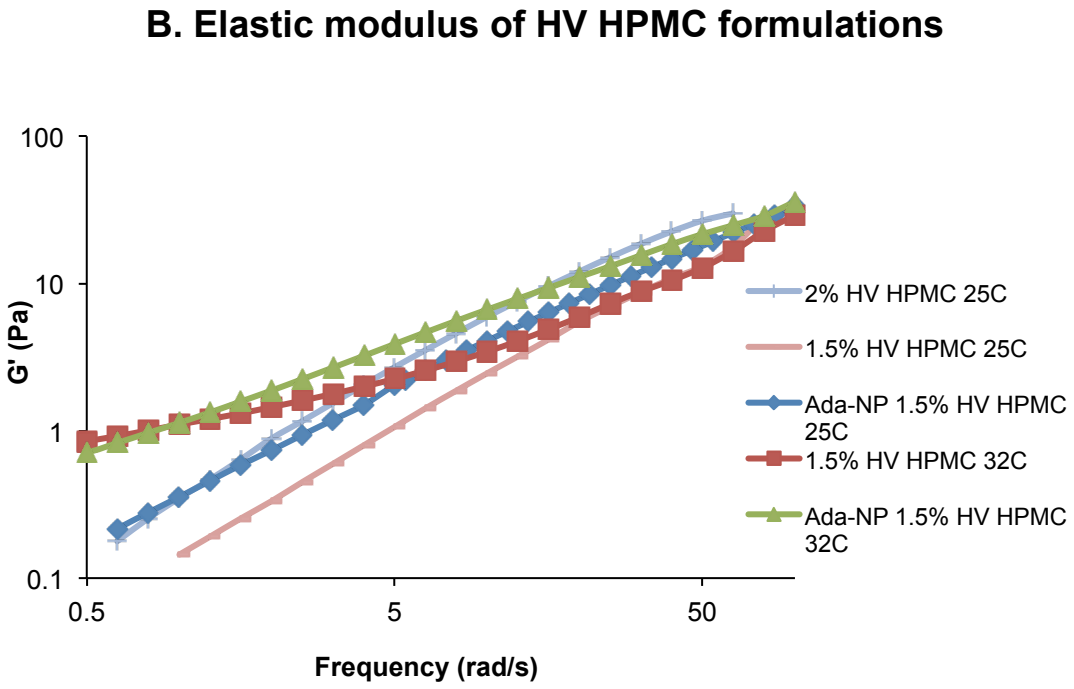

Figure 4.6. Oscillatory viscometry of HV HPMC formulations. A) The influence of oscillation rate on shear moduli of 2% and 1.5 wt% HV HPMC at 25°C. B) The influence of oscillation on elastic modulus (*G'*) in HV HPMC formulations at 25 and 32°C with and without adapalene-TyroSpheres (Ada-Tyr).

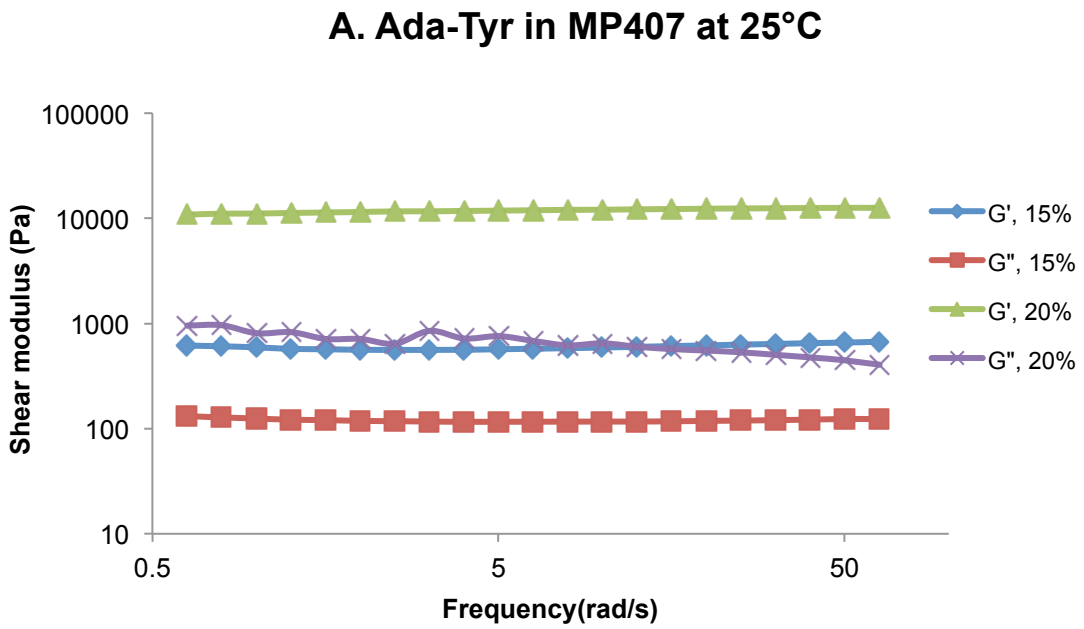

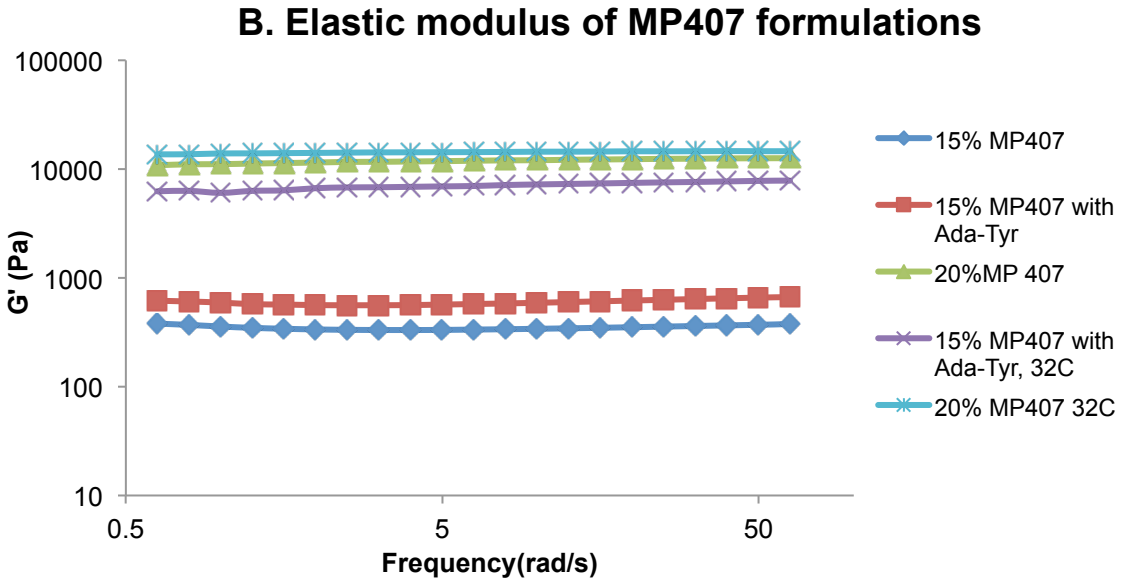

Figure 4.7. Oscillatory viscometry of MP407 gels. A) The influence of oscillation rate on shear moduli of 20 and 15 wt% MP407 gels at 25°C. B) The influence of oscillation rate on elastic modulus (G') in MP407 formulations at 25 and 32 °C with and without adapalene-TyroSpheres (Ada-Tyr).

The gelling agent in Differin® is Carbomer 940, which is a cross-linked polyacrylate polymer capable of providing high viscosity and forming clear aqueous and hydroalcoholic gels.[24] The results of frequency sweep test for Differin® gel is demonstrated in Figure 4.8. Rheological measurements of *G′* and *G″* for Differin® showed independency of both shear moduli from oscillation rate. At both temperatures the *G′* is much more than *G″* indicating the system is elastic. Both shear moduli were not affected by change in the temperature.

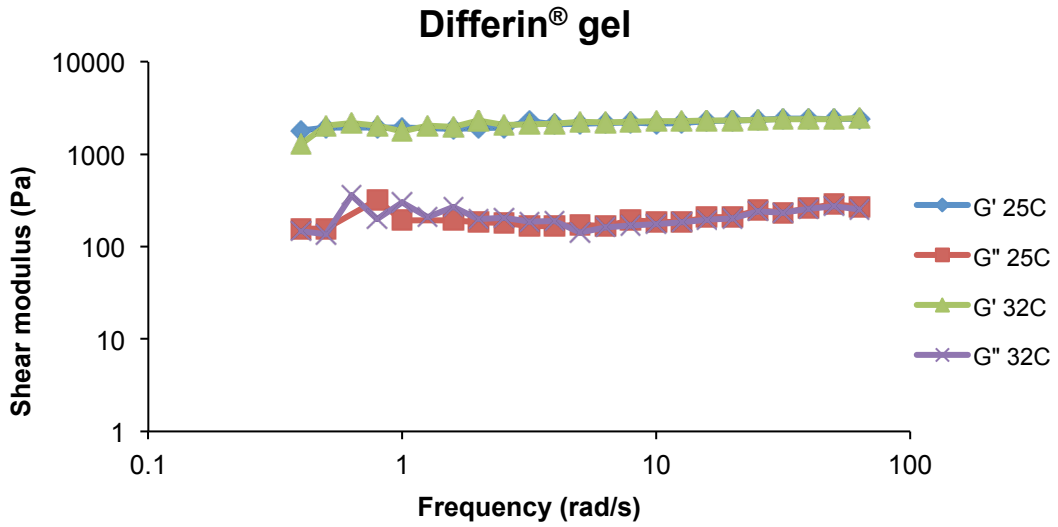

Figure 4.8. Oscillatory viscometry of Differin® gel recorded at 25 and 32°C.

The results of the frequency sweep tests on the viscous formulations revealed that the gels made with MP407 behaved similar to Differin® gel. In both gels, *G′* and *G″* are independent of the frequency. In both systems, elastic modulus dominates the complex modulus meaning the system is very elastic. In the gels made with HV HPMC, the loss and storage moduli are both enhanced with increase in the frequency. Presence of

TyroSpheres in the gels slightly increased the shear viscosity but did not change the rheological behavior and strength of the gels.

4.3.3.2. Strain sweep test

The strain sweep test (Figure 4.9) was performed on TyroSphere viscous formulations and Differin® in order to establish the regime of linear viscoelasticity (LVE) and to study mechanical strength of the gels. In the cellulose-based system (HPMC) the loss modulus (*G″*) dominates and relative to MP407 and Differin® gel, this formulation showed the highest resistance to structural change following increase in shear strain. But in MP407 and Differin® storage modulus (*G′*) was higher than loss modulus, confirming both systems are elastic. Also the structure of both gels break down at nearly 5% shear strain.

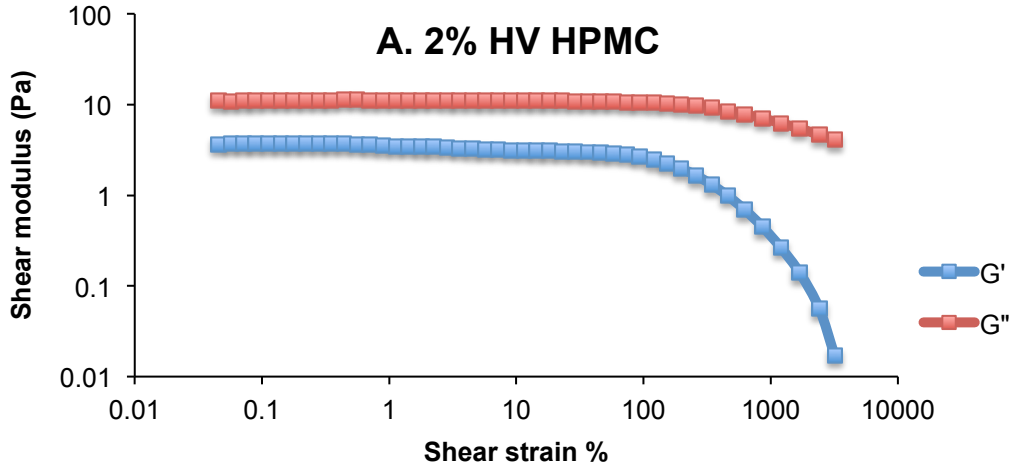

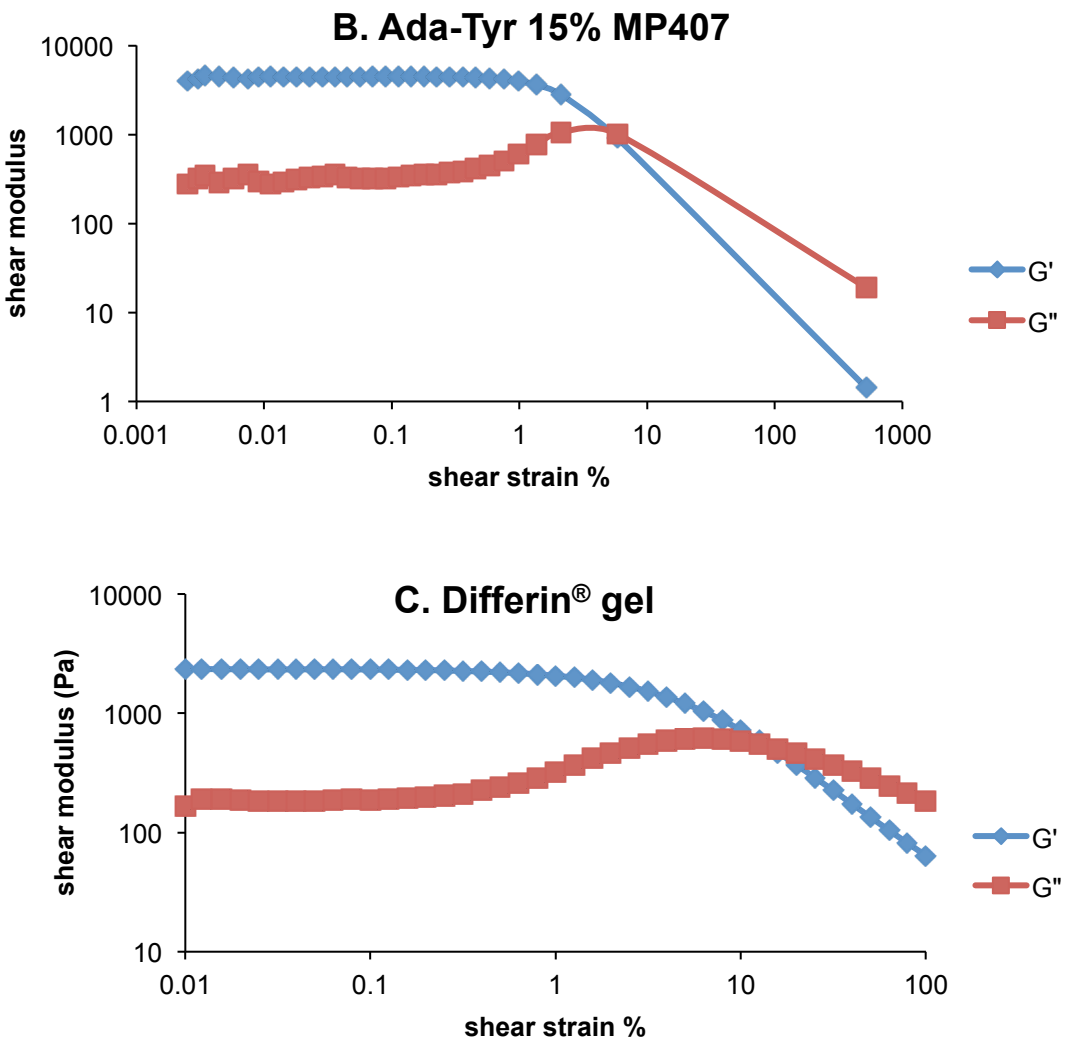

Figure 4.9. Strain sweep test on A) adapalene-TyroSpheres in 2% HV HPMC, B) adapalene-TyroSpheres in 15% MP407, and C) Differin® to establish the linear viscoelasticity regime of the gels.

4.3.3.3. Temperature sweep test

The results of temperature sweep test are provided in Figure 4.10. The viscosity of Differin® and the formulations made with HV HPMC are not highly dependent on the temperature. Slight decrease in the shear viscosity of the HV HPMC formulations was observed with increase in temperature.

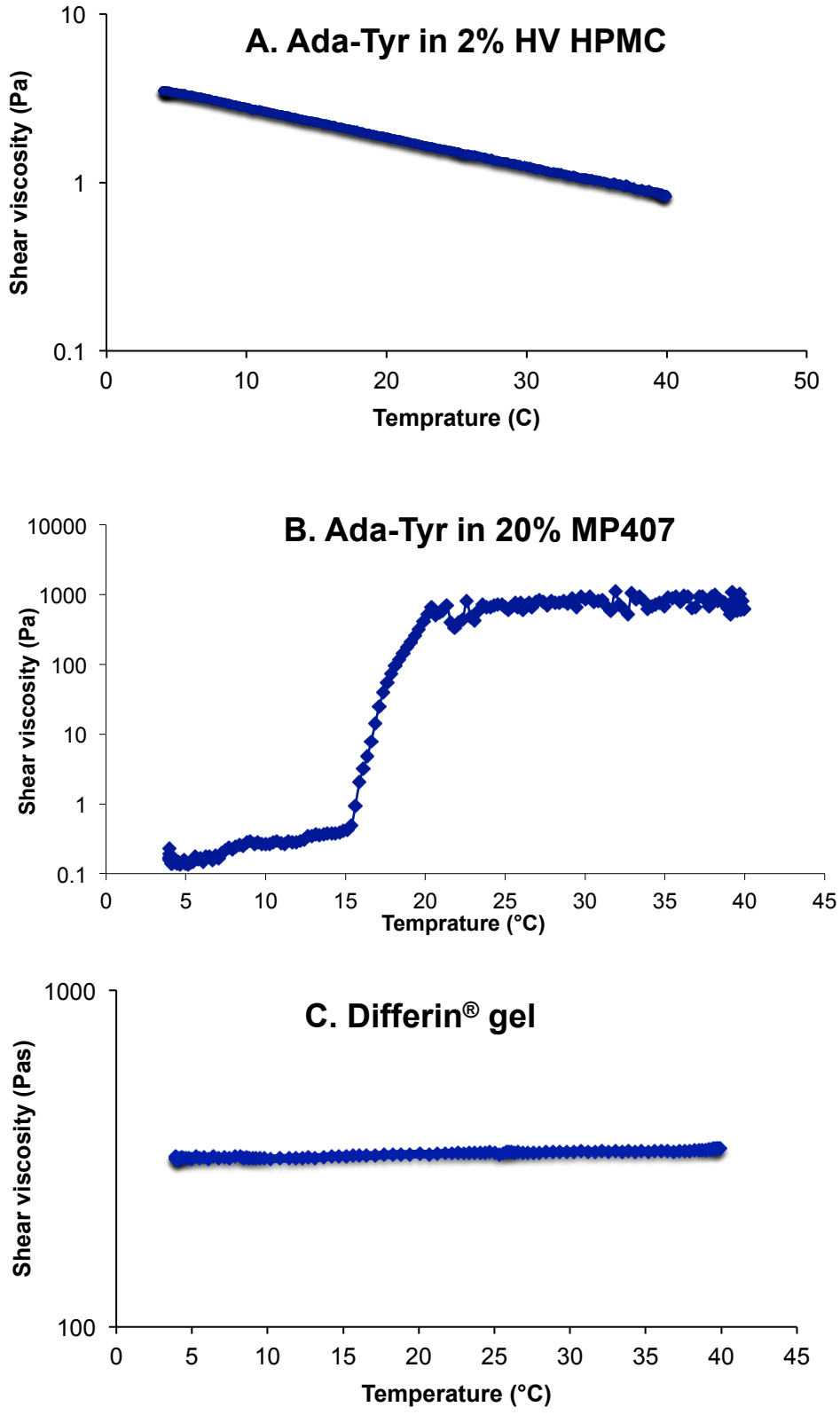

Figure 4.10. Results of temperature sweep test on adapalene-TyroSpheres (Ada-Tyr) in A) 1.5% HV HPMC, B) 20% MP407 and C) Differin®.

On the other hand, the formulations made with MP407 showed flow properties similar to liquids at lower temperatures (<15°C) and shear viscosity of less than 1 Pas. However, at temperature range of 15-18 °C the solutions transitioned to a viscous gel and shear viscosity drastically increased (Figure 4.10.B). At temperatures higher than 20°C, MP407 gel behaved similar to Differin® and the shear viscosity did not significantly change with increased temperature.

Based on the results we obtained from the rheological characteristics of TyroSphere viscous formulations, we found 15% MP407 the best gel system to use for TyroSpheres with closest rheological properties to Differin®.

4.3.4. Other adapalene-TyroSphere MP407 characteristics

In the commercial formulation (Differin®) adapalene exists in form of microcrystals dispersed in the vehicle and these microcrystals can be visualized under fluorescent microscope (Figure 4.11.A). However, in fluorescent images taken from adapalene-TyroSphere MP407 gels no microcrystal was observed even after one month storage at room temperature (Figure 4.11.B). This confirms drug encapsulation by TyroSpheres and lack of drug leakage from nanoparticles in short-term storage.

FE SEM images taken from adapalene-TyroSphere MP407 gel demonstrate homogenous dispersion of nanoparticles in the gel structure and lack of particle agglomeration (Figure 4.12). The nanoparticles are seen as white 20-40 nm size spheres in the gel system. The particle size of TyroSpheres found to be similar to what was observed with TEM.

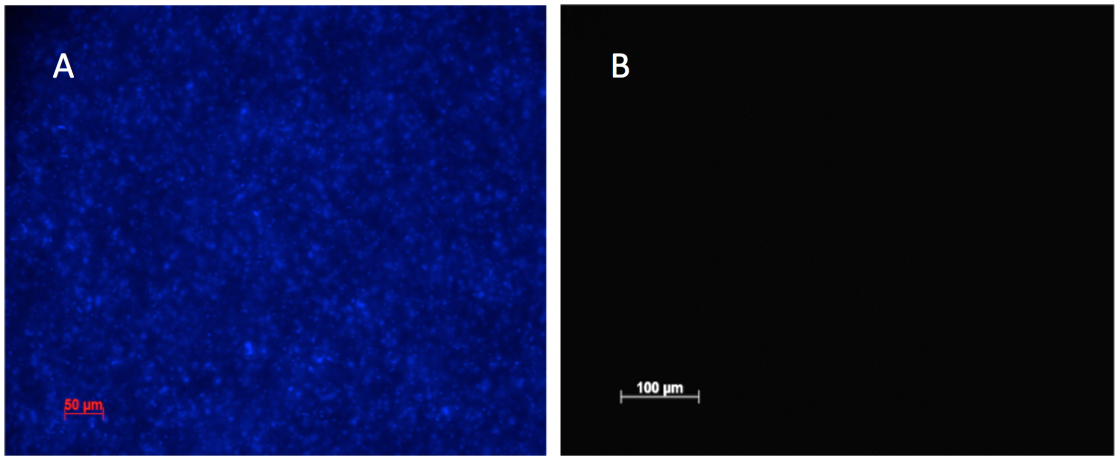

Figure 4.11. Fluorescent images of A) Differin® gel and B) adapalene-TyroSphere MP407 gel. Adapalene microcrystals (in blue) are observed in Differin® sample, but not in TyroSphere gel formulation.

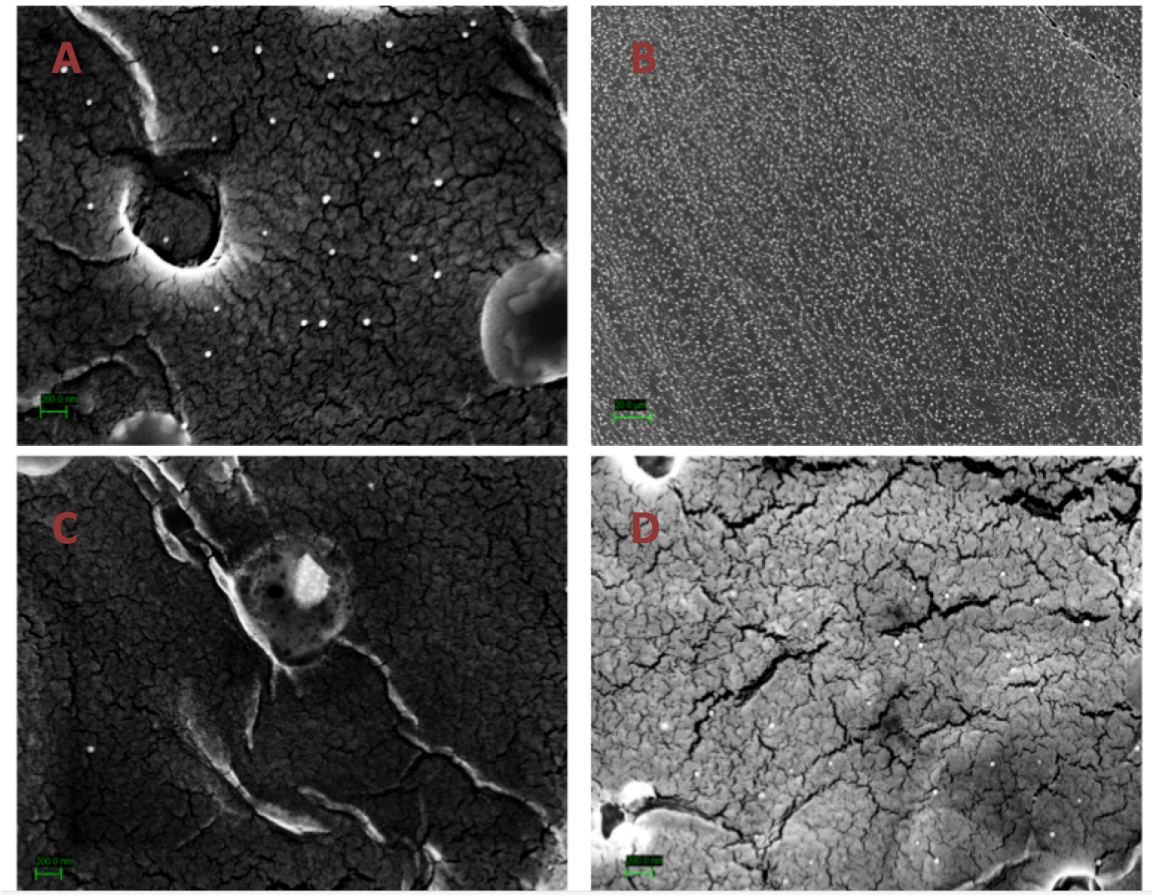

Figure 4.12. FE SEM micrograph of A-C) adapalene-TyroSpheres in 15% MP407 gel, (the scale bars are 200 nm, 20µm and 200nm respectively) and D) TyroSphere MP407 gel without drug (scale bar = 200 nm). TyroSpheres are the white spherical particles in the images.

4.3.5. Adapalene release from TyroSpheres and diffusion through stratum corneum

Previous studies reported in Chapter 3 showed that adapalene release from TyroSpheres occurs in a sustained manner and follows Higuchi square root model. Drug release from TyroSpheres and diffusion through SC was studied for both liquid dispersion and gel formulations. SC was chosen to better understand release behavior of adapalene from TyroSpheres while mimicking cutaneous conditions. DMF was added to the receptor compartment (20 vol% in PBS) to provide a sink condition and also an adequate driving force for the released drug to diffuse across the SC. Figure 4.13 shows the *in vitro* release profile of adapalene from liquid and gel formulation of TyroSpheres and diffusion across SC. The cumulative drug release during 51 h was around 42% and 73% for TyroSphere liquid dispersion and MP407 gel formulation respectively.

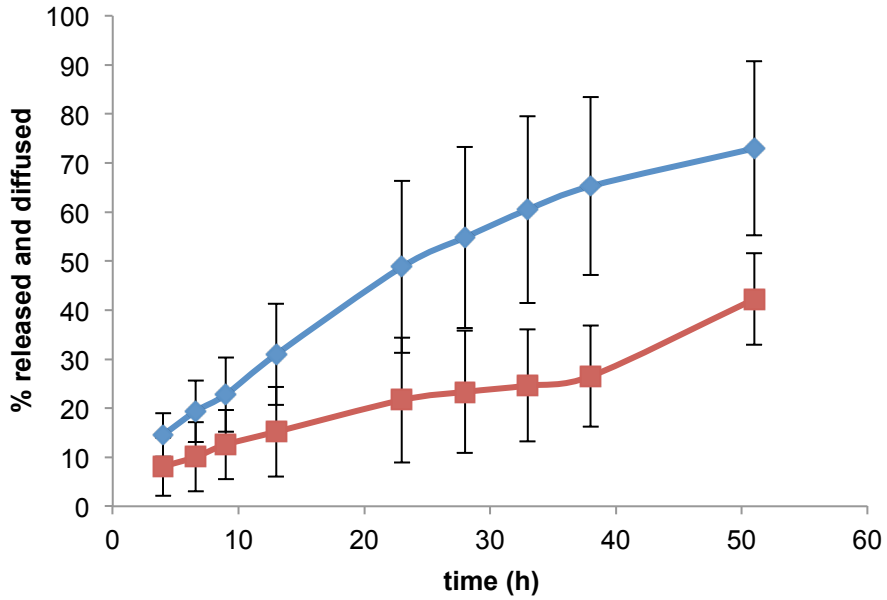

Figure 4.13. Cumulative adapalene release and diffusion across the SC from TyroSpheres in liquid dispersion (blue) and MP407 gel formulation (red). Results are shown as mean ± SD (n = 5).

Incorporation of the nanoparticulate dispersion into a gel system further decreased the drug release. This was probably due to the release-retarding effect of the polymeric matrix of the MP407.

4.3.6. *In vitro* Irritation study

The most frequent side effect of topical retinoids is known as the "retinoid reaction", which is characterized by pruritus, peeling, burning, and redness in the site of application and peaks within the first few weeks of the treatment. This phenomenon is due to the free carboxylic acid in the structure of retinoids and occurs more with application of tretinoin and tazarotene than with adapalene. Release of pro-inflammatory cytokines such as IL-1α, IL-6, TNF-α, and IL-8 in is known to initiate this retinoid reaction.[4, 25]

4.3.6.1. Irritation study on monolayer keratinocytes

Even though cell culture models lack barrier properties of the intact skin and may overestimate the irritancy of the chemicals, they can function as a useful tool to compare irritation potential of different formulations/compounds.[26] In our study, we used immortalized human keratinocyte line, HaCaT, to analyze skin irritation of adapalene commercial gel and TyroSphere gels. Figure 4.14 shows the metabolic activity of HaCaTs (obtained from AlamarBlue® assay) that were exposed to 0.5-10 μg/mL adapalene in different formulations. At all three adapalene concentrations that were studied, TyroSphere MP407 formulations did not induce cytotoxicity and irritation on the HaCaTs and at drug concentrations of 2 and 10 μg/mL this formulation was found to be

significantly less irritant and cytotoxic compared to the commercial formulation as well as the control adapalene solution. Based on these results, adapalene encapsulation in the TyroSpheres significantly decreased the irritation potential of the drug. This can be attributed to controlled release of the drug from nanoparticles dispersed in the gel system, which prevents direct contact of all dose of the drug with the skin cells. Additionally, the irritation potential of adapalene-TyroSphere MP407 gel system was compared with TyroSphere suspension at drug concentration of 10 µg/ml (see Figure 4.15). The highest cell viability was obtained from adapalene-TyroSphere in MP407 formulation and this can be explained by slower release of the drug from the TyroSpheres in the hydrogel system compared with the suspension dosage form.

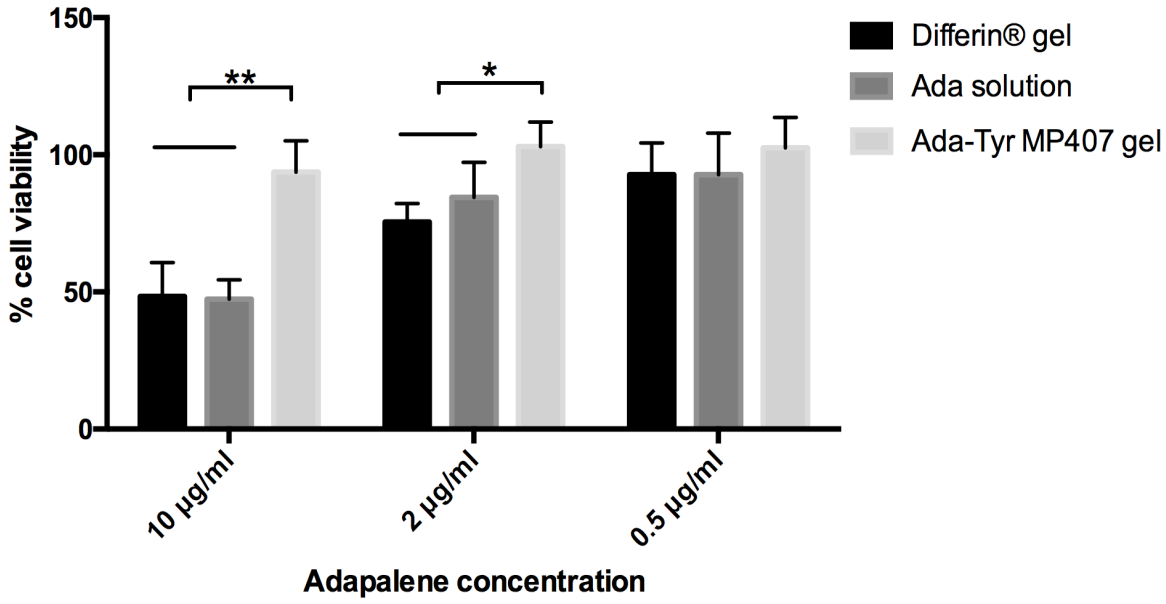

Figure 4.14. Percentage cell viability of HaCaTs treated with different content of adapalene in TyroSphere gel formulation (Ada-Tyr) MP407, Differin® and solution form. Under the same adapalene concentrations, the cells treated with Ada-Tyr MP407 had highest cell viability comparing to ones treated with Differin® and drug solution. Results are shown as mean ± SD (n=9), * $P<0.05$ and ** $P<0.01$ from one-way ANOVA and Tukey's post hoc test.

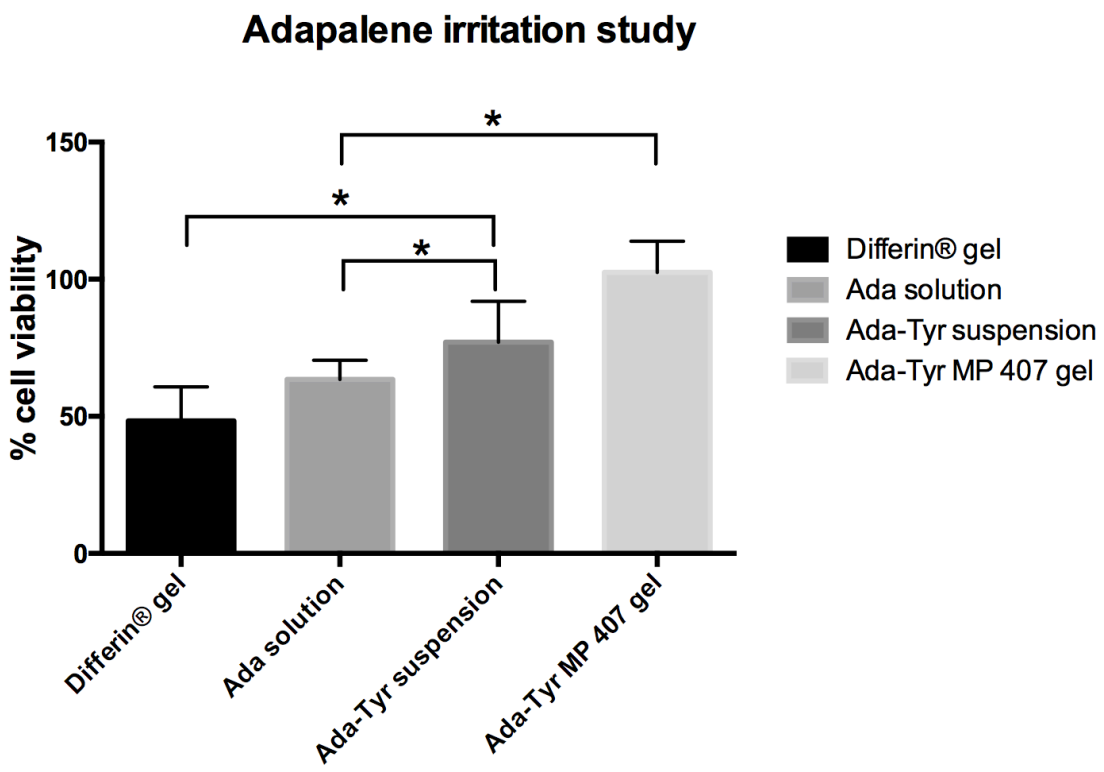

Figure 4.15. Percentage cell viability of HaCaTs treated with 10µg/mL adapalene in various formulations: Differin®, solution form, TyroSpheres (Ada-Tyr), and TyroSpheres in MP407 gel. Data are shown as mean ± SD (n = 6), * $P<0.05$ from one-way ANOVA and Tukey's post hoc test.

4.3.6.2. Irritation study on MatTek epidermal skin model (EpiDerm™)

Commercially available artificial skin models such as EPISKIN and EpiDerm™ are widely used nowadays to assess acute irritation potential of the topically applied compounds. They have proved to be a reliable alternative to the *in vivo* irritation test that is conducted on albino rabbits.[27] We used EpiDerm™ skin model from MatTek corp. to compare irritation potential of adapalene-TyroSphere MP407 gel with the commercial adapalene gel, Differin®. Based on MTT tissue viability assay performed on EpiDerm™ treated with the adapalene formulations, both Differin® and TyroSphere formulations were found to be non-irritant (Figure 4.16). No significant difference was found with the

tissue viability of the skin treated with both formulation during 3, 24 and 40 h application.

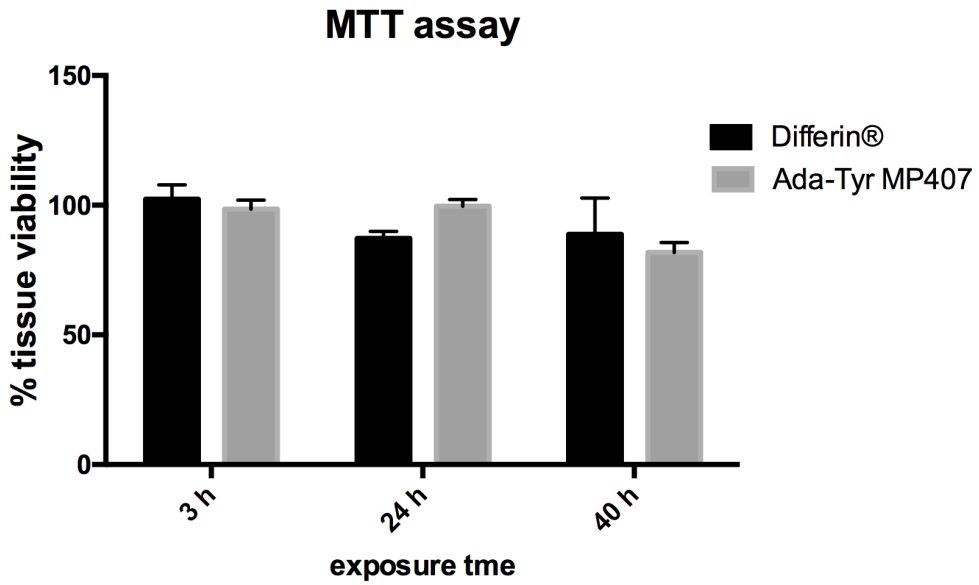

Figure 4.16. Percentage (%) tissue viability of EpiDerm™, treated with adapalene-TyroSpheres MP407 gel (Ada-Tyr Mp407) and Differin® for 3, 24, and 40 h. Data are shown as mean ± SE.

Release of proinflammatory cytokines (a well-established biomarker of acute irritation) was used to quantify the amount of irritation in EpiDerm™ skin model. ELISA assays were used to measure concentrations of IL-1α and IL-8 that were secreted from EpiDerm™ treated with adapalene formulations. At some of the time points (especially with shorter exposure time) application of adapalene-TyroSpheres MP407 resulted in less secretion of IL-1α and IL-8 compared to treatment with Differin® (Figures 4.17-18). There was no significant difference in release of pro-inflammatory cytokines from EpiDerm™ treated with adapalene-TyroSphere and negative control (PBS) except the IL-1α secretion during 40 h application of the formulations. We assume that encapsulation of adapalene in the nanoparticles and the sustained release manner that was observed

earlier with TyroSphere gel formulation prevent the non-physiological overload of adapalene in the skin; and therefore, reduce irritation potential of the retinoid formulation compared to the commercial product. With Differin® since the drug crystals are dispersed in the vehicle they directly contact the skin, inducing release of inflammatory cytokines. Similar observations have been reported in the literature, where irritant drugs like retinoic acid were encapsulated in particulate systems. Castro et al.[21] reported significant decrease in skin irritation of retinoic acid in solid lipid nanoparticle formulations without reduction in efficacy *in vivo*. Moreover, the absence of other potentially irritant ingredients such as chemical penetration enhancers in the TyroSphere MP407 gel could be another reason for decreased skin irritation that was observed from our formulation relative to the commercial gel.

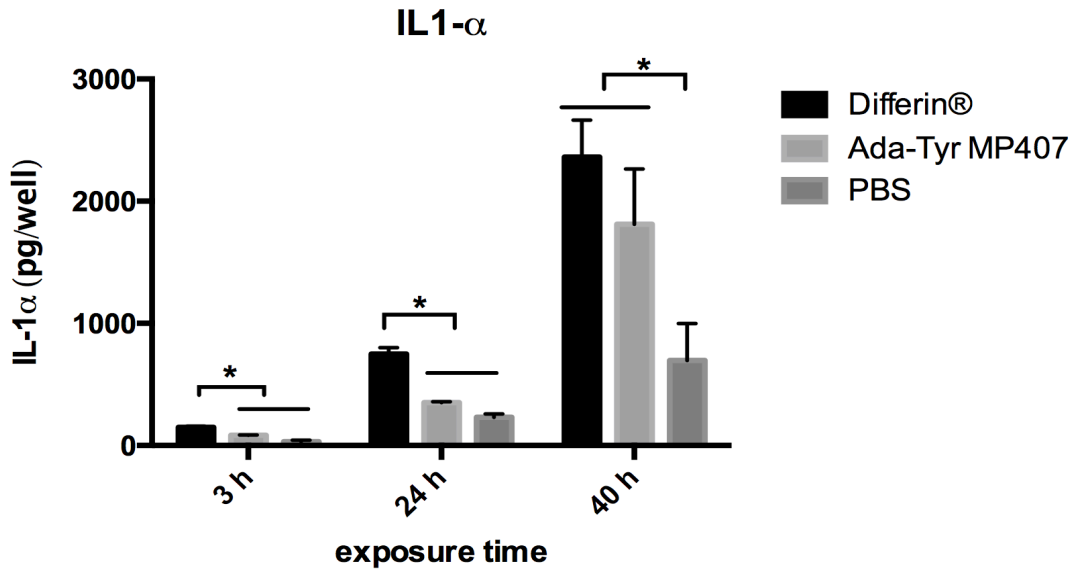

Figure 4.17. Release of IL-1α from EpiDerm™ treated with adapalene-TyroSpheres in 15% MP407 (Ada-Tyr MP407), Differin®, and phosphate buffered saline (PBS) for 3 and 24, and 40 h. Data are shown as mean ± SE, * $P<0.05$ from one-way ANOVA and Tukey's post hoc test.

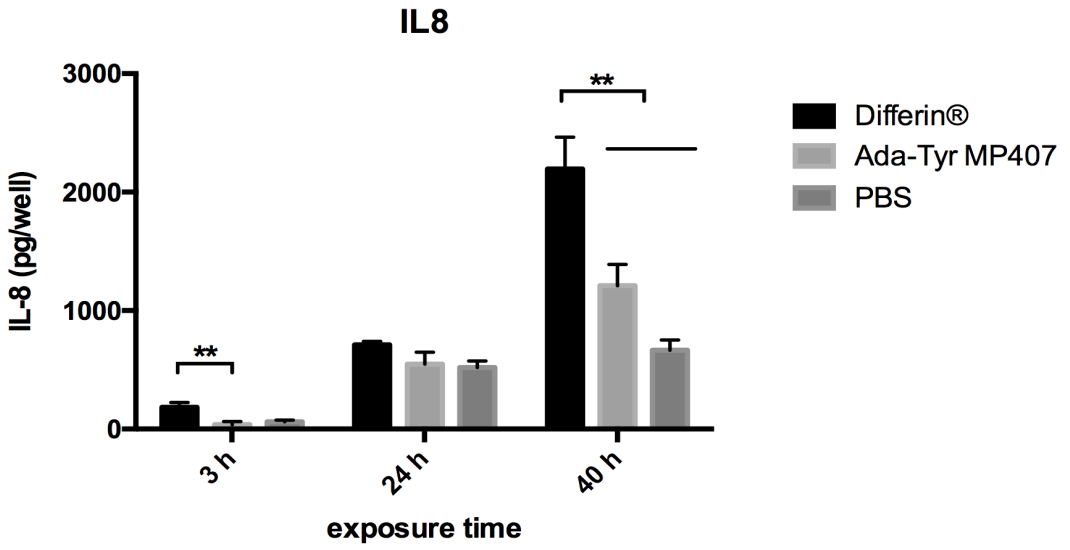

Figure 4.18. Release of IL-8 from EpiDerm™ treated with adapalene-TyroSpheres in 15% MP40 (Ada-Tyr MP407), Differin®, and phosphate buffered saline (PBS) for 3 and 24, and 40 h. Data are shown as mean ± SE, ** $P<0.01$ from one-way ANOVA and Tukey's post hoc test.

4.3.7. Efficacy of adapalene-TyroSphere gel on acne animal model

The rhino mouse model has been frequently used to assess the potential efficacy of the topical retinoids. The epidermal sheets of rhino mice that were obtained by acetic acid splitting and alcohol/xylene clearing were analyzed under microscope (Figure 4.19). Circular-shaped utricules (representing microcomedones) were observed in rhino mouse epidermis. In the untreated area of the skin, the utricles are found to be much bigger and had larger openings (Figure 4.19.A). Following treatment with adapalene formulations there was significant shrinkage in size of the utricles on rhino mouse skin (Figure 4.19.B).

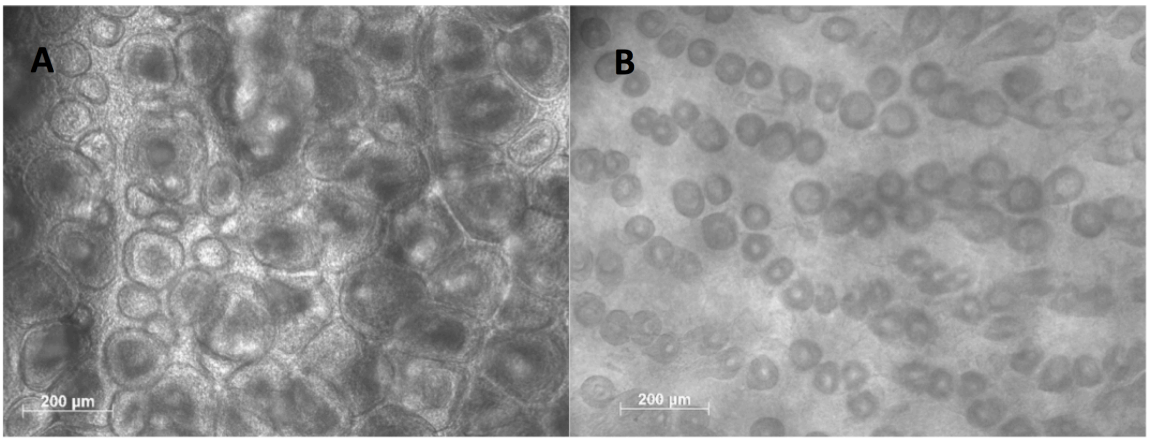

Figure 4.19. Horizontal images of the rhino mouse epidermis. A) not treated with adapalene and B) treated with adapalene-TyroSphere MP407 gel. The epidermal sheets were prepared from acetic acid splitting and ethanol/xylene processing.

Reduction in size of utricles and epidermal hyperplasia (increase in number of cells) in rhino mouse skin are indication of the retinoid efficacy. In order to capture these effects, H&E stained vertical cross sections of the rhino mouse skin were prepared. As it is demonstrated in Figures 4.20.A, C, and E, in untreated skin areas most of the utricles are opened to the surface and often contain keratin-like sheets. The utricle walls and the epidermal layer are thinner than the skin areas treated with adapalene. The comedolytic effect of adapalene is confirmed by promoting thickness of viable epidermal layers and reduction of utricles size and density (Figures 4.20.B, D, and F). These effects were observed in all the mice which received either Differin® or adapalene-TyroSphere gel formulations. In addition, no sign of skin irritation was observed on the mice.

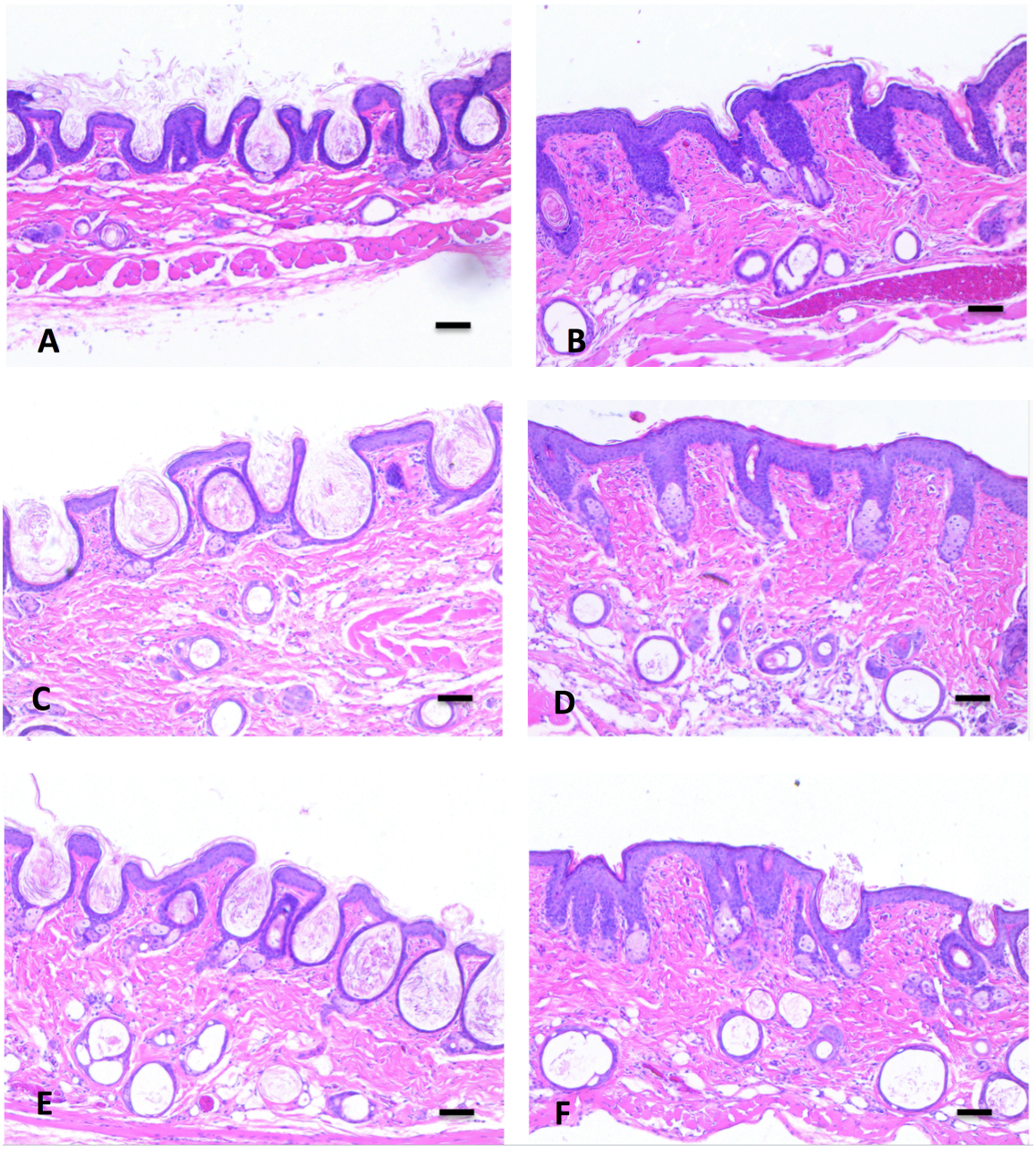

Figure 4.20. Cross section view of rhino mouse skin A) untreated and B) treated once daily for 14 days with adapalene-TyroSphere MP407-2 gel 0.03 wt% (20 µg/cm^2), C) untreated and D) treated with adapalene-TyroSphere MP407-1 gel 0.05 wt% (35 µg/cm^2), E) untreated and F) treated with Differin® gel 0.1 wt% (35 µg/cm^2). The vertical paraffin sections of skin specimens were stained with haematoxylin and eosin. Scale bar = 100µm.

Figure 4.21 depicts effects of topically applied adapalene-TyroSphere gel formulation on morphological characteristics of rhino mouse epidermis. The number of

cell layers and the thickness of epidermal layer, especially stratum granulosum increased in the skin areas treated with adapalene formulations. The epidermal hyperplasia is more clear in utricle walls. These findings suggest that encapsulation of adapalene in TyroSpheres preserved its therapeutic efficacy.

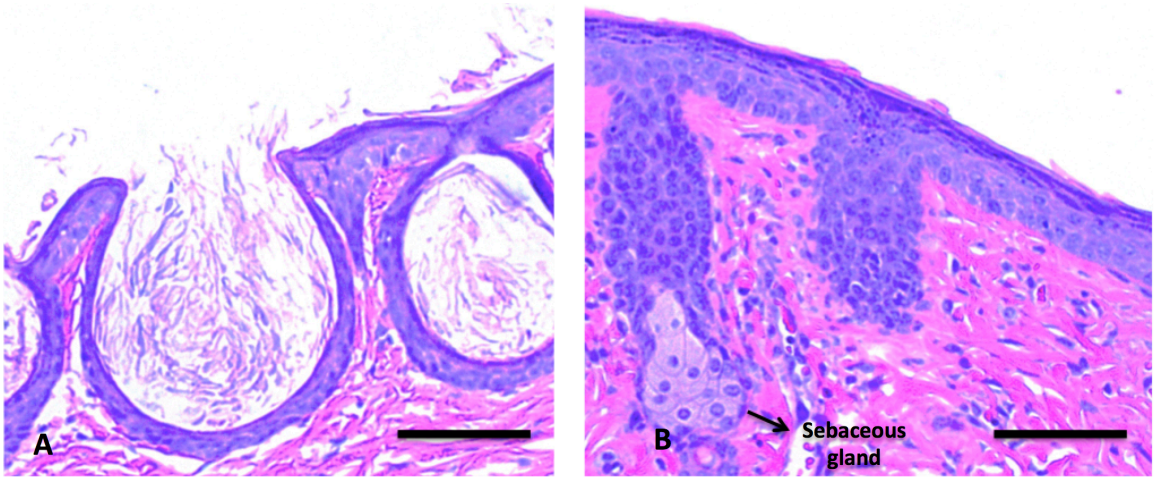

Figure 4.21. Rhino mouse skin A) untreated and B) treated with adapalene-TyroSphere MP407 gel. Adapalene induced significant epidermal hyperplasia, especially in the utricle wall. The vertical paraffin sections of skin specimens were stained with haematoxylin and eosin. Scale bar = 100μm.

In order to compare comedolytic effect of the TyroSphere gels with the adapalene commercial product, the diameter size, depth and density of the utricles were measured in the cross section samples. The efficacy of the formulations was assessed by calculating percentage reduction of the number and size of utricles in each mouse after 2 weeks of adapalene daily treatment. Figure 4.22 shows the change in utricle density between untreated skin areas and areas treated with adapalene formulations. In all experimental groups there was a highly significant reduction in number of open utricles (representing microcomedones in human) after treatment with adapalene ($p<0.001$). The percentage change in utricle density was calculated as 33.7±7.6, 53.4±7.4, and 43.8±6.7 % for

Differin®, adapalene-TyroSphere-MP407-1 and 2 respectively. TyroSphere gel formulation —with similar drug content—was significantly more effective than Differin® in reducing number of open utricles in rhino mice skin (p<0.01).

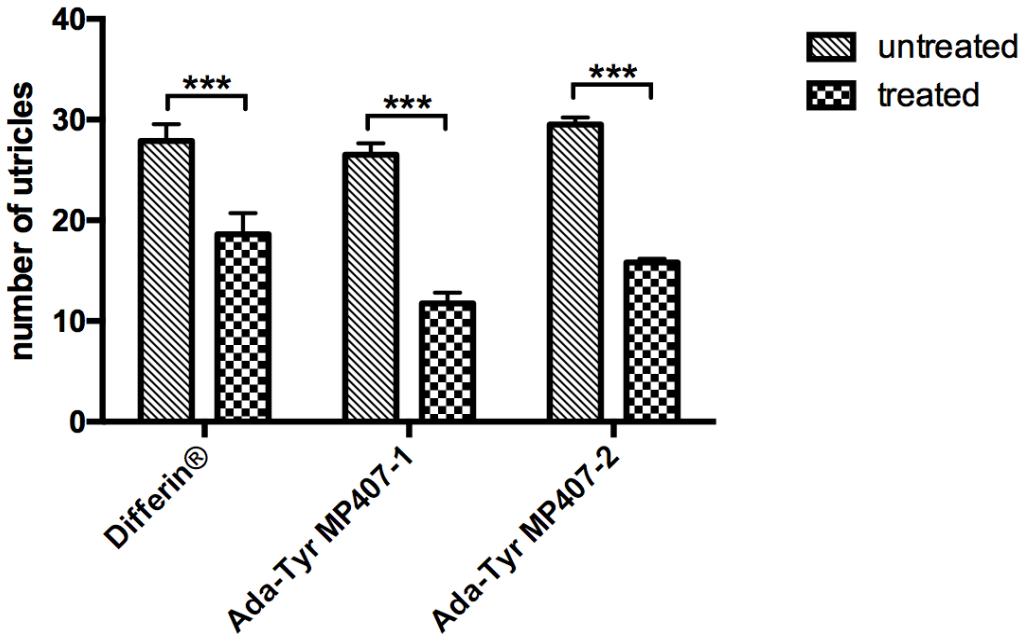

Figure 4.22. The average utricle density in rhino mouse skin counted from the areas not treated with adapalene formulations (untreated) and the areas that received the adapalene-TyroSphere MP407 gels (Ada-Tyr MP407) or Differin® (treated). The results are shown as average number of utricles in 6 mm cross-section skin biopsy ± SE. *** P<0.01 determined by one-way ANOVA followed by Tukey's post hoc test.

The effect of adapalene treatments on reduction of utricle size is shown in Table 4.1 and Figure 4.23. The utricles' depth and diameter were substantially decreased following two weeks of topical adapalene daily treatment. Adapalene-TyroSphere MP407-1 was significantly more effective in reducing the size of rhino mice utricles (p<0.001). There was no significant difference between Differin® and adapalene-MP407-2 in reducing the diameter of utricle opening. However both TyroSphere gels (with

similar and less drug content than Differin®) were more successful than the commercial product in reducing the depth of utricles.

Table 4.1. The average utricle diameter and depth in rhino mice skin.
The utricle size was measured from the areas not treated with adapalene formulations (untreated) and the areas that received the adapalene-TyroSphere MP407 gels (Ada-Tyr MP407) or Differin® (treated). The data are shown as mean±SD.

	Utricle diameter (µm)		**Utricle depth (µm)**	
	untreated	After treatment	untreated	After treatment
Differin®	77.8±8.5	45.6±10.2	121.3±27.3	76.8±26.9
Ada-Tyr MP407-1	74.4±6.3	27.6±14.5	111.0±13.8	41.7±10.1
Ada-TyrMP407-2	67.7±4.5	38.2±4.9	116.2±12.1	51.9±14.9

In general our data show that adapalene encapsulation in TyroSpheres not only preserve its efficacy, but also have promoted the comedolytic effect significantly better than what observed with the commercial adapalene gel. Adapalene-TyroSphere gel (0.03 wt%) showed comedolytic effect similar to Differin® (0.1 wt%). The improved retinoid efficacy that was observed with TyroSpheres can be attributed to penetration and accumulation of the nanospheres in the utricles and gradual release and delivery of the retinoid at its target site.

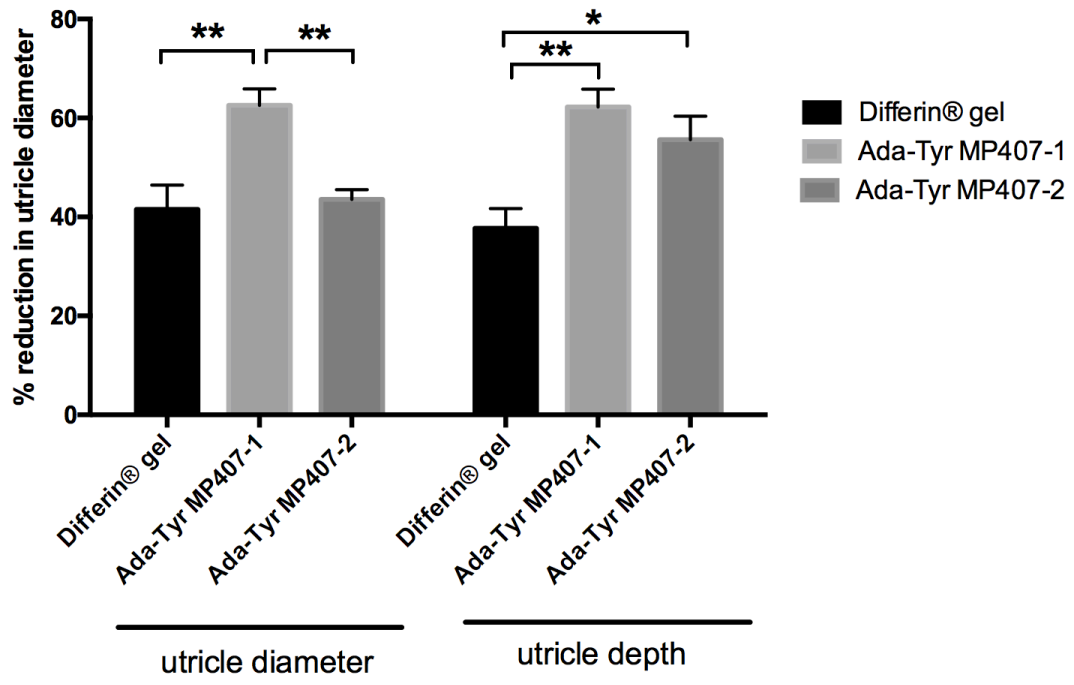

Figure 4.23. The % reduction in diameter and depth of utricles in rhino mouse skin following two weeks of daily treatment with Differin® 0.1 wt% (35 μg/cm^2) and adapalene-TyroSphere (Ada-Tyr) MP407 gel-1 0.05 wt% (35 μg/cm^2) and adapalene-TyroSphere MP407 gel-2 0.03 wt% (20 μg/cm^2). The data are shown as mean±SE, n=5. ** P<0.01 and * P<0.05 determined by one-way ANOVA followed by Tukey's post hoc test.

4.4. Conclusions

A topical formulation of adapalene was developed and characterized using TyroSpheres as the carrier system and MP407 as the viscous agent. This oil-free and alcohol-free aqueous-based formulation of adapalene has rheological properties similar to Differin® but is potentially less irritant and suited to be applied on oily and acneic skin. TyroSphere formulations with less drug content than the marketed product were able to deliver comparable amounts of adapalene to the epidermis. The TyroSphere formulation of adapalene was tested on a preclinical *in vivo* acne model, which confirmed that the

comedolytic and epidermal differentiation effects of the drug were preserved after loading in the nanoparticles. TyroSpheres were able to enhance adapalene distribution in the skin, and particularly utricles, and were more effective in shrinking the microcomedones. Together, these results suggest that TyroSpheres have considerable potential in the drug delivery to skin and can be employed as an innovative and effective approach for topical acne therapy.

4.5. References

1. Greenman, J., Follicular pH and the development of acne. *Int J Dermatol* 1981, *20* (10), 656-8.
2. Well, D., Acne vulgaris: A review of causes and treatment options. *Nurse Pract* 2013, *38* (10), 22-31; quiz 32.
3. Akhavan, A.; Bershad, S., Topical acne drugs: review of clinical properties, systemic exposure, and safety. *Am J Clin Dermatol* 2003, *4* (7), 473-92.
4. Mukherjee, S.; Date, A.; Patravale, V.; Korting, H. C.; Roeder, A.; Weindl, G., Retinoids in the treatment of skin aging: an overview of clinical efficacy and safety. *Clin Interv Aging* 2006, *1* (4), 327-48.
5. Waugh, J.; Noble, S.; Scott, L. J., Adapalene: a review of its use in the treatment of acne vulgaris. *Drugs* 2004, *64* (13), 1465-78.
6. Batheja, P.; Sheihet, L.; Kohn, J.; Singer, A. J.; Michniak-Kohn, B., Topical drug delivery by a polymeric nanosphere gel: Formulation optimization and in vitro and in vivo skin distribution studies. *J Control Release* 2011, *149* (2), 159-67.
7. Kilfoyle, B. E.; Sheihet, L.; Zhang, Z.; Laohoo, M.; Kohn, J.; Michniak-Kohn, B. B., Development of paclitaxel-TyroSpheres for topical skin treatment. *J Control Release* 2012, *163* (1), 18-24.
8. Alvarez-Roman, R.; Barre, G.; Guy, R. H.; Fessi, H., Biodegradable polymer nanocapsules containing a sunscreen agent: preparation and photoprotection. *Eur J Pharm Biopharm* 2001, *52* (2), 191-5.
9. Gao, W.; Vecchio, D.; Li, J.; Zhu, J.; Zhang, Q.; Fu, V.; Li, J.; Thamphiwatana, S.; Lu, D.; Zhang, L., Hydrogel containing nanoparticle-stabilized liposomes for topical antimicrobial delivery. *ACS Nano* 2014, *8* (3), 2900-7.
10. Pople, P. V.; Singh, K. K., Development and evaluation of topical formulation containing solid lipid nanoparticles of vitamin A. *AAPS PharmSciTech* 2006, *7* (4), 91.
11. Valenta, C.; Christen, B.; Bernkop-Schnurch, A., Chitosan-EDTA conjugate: A novel polymer for topical gels. *J Pharm Pharmacol* 1998, *50* (5), 445-452.

12. Levina, M.; Rajabi-Siahboomi, A. R., The influence of excipients on drug release from hydroxypropyl methylcellulose matrices. *J Pharm Sci-Us* 2004, *93* (11), 2746-2754.
13. Pereira, G. G.; Dimer, F. A.; Guterres, S. S.; Kechinski, C. P.; Granada, J. E.; Cardozo, N. S. M., Formulation and Characterization of Poloxamer 407 (R): Thermoreversible Gel Containing Polymeric Microparticles and Hyaluronic Acid. *Quim Nova* 2013, *36* (8), 1121-+.
14. Dumortier, G.; Grossiord, J. L.; Agnely, F.; Chaumeil, J. C., A review of poloxamer 407 pharmaceutical and pharmacological characteristics. *Pharm Res* 2006, *23* (12), 2709-2728.
15. Bernerd, F.; Ortonne, J. P.; Bouclier, M.; Chatelus, A.; Hensby, C., The rhino mouse model: the effects of topically applied all-trans retinoic acid and CD271 on the fine structure of the epidermis and utricle wall of pseudocomedones. *Arch Dermatol Res* 1991, *283* (2), 100-7.
16. Kligman, L. H.; Kligman, A. M., The effect on rhino mouse skin of agents which influence keratinization and exfoliation. *J Invest Dermatol* 1979, *73* (5), 354-8.
17. Plewig, G.; Kligman, A. M., Rhino Mouse Model. In *ACNE and ROSACEA*, Springer: 1993; pp 241-243.
18. Beehler, B. C.; Chen, S.; Tramposch, K. M., Gene expression of retinoic acid receptors and cellular retinoic acid-binding proteins in rhino and hairless mouse skin. *Arch Dermatol Res* 1995, *287* (5), 488-93.
19. Sheihet, L.; Dubin, R. A.; Devore, D.; Kohn, J., Hydrophobic drug delivery by self-assembling triblock copolymer-derived nanospheres. *Biomacromolecules* 2005, *6* (5), 2726-31.
20. Sheihet, L.; Piotrowska, K.; Dubin, R. A.; Kohn, J.; Devore, D., Effect of tyrosine-derived triblock copolymer compositions on nanosphere self-assembly and drug delivery. *Biomacromolecules* 2007, *8* (3), 998-1003.
21. Castro, G. A.; Oliveira, C. A.; Mahecha, G. A.; Ferreira, L. A., Comedolytic effect and reduced skin irritation of a new formulation of all-trans retinoic acid-loaded solid lipid nanoparticles for topical treatment of acne. *Arch Dermatol Res* 2011, *303* (7), 513-20.
22. Hayashi, N.; Watanabe, H.; Yasukawa, H.; Uratsuji, H.; Kanazawa, H.; Ishimaru, M.; Kotera, N.; Akatsuka, M.; Kawashima, M., Comedolytic effect of topically applied active vitamin D3 analogue on pseudocomedones in the rhino mouse. *Br J Dermatol* 2006, *155* (5), 895-901.
23. Edsman, K.; Carlfors, J.; Petersson, R., Rheological evaluation of poloxamer as an in situ gel for ophthalmic use. *Eur J Pharm Sci* 1998, *6* (2), 105-12.
24. https://www.lubrizol.com/PersonalCare/Products/Carbopol/Carbopol940.html.
25. Orfanos, C. E.; Zouboulis, C. C.; Almond-Roesler, B.; Geilen, C. C., Current use and future potential role of retinoids in dermatology. *Drugs* 1997, *53* (3), 358-88.
26. Van de Sandt, J.; Roguet, R.; Cohen, C.; Esdaile, D.; Ponec, M.; Corsini, E.; Barker, C.; Fusenig, N.; Liebsch, M.; Benford, D., The use of human keratinocytes and human skin models for predicting skin irritation. *ATLA-NOTTINGHAM-* 1999, *27*, 723-744.
27. Spielmann, H.; Hoffmann, S.; Liebsch, M.; Botham, P.; Fentem, J. H.; Eskes, C.; Roguet, R.; Cotovio, J.; Cole, T.; Worth, A.; Heylings, J.; Jones, P.; Robles, C.; Kandarova, H.; Gamer, A.; Remmele, M.; Curren, R.; Raabe, H.; Cockshott, A.; Gerner,

I.; Zuang, V., The ECVAM international validation study on in vitro tests for acute skin irritation: report on the validity of the EPISKIN and EpiDerm assays and on the Skin Integrity Function Test. *Altern Lab Anim* 2007, *35* (6), 559-601.

Chapter 5: Evaluation of Vitamin D3-TyroSpheres for topical delivery

5.1. Introduction

Vitamin D3 (VD3) or cholecalciferol is a steroid hormone generated in the skin by UVB radiation of 7-dehydrocholesterol or it is obtained from dietary sources. The active form of cholecalciferol, 1,25-dihydroxycholecalciferol (calcitriol) plays an important role in regulation of calcium homeostasis and mineralization of bones.[1] VD3 and its analogues have been also associated with other functions in the body. For example, they can influence keratinocyte differentiation and are therefore used in treatment of several skin disorders including psoriasis.[2] Vitamin D3 and its analogues are also involved in the control of multiple intracellular pathways responsible for the melanin synthesis and melanocyte survival. They can control the activation, proliferation, and migration of melanocytes and therefore induce skin pigmentation, which is potentially useful in treatment of vitiligo.[3] Maxacalcitol, one of the active analogues of VD3, has proven to be effective in treatment of comedones,[4-5] and there are a few studies reporting antineoplastic activity of calcitriol.[6] The anti-psoriatic properties of VD3 analogues are suggested to result from their effects in decreasing proliferation and promoting differentiation of keratinocytes, as well as immunomodulatory actions.[7] Even though the exact mechanism behind these effects is not completely understood, it is well-known that VD3 anti-psoriatic effects are partially genomic and mediated via the vitamin D receptor.[8] As far back as the 1930s, VD3 was used as an oral therapy for psoriasis but eventually fell out of favor due to hypercalcemic side effects. After the discovery of VD3

receptors on keratinocytes and fibroblasts, interest in topical therapy with VD3 analogues resurfaced.[9] Human keratinocytes have an autonomous VD3 pathway and can convert VD3 to its hormonally active form, calcitriol.[8]

Skin, despite its strong barrier properties provides several advantages as a route of delivery. Dermal drug delivery via topical application can localize a high concentration of active in the upper skin layers —which is the site of action for many drugs that treat dermatological disorders— and also minimize systemic exposure of the drug. Successful drug delivery depends on the physicochemical characteristics of the active and its carriers in the formulation. One of the approaches for formulating unstable and highly lipophilic compounds is by using particulate systems. Many studies have been focused on using nanoparticles for enhanced topical delivery of small and large molecules. A broad spectrum of particles (including liposomes, solid lipid nanoparticles[10], polymeric micelles[11], and microemulsions[12]) have been studied for delivery of drugs and cosmetic actives to the skin. These delivery systems may be capable of providing chemical and/or physical protection of the active, sustained and controlled release of the drug, enhanced solubility of the active, and eventual enhancement of the biological absorption of the drug.[13]

VD3 is very hydrophobic (log P = 9) and sensitive to many environmental factors (e.g. moisture, heat and light), which can induce isomerization or oxidation of its structure and adversely affecting its activity.[14] In recent years, encapsulation of lipophilic compounds to increase their stability and preserve their bioactivity has received significant attention in both the food and the pharmaceutical industry. There are few reports in literature where these approaches have been used for VD3. However,

preparation of some of these carrier systems involves using high temperature[15-16] (which would induce inactivation of VD) or toxic solvents e.g. tetrachloride or petroleum ether[16], which poses potential problems if the solvent residues exist in the final product. In this study, we propose to utilize a TyroSphere-containing formulation made from PEG_{5K}-*b*-oligo(desaminotyrosyl-tyrosine octyl ester suberate)-*b*-PEG_{5K} (DTO-SA/5K) copolymer for the topical delivery of VD3. To best of our knowledge there is no published study on topical delivery of VD3 using nanocarriers.

The initial studies on VD3-TyroSpheres fabrication and characterization were conducted by Dr. Brian Kilfoyle, the former Ph.D. student at New Jersey Center for Biomaterials. In those studies, VD3 was loaded in TyroSpheres at range of about 1 to 30% of initial drug to polymer input (w/w). There has been substantial increase in the aqueous solubility of VD3 by means of TyroSpheres and the maximum drug concentration was about 3.5 mg/ml in the nano-dispersion. Figure 5.1 depicts VD3 binding and loading efficiencies in TyroSpheres. The drug-to-polymer ratio highly influences the drug loading. As the drug initial input increased, higher loading was obtained in the TyroSpheres. TyroSpheres encapsulated VD3 to a maximum of 30.2 wt%. The high drug loading efficiency is due to high affinity of the VD3 structure to the hydrophobic section of the copolymer. VD3-TyroSpheres had particle size in the range of 65-75 nm. The loading input of VD3 had a small impact on the diameter size of TyroSpheres; larger nanoparticles were obtained by increasing VD3 initial loading.[17] In this chapter we report on the characterization of VD3-TyroSpheres for stability, drug release, and permeation to human skin. This work aims to address the need of a suitable

carrier system for enhancing dermal delivery of VD3 and improving its stability in the formulation.

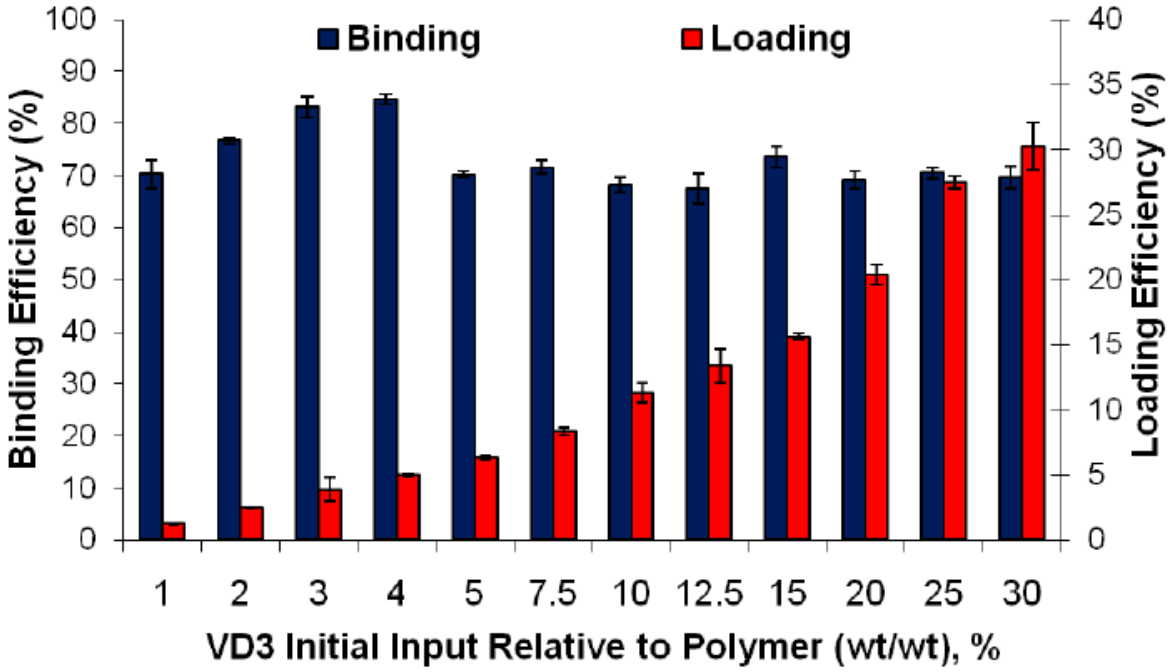

Figure 5.1. Percentage binding and loading efficiencies of Vitamin D3 (VD3) in TyroSphere formulations. The results are shown as mean ± SD.[17]

5.2. Materials and Methods

5.2.1. Materials

Suberic acid (SA), poly(ethylene glycol) monomethyl ether MW 5000 (PEG5K), Tween-80, Dimethylformamide (DMF), and Dulbecco's Phosphate Buffered Saline (PBS), cholecalciferol, and diethylene glycol monoethyl (Transcutol®) were purchased from Sigma Aldrich (St. Louis, MO). Dulbecco's Modified Eagle Medium, high glucose (DMEM), trypsin (0.25% Trypsin-EDTA), Penicillin Streptomycin (10,000 U/mL), fetal bovine serum (FBS), and Dulbecco's Phosphate Buffered Saline without calcium

chloride and magnesium chloride (DPBS) were purchased from Life Technologies (Grand Island, NY). HPLC grade water, acetonitrile, and methanol were obtained from Fisher Scientific (Pittsburgh, PA). HaCaT cells were received as a generous gift from Dr. Qing Ren (Department of Radiation Oncology at Thomas Jefferson University). AlamarBlue® Reagent was obtained from AbD Serotec (Raleigh, NC). PEG_{5K}-*b*-oligo(desaminotyrosyl-tyrosine octyl ester suberate)-*b*-PEG_{5K} (M_n = 22.9 kDa, Mw = 31.9 kDa, PD = 1.39 obtained from gel permeation chromatography) was synthesized according to previously published and established procedures at the New Jersey Center for Biomaterials, Rutgers-The State University of New Jersey. The chemical structure and purity were confirmed by ^{1}H NMR.[18,19] All reagents were used as received.

5.2.2. Preparation of VD3 loaded-TyroSphere formulations

ABA triblock copolymers composed of hydrophilic A blocks of poly(ethylene glycol) and hydrophobic B blocks of desaminotyrosyl-tyrosine octyl ester and suberic acid were used for preparation of TyroSpheres. VD3 loaded-TyroSpheres was prepared and purified by methods described previously.[17, 19-20] The final VD3-TyroSphere nano-dispersion was obtained by redispersing the pellet formed from ultracentrifugation in 3 mL PBS and filtering through 0.22 μm PVDF syringe filters (Merck Millipore). All VD3 solutions/formulations were prepared and stored in amber vials to protect the active against photodegradation.

5.2.3. VD3 high performance liquid chromatography (HPLC) method

An Agilent 1100 high-performance liquid chromatography (HPLC) system (Agilent Technologies, USA) equipped with a UV/Vis detector and C18 column (Waters XBridge 3.5μm particle size, 4.6 x 50 mm) was used for chromatographic separations at 25 °C. A mixture of acetonitrile: water (isocratic A:B, 98:2) was applied as the mobile phase at a flow rate of 1 mL/min. The injection volume was 20 μL and the detection wavelength was set at 265 nm. Standard calibration curves were prepared at drug concentrations ranging from 0.1 to 100 μg/mL in both methanol and DMF. The HPLC method was previously validated for variability, specificity, linearity, robustness, limit of detection, and limit of quantification.[17]

5.2.4. Cytotoxicity in keratinocyte cell line

HaCaTs (a cell line of human keratinocytes) were cultured in a 37°C incubator with 97% relative humidity and 10% CO2. DMEM with 10% FBS and 1% Penicillin/Streptomycin applied as culture medium. When 90% confluency was reached, the cells were rinsed with DPBS and trypsinized. The cells were seeded in 96-well plates at 3,000 cells/well seeding density. The cytotoxicity of VD3-TyroSpheres (at approximately 4% loading) and free VD3 (dissolved in DMSO and diluted in the medium) were tested on HaCaT's at the concentration range of 1-50 μM. AlamarBlue® assay was performed to evaluate the 3-day cytotoxicity according to the method described by Kilfoyle et al.[11] The IC50 was determined based on results of 3 independent experiments.

5.2.5. Drug release and diffusion through stratum corneum

Dermatomed human cadaver skin samples (500-700 μm) from the posterior torso of a male Caucasian donor were obtained from New York Firefighters Skin Bank (New York, NY). The frozen skin was thawed in room temperature and the epidermis was separated by immersing the skin pieces in deionized water and heating up to 60°C.[21] Next, the epidermal layer was transferred to a Petri dish containing 0.025% trypsin solution and incubated at room temperature for 4 h. Then the viable layers of epidermis were removed by a cotton swab and the remaining SC membranes were rinsed with PBS (pH 7.4), dried in in a desiccator overnight and stored at -20°C until use.

SC separated from human cadaver skin was mounted on vertical jacketed Franz diffusion cells with receiver volume of 5 ml and 0.64 cm^2 donor-receptor area (PermeGear, Hellertown, PA). 20% DMF was added as the releasing medium, which was stirred with a magnetic bar at 300 rpm during the experiment at 37 °C. 200 μL of VD3-TyroSphere with 4 and 15 wt.% initial drug loading were applied on the SC. At pre-determined time-points, 300 μL of releasing medium was collected from the receptor compartment and were replaced with the equivalent amount of the DMF. The drug content in the samples was analyzed by HPLC.

5.2.6. *Ex vivo* skin distribution study on human cadaver skin

Dermatomed human skin samples (300-600 μm) from the posterior torso of a Caucasian male donor obtained from New York Firefighters Skin Bank (New York, NY) were used to evaluate skin delivery of VD3 from the TyroSphere and the commercial formulation Differin®. The permeation studies were carried out using vertical Franz

diffusion cells with donor area of 0.64 cm^2 (PermeGear, Inc., Hellertown PA) according to previously described methods.[11] PBS pH 7.4 containing 20% DMF was added to the receptor compartment. The skin samples were treated with either 200 μL VD3-TyroSphere liquid dispersion with 4 and 15 wt.% initial drug loading or VD3 solution in Transcutol® (1.5 mg/ml, similar concentration to VD3-TyroSpheres 15 wt%). The temperature of the Franz cells was maintained at 37 °C. At predetermined time points (3, 6, and 12 h) the skin pieces were washed and removed from the Franz cells. Epidermal and dermal layers were manually separated using tweezers. VD3 was extracted in DMF from skin layers with the aid of bead bug microtube homogenizer (Benchmark Scientific, Atkinson, NH). The drug content in epidermis, dermis, receptor media and donor compartment was determined by HPLC.

5.2.7. Stability of VD3 against photodegradation

VD3-TyroSphere dispersion and methanolic solution of VD3 (both about 200 μg/mL) were prepared for photochemical stability measurement. Samples were transferred into transparent glass vials and were placed in a safety cabinet exposed to 254 nm UV light. At various exposure time intervals 100 μL of sample was withdrawn from each treatment. The samples from VD3 in methanol were directly subjected for HPLC analysis. The VD3-TyroSphere samples were lyophilized, redispersed in methanol and analyzed by HPLC. This experiment was performed in triplicate.

5.2.8. Stability of the VD3-TyroSphere during storage

Formulations with different target drug loadings (4, 8, and 15% VD3/copolymer w/w) were prepared and stored at 4 °C for 6 months. Particle size and drug content were measured at selected time-points for 6 months. The formulations were also visually analyzed for existence of any precipitation. Short-term stability of VD3 in TyroSphere formulations and VD3 in Transcutol® (1 mg/ml) at room temperature was also assessed. The formulations were kept in amber vials to protect the active from photo-induced degradation.

5.2.9. Statistical analysis

Statistical analysis was performed using Prism Version 6 (GraphPad software, La Jolla California). Student t-test and one-way analysis of variance (ANOVA) followed by Tukey's post hoc was applied to determine the difference among the groups in every study. For skin distribution study, two-way ANOVA was used to compare drug delivery from different formulations at different time points. For all analysis, a *P* value of less than 0.05 derived from a two-tailed test was considered significant unless specified.

5.3. Results and Discussion

DTO-SA copolymers are composed of hydrophilic PEG segments and hydrophobic desaminotyrosyl alkyl ester segment. These copolymers self-assemble to form polymeric micelles (TyroSpheres) in aqueous media. TyroSpheres have a core-shell structure with hydrophobic blocks making the core and the hydrophilic blocks stabilizing

the system in an aqueous environment. This structure allows TyroSpheres to "stabilize" significant amounts of hydrophobic drug in the aqueous solution. Previous studies reported that TyroSpheres were able to encapsulate a wide range of hydrophobic actives and significantly enhance their solubility.[22] VD3 is a hydrophobic molecule and practically insoluble in aqueous media like PBS. It has logP of approximately 9.09 and a molecular weight of 384.64. The molecular structure of VD3 has 7 rotatable bonds, 1 hydrogen acceptor, and 1 hydrogen donor. The chemical structure of VD3 is shown in Figure 5.2. A computational modeling study performed at the New Jersey Center for Biomaterials revealed that the high binding affinity of VD3 to the core of nanospheres is the result of hydrogen bonding and hydrophobic interactions between drug and the copolymer. VD3 is less rigid than other studied molecules, and its flexibility and extremely high hydrophobicity allowed for many hydrophobic interactions within the hydrophobic core of TyroSpheres.[23]

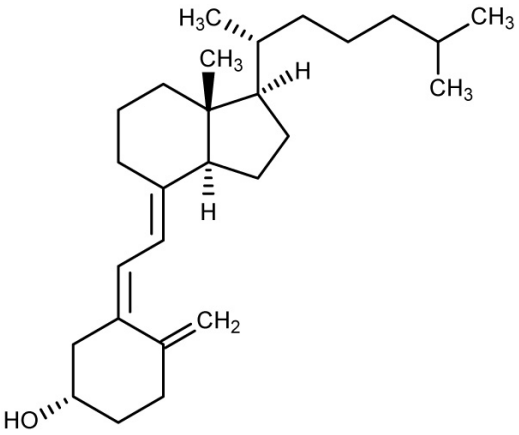

Figure 5.2. Chemical structure of cholecalciferol (Vitamin D3).

5.3.1. Cytotoxic effect of VD3 loaded and unloaded in TyroSpheres on HaCaTs

One of the main characteristics of the psoriatic skin is the over-proliferation of the keratinocytes. Therefore, in order to test whether VD3 can remain active in TyroSpheres, we evaluated cytotoxic effect of VD3 (in form of solution and entrapped in TyroSpheres) on HaCaTs. AlamarBlue® assay has been used to assess metabolic activity of the cell lines following exposure to the tested chemicals. The conversion of the fluorescent Resazurin in AlamarBlue® to Resorufin, in response to cellular metabolic activity, is a marker for cell viability. TyroSpheres that were not loaded with drug did not show cytotoxicity on keratinocytes at concentration range of 1-500 µg/ml. Figure 5.3 depicts % cell viability of HaCaTs following 3-day treatment with either free VD3 or VD3-TyroSphres.

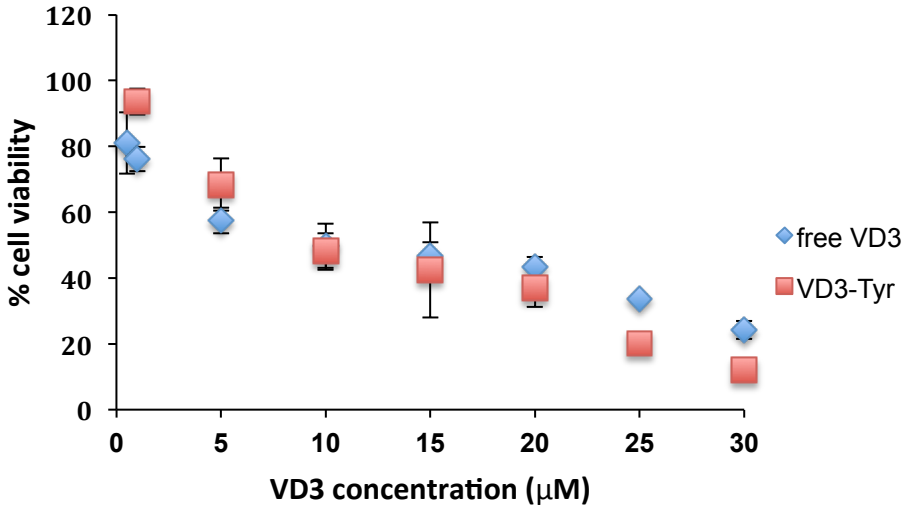

Figure 5.3. Viability of HaCaT epithelial cell line exposed to free Vitamin D3 (VD3) and VD3 encapsulated in TyroSpheres (VD3-Tyr). The percentage viability was measured by AlamarBlue® assay based on metabolic activity of the cells.

The IC_{50} of free VD3 and VD3-TyroSpheres were calculated as 9.3±1.2 μM and 12.0±3.0 μM respectively. Thus, no significant change in metabolic activity of HaCaTs was observed between the two treatment groups, indicating that TyroSpheres do not induce short-term cytotoxicity on keratinocytes and the encapsulated VD3 do not lose its activity.

5.3.2. Release of VD3 from TyroSpheres

The ability of a carrier to release the drug is very important and is usually measured *in vitro* using a semi-permeable membrane in an aqueous environment. However, this method for drug release studies cannot predict the behavior of nanocarriers in contact with SC, which has lipophilic nature. Additionally, for VD3-TyroSpheres, when release studies were conducted with dialysis cassette in an aqueous environment (PBS+1% Tween 80 w/v), VD3 was not detected in the release compartment.[17] This was not unexpected because of the low water solubility of VD3 and its instability in PBS. Therefore, in order to mimic skin application and better understand VD3 release behavior from TyroSpheres in a lipophilic environment, we studied drug release and diffusion through SC. 20% DMF was added to the receptor chamber to provide an adequate driving force for the released drug to diffuse across the SC and prevent instability issues of VD3 that is observed in aqueous media. Figure 5.4 depicts the cumulative % VD3 release from TyroSpheres, which occurred in a sustained manner. Minimal change in particle size of TyroSphere dispersion —applied on SC— after the majority of the loaded drug was released, assured that DMF diffusion to the donor compartment was negligible. Therefore, the drug release did not occur due to dissociation and degradation of the

nanoparticles and the VD3 detected in the receptor compartment is the portion of drug released from TyroSpheres and diffused across the SC.

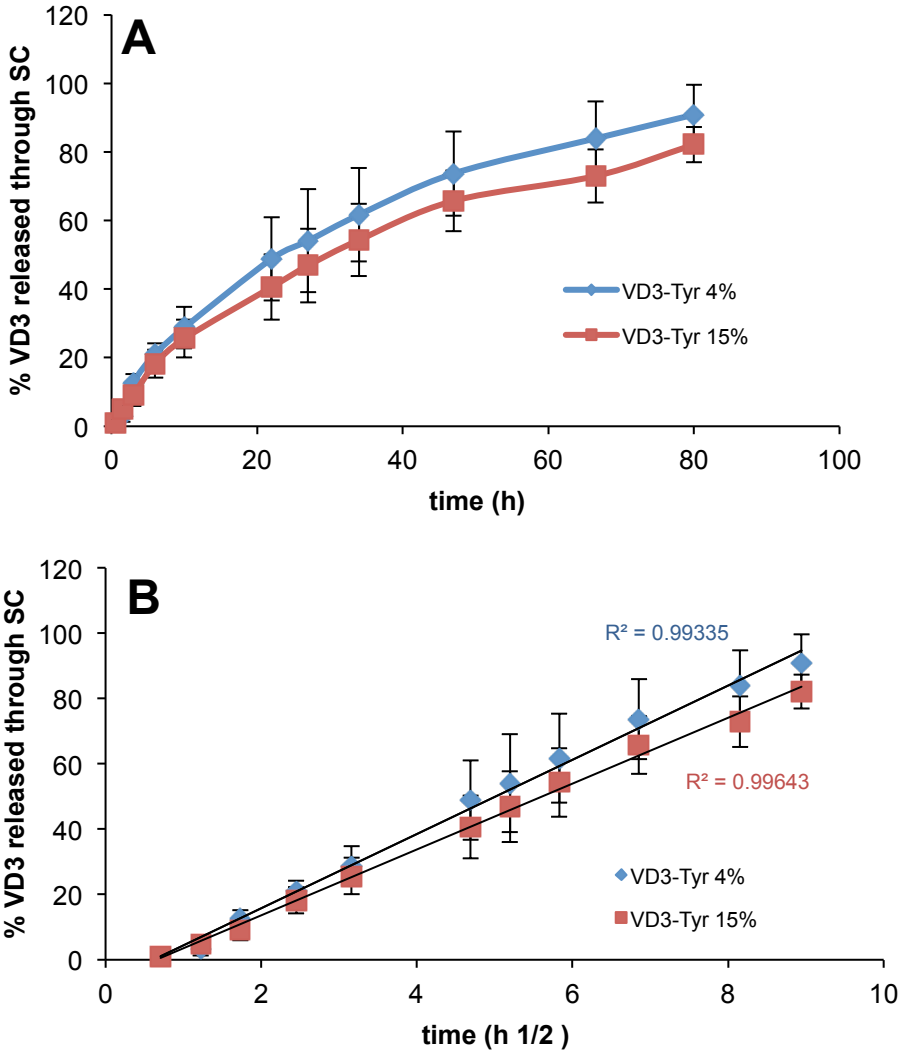

Figure 5.4. Cumulative Vitamin D3 release from TyroSpheres and diffusion through stratum corneum (SC). A) as a function of time and B) as a function of the square root of time (Higuchi model). Study was done with 4 and 15 wt% initial loading VD3 in TyroSpheres (D3-Tyr). Data are shown as mean ± SD (n=5).

The influence of drug loading on release rate from TyroSpheres was also studied. VD3 release profile from both 4 wt% and 15wt% VD3-TyroSpheres were very similar

and there was no significant difference in the percentage drug release ($p<0.05$). Therefore, the drug loading did not affect the release kinetic. According to Figure 5.3.A, the cumulative drug release was not linear. We fit the release data to Higuchi square root model, where the cumulative drug release has a linear correlation with root of time ($R^2=0.99$) irrespective of drug loading (see Figure 5.4.B). This indicates that the drug release from TyroSpheres is controlled by the diffusion and concentration gradient and not polymer erosion.

5.3.3. Skin distribution studies

Skin distribution study was conducted at 3, 6 and 12 h to assess TyroSphere ability to enhance delivery of VD3 to skin. Transcutol® has been reported to be an effective dermal penetration enhancer by enhancing drug solubility in the skin.[24] Thus, VD3 solution in Transcutol® (at similar drug concentration to VD3-TyroSphere 15%) was used to compare delivery efficiency of this vehicle to that of TyroSpheres. Figure 5.5 provides the results of skin permeation study that were analyzed by HPLC. At all the time points, VD3 diffusion to epidermis, which is the target layer for VD3 delivery, was significantly higher than dermis for VD3-TyroSpheres 15 wt% formulation ($p<0.01$). Drug content in receptor compartment was below detection limit of our analytical technique, which was expected due to high lipophilicity of VD3. Following 6 h and 12 h exposure of VD3 formulations with human skin, VD3-TyroSpheres 15 wt% was found to be the most efficient formulation to deliver the drug to epidermis and dermis. According to Fick's law of diffusion ($J=-D\times\partial\varphi/\partial x$, where J is diffucion flux, D is diffusion coefficient, and $d\varphi/dx$ is concentration gradient)[13] it is expected that by increasing drug

concentration in the formulation the diffusion flux increases, which explains higher VD3 delivery to skin layers from VD3-TyroSphere 15 wt% than 4wt% drug loading. By increasing the exposure time of skin with the formulation (from 6 h to 12 h) significant increase in the VD3 diffusion to epidermis observed with VD3-TyroSphere 15 wt% ($p<0.05$), while VD3-Transcutol® with similar drug concentration did not show statistically significant increase in the delivery with longer application time. This observation is probably due to sustained release of VD3 from TyroSpheres that affects the rate of drug permeation to the skin and does not occur with VD3 solution in Transcutol®. The results from *ex vivo* skin distribution study are in agreement with previous published studies[11, 20, 25] and confirmed TyroSpheres efficiency for topical drug delivery and show that these nanocarriers are more effective than some other dermal penetration enhancers, such as propylene glycol[20] and Transcutol®. The exact mechanism behind dermal penetration enhancement effect of polymeric nanoparticles is still unknown. However according to the recent investigations in this area, this enhancement in skin penetration can be attributed to accumulation of nanoparticles in skin appendages, their penetration into the superficial layers of the SC, and/or providing higher concentration gradient by increasing apparent solubility of the loaded drugs. [26-27]

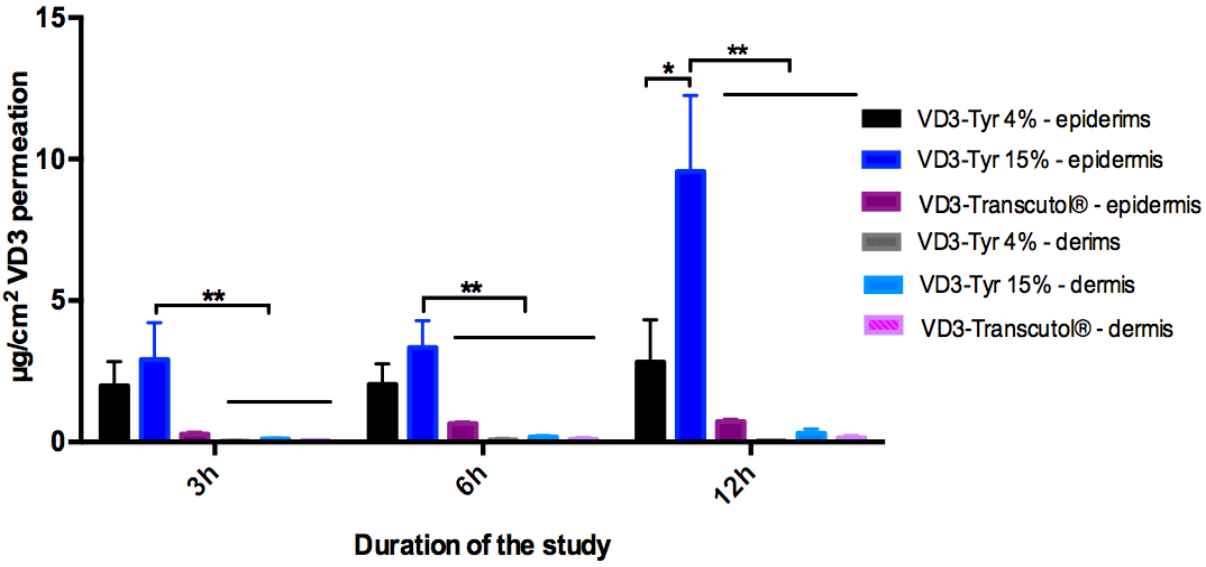

Figure 5.5. Skin distribution of Vitamin D3 loaded in TyroSphere (VD3-Tyr) at 4 and 15 wt% initial loading and VD3 dissolved in Transcutol®, in human cadaver skin during 3, 5 and 12 h exposure. The statistical data is expressed as mean ± SE (n = 5), * P<0.05, ** P<0.01.

5.3.4. Stability of VD3 in TyroSphere formulation

5.3.4.1. Stability against photodegradation

Photochemical stability of VD3 encapsulated in TyroSpheres was studied and compared with free VD3 dissolved in methanol. As it is shown in Figure 5.6, VD3 in methanol underwent photodegradation much faster than in TyroSphere formulation. In the first 24 h exposure to UV light, no significant VD3 degradation was observed in TyroSphere formulation while nearly 20% of the drug was lost in methanolic solution. After 134 h only 21% of VD3 was left in methanol formulation, which is significantly lower than 49%, VD3 left in TyroSphere formulation (p<0.01 from Student t-test).

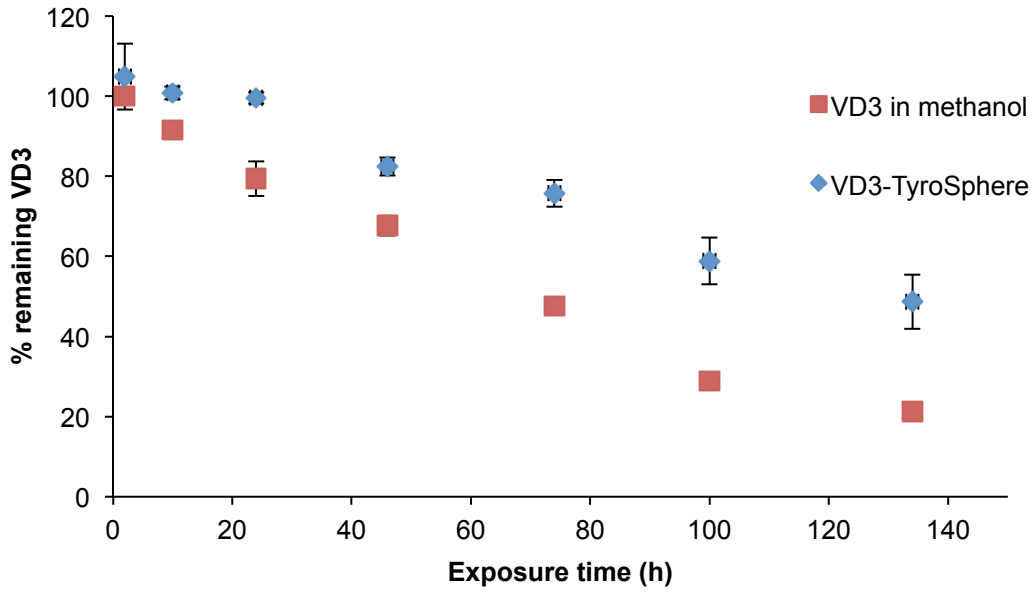

Figure 5.6. Photostability of Vitamin D3 (VD3) encapsulated in TyroSpheres and dissolved in methanol (as control). The results are the average % of VD3 remained in the formulation ± SD (n=3).

Photodegradation of VD3 in both vehicles followed zero-order kinetics (R>0.97). The degradation rate constants were found to be -1.194 and -0.757 $ug.ml^{-1}.h^{-1}$ for VD3 in methanol and TyroSpheres respectively (Figure 5.7). The half-life of VD3 was calculated as 76 and 127 h in methanolic solution and TyroSpheres aqueous dispersion, respectively. Our results demonstrate that TyroSpheres could improve stability of VD3 when exposed to UV light. This can be ascribed to accommodation of VD3 inside the inner core of TyroSpheres which is surrounded by PEG layer. As a result, VD3 is protected from harsh environmental factors (like light and moisture).[28] It is noteworthy that we chose methanol as a solvent that completely dissolves VD3 and other researchers have used it as a control solvent for evaluating photoprotective properties of the nanomaterial.[29,30] Light-induced degradation of VD3 can further be accelerated when VD3 is dispersed in aqueous media. Luo et al.[31] reported that only about 30% of VD3 was remained when VD3 dispersion in water was exposed to UV light for 9.5 h. Therefore, TyroSpheres not only enhance water

solubility of VD3, but also substantially decrease degradation of this compound in the aqueous medium.

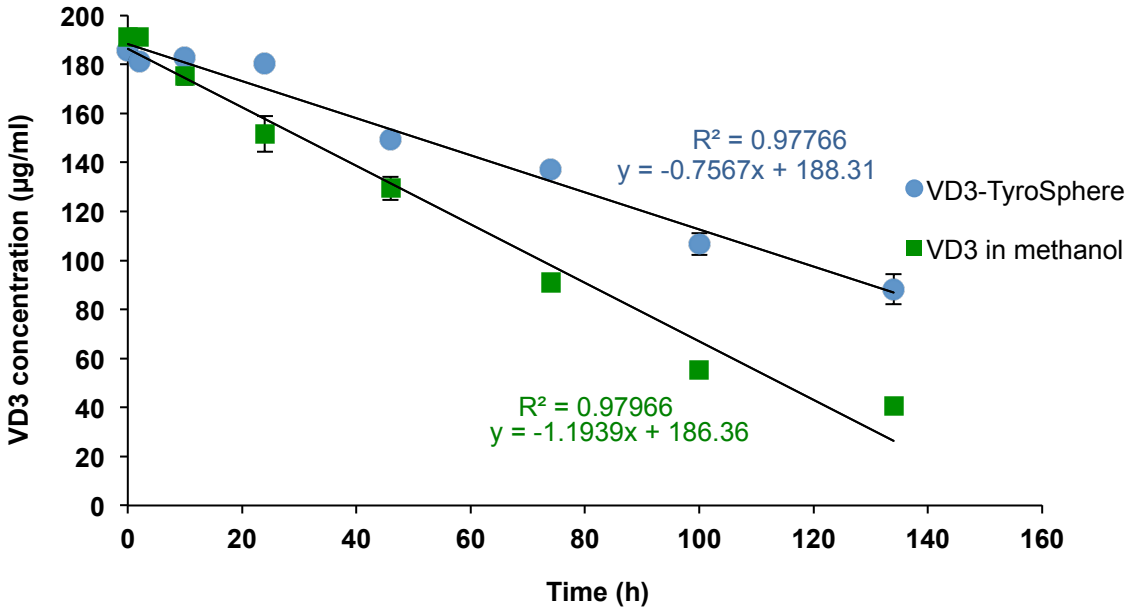

Figure 5.7. Variation of Vitamin D3 (VD3) concentrations in methanol and TyroSphere formulation when exposed to UV light. Data is shown as mean ± SD (n=3). Results from both formulations fit to the zero-order kinetic model.

5.3.4.2. Stability of VD3 in TyroSpheres during long-term and short-term storage

Encapsulation of VD3 with TyroSpheres aims to protect VD3 from environmental factor (e.g. moisture and light) that affect its activity. Stability of VD3-TyroSphere formulations was studied by measuring particle size and drug content at different time points. During 6 months storage at 4°C, precipitation or change in turbidity of the colloidal dispersion was not visually observed. Additionally, there was no significant change in the average diameter size of nanoparticles (measured by DLS technique) and the particle size remained around 65 nm and 71 nm for both VD3-TyroSphere 4 and 15 wt% loading respectively. The PDI was also less than 0.16 showing narrow size

distribution and lack of agglomeration of TyroSpheres. TyroSpheres have micelle–like structure with hydrophobic core and hydrophilic shell. The highly hydrated outer shells of these polymeric micelles — due to the presence of PEG — can inhibit intermicellar aggregation of their hydrophobic inner cores. As a result, TyroSpheres maintained a satisfactory aqueous stability irrespective of high contents of hydrophobic drug incorporated into their inner core.[32]

Following 6 months storage of VD3-TyroSpheres at 4°C, 93.2± 9.6 and 89.0±2.6 % of VD3 were remained in 4 and 8 wt% VD3-TyroSphere formulations. Short-term stability assessment of VD3-TyroSpheres at 25°C confirmed that TyroSpheres can significantly increase drug stability in the formulation. As expected, the rate of VD3 degradation was less at 4°C relative to room temperature. After 2 months storing at room temperature, only 2% of VD3 was detected in Transcutol® (control vehicle for VD3 that was used in skin permeation study), while VD3 recovery in 4 and 15 wt% VD3-TyroSphere was 92 and 74% (Table 5.1). Our results suggest that at both storage conditions, the initial drug loading can influence the rate of VD3 degradation. This observation can be explained by the results of computational modeling study conducted by Costache et al.[23] They concluded that there are sites with different binding affinities to the drug in TyroSpheres. The sites with higher binding affinity are occupied first and by increasing the initial VD3 loading, these sites get saturated and the excess drug binds to sites with weaker affinities. During the storage, the portion of VD3 that is bound weakly to the polymer, may release from TyroSpheres and leak to the surrounding aqueous medium, which results in its degradation.

Table 5.1. Vitamin D3 (VD3) stability in the formulations during storage at 25°C. The results are shown as average %VD3 remaining in the formulations.

Formulations	1 week	3 weeks	5 weeks	8 weeks
VD3-Tyr 4%	101%	98%	95%	92%
VD3-Tyr 15%	98%	87%	80%	74%
VD3 in Transcutol®	54%	16%	7%	2%

5.4. Conclusions

There is limited work that has been performed on the topical delivery of VD3. In the present study we introduced TyroSpheres as a novel carrier system to formulate VD3 for dermal delivery. We highlighted the importance of carrier selection to improve solubility, efficacy and stability of challenging-to-formulate drugs such as VD3. TyroSpheres were able to substantially enhance solubility of VD3 in aqueous medium without affecting activity of the drug. These biocompatible nanocarriers form a protective layer around the lipophilic drug that can protect it against environmental-induced degradation. Moreover, the skin delivery efficiency of TyroSpheres was found to be higher than for some other dermal penetration enhancers, such as Transcutol®. This study provides supplementary evidence of TyroSpheres' significant potential for targeted delivery of hydrophobic actives to skin layers.

5.5. References

1. Picciano, M. F., Vitamin D Status and Health. *Crit Rev Food Sci* 2010, *50*, 24-25.
2. Barker, J. N. W. N.; Ashton, R. E.; Marks, R.; Harris, R. I.; Berth-Jones, J., Topical maxacalcitol for the treatment of psoriasis vulgaris: a placebo-controlled, double-blind, dose-finding study with active comparator. *Brit J Dermatol* 1999, *141* (2), 274-278.
3. Birlea, S. A.; Costin, G. E.; Norris, D. A., New insights on therapy with vitamin D analogs targeting the intracellular pathways that control repigmentation in human vitiligo. *Med Res Rev* 2009, *29* (3), 514-46.
4. Hayhoe, R. P. G.; Henson, S. M.; Akbar, A. N.; Palmer, D. B., Variation of human natural killer cell phenotypes with age: Identification of a unique KLRG1-negative subset. *Hum Immunol* 2010, *71* (7), 676-681.
5. Nieves, N. J.; Ahrens, J. M.; Plum, L. A.; DeLuca, H. F.; Clagett-Dame, M., Identification of a Unique Subset of 2-Methylene-19-Nor Analogs of Vitamin D with Comedolytic Activity in the Rhino Mouse. *Journal of Investigative Dermatology* 2010, *130* (10), 2359-2367.
6. Krishnan, A. V.; Feldman, D., Mechanisms of the Anti-Cancer and Anti-Inflammatory Actions of Vitamin D. *Annu Rev Pharmacol* 2011, *51*, 311-336.
7. Nagpal, S.; Na, S.; Rathnachalam, R., Noncalcemic actions of vitamin D receptor ligands. *Endocr Rev* 2005, *26* (5), 662-87.
8. Lehmann, B., The vitamin D3 pathway in human skin and its role for regulation of biological processes. *Photochem Photobiol* 2005, *81* (6), 1246-51.
9. DiSepio, D.; Chandraratna, R. A.; Nagpal, S., Novel approaches for the treatment of psoriasis. *Drug Discov Today* 1999, *4* (5), 222-231.
10. Jenning, V.; Gysler, A.; Schafer-Korting, M.; Gohla, S. H., Vitamin A loaded solid lipid nanoparticles for topical use: occlusive properties and drug targeting to the upper skin. *European journal of pharmaceutics and biopharmaceutics : official journal of Arbeitsgemeinschaft fur Pharmazeutische Verfahrenstechnik e.V* 2000, *49* (3), 211-8.
11. Kilfoyle, B. E.; Sheihet, L.; Zhang, Z.; Laohoo, M.; Kohn, J.; Michniak-Kohn, B. B., Development of paclitaxel-TyroSpheres for topical skin treatment. *Journal of controlled release : official journal of the Controlled Release Society* 2012, *163* (1), 18-24.
12. Bhatia, G.; Zhou, Y.; Banga, A. K., Adapalene microemulsion for transfollicular drug delivery. *Journal of pharmaceutical sciences* 2013, *102* (8), 2622-31.
13. Zhang, Z.; Tsai, P. C.; Ramezanli, T.; Michniak-Kohn, B. B., Polymeric nanoparticles-based topical delivery systems for the treatment of dermatological diseases. *Wires Nanomed Nanobi* 2013, *5* (3), 205-218.
14. Ballard, J. M.; Zhu, L.; Nelson, E. D.; Seburg, R. A., Degradation of vitamin D3 in a stressed formulation: the identification of esters of vitamin D3 formed by a transesterification with triglycerides. *J Pharm Biomed Anal* 2007, *43* (1), 142-50.
15. Delaurent, C.; Siouffi, A. M.; Pepe, G., Cyclodextrin inclusion complexes with vitamin D-3: Investigations of the solid complex characterization. *Chem Anal-Warsaw* 1998, *43* (4), 601-616.

16. Shi, X. Y.; Tan, T. W., Preparation of chitosan/ethylcellulose complex microcapsule and its application in controlled release of vitamin D-2. *Biomaterials* 2002, *23* (23), 4469-4473.
17. Kilfoyle, B. E. Tyrosine-derived nanoparticles for the topical treatment of psoriasis. Rutgers University-Graduate School-New Brunswick, 2011.
18. Sheihet, L.; Dubin, R. A.; Devore, D.; Kohn, J., Hydrophobic drug delivery by self-assembling triblock copolymer-derived nanospheres. *Biomacromolecules* 2005, *6* (5), 2726-31.
19. Sheihet, L.; Piotrowska, K.; Dubin, R. A.; Kohn, J.; Devore, D., Effect of tyrosine-derived triblock copolymer compositions on nanosphere self-assembly and drug delivery. *Biomacromolecules* 2007, *8* (3), 998-1003.
20. Batheja, P.; Sheihet, L.; Kohn, J.; Singer, A. J.; Michniak-Kohn, B., Topical drug delivery by a polymeric nanosphere gel: Formulation optimization and in vitro and in vivo skin distribution studies. *Journal of controlled release : official journal of the Controlled Release Society* 2011, *149* (2), 159-67;
21. KLIGMAN, A. M.; CHRISTOPHERS, E., Preparation of isolated sheets of human stratum corneum. *Archives of dermatology* 1963, *88* (6), 702-705.
22. Zhang, Z.; Ramezanli, T.; Tsai, P.-C., Drug Delivery Systems Based on Tyrosine-derived Nanospheres (TyroSpheres™). *Nanotechnology and Drug Delivery, Volume One: Nanoplatforms in Drug Delivery* 2014, *1*, 210.
23. Costache, A. D.; Sheihet, L.; Zaveri, K.; Knight, D. D.; Kohn, J., Polymer-drug interactions in tyrosine-derived triblock copolymer nanospheres: a computational modeling approach. *Molecular pharmaceutics* 2009, *6* (5), 1620-7.
24. Harrison, J. E.; Watkinson, A. C.; Green, D. M.; Hadgraft, J.; Brain, K., The relative effect of Azone and Transcutol on permeant diffusivity and solubility in human stratum corneum. *Pharmaceutical research* 1996, *13* (4), 542-6.
25. Goyal, R.; Macri, L.; Kohn, J., Formulation Strategy for the Delivery of Cyclosporine A: Comparison of Two Polymeric Nanospheres. *Sci Rep* 2015, *5*, 13065.
26. Chen-yu, G.; Chun-fen, Y.; Qi-lu, L.; Qi, T.; Yan-wei, X.; Wei-na, L.; Guang-xi, Z., Development of a quercetin-loaded nanostructured lipid carrier formulation for topical delivery. *International journal of pharmaceutics* 2012, *430* (1-2), 292-8.
27. Desai, P.; Patlolla, R. R.; Singh, M., Interaction of nanoparticles and cell-penetrating peptides with skin for transdermal drug delivery. *Mol Membr Biol* 2010, *27* (7), 247-59.
28. Wichit, A.; Tangsumranjit, A.; Pitaksuteepong, T.; Waranuch, N., Polymeric micelles of PEG-PE as carriers of all-trans retinoic acid for stability improvement. *AAPS PharmSciTech* 2012, *13* (1), 336-43.
29. Ourique, A. F.; Melero, A.; de Bona da Silva, C.; Schaefer, U. F.; Pohlmann, A. R.; Guterres, S. S.; Lehr, C. M.; Kostka, K. H.; Beck, R. C., Improved photostability and reduced skin permeation of tretinoin: development of a semisolid nanomedicine. *European journal of pharmaceutics and biopharmaceutics : official journal of Arbeitsgemeinschaft fur Pharmazeutische Verfahrenstechnik e.V* 2011, *79* (1), 95-101.
30. Ourique, A. F.; Pohlmann, A. R.; Guterres, S. S.; Beck, R. C., Tretinoin-loaded nanocapsules: Preparation, physicochemical characterization, and photostability study. *International journal of pharmaceutics* 2008, *352* (1-2), 1-4.

31. Luo, Y.; Teng, Z.; Wang, Q., Development of zein nanoparticles coated with carboxymethyl chitosan for encapsulation and controlled release of vitamin D3. *J Agric Food Chem* 2012, *60* (3), 836-43.
32. Opanasopit, P.; Ngawhirunpat, T.; Rojanarata, T.; Choochottiros, C.; Chirachanchai, S., N-phthaloylchitosan-g-mPEG design for all-trans retinoic acid-loaded polymeric micelles. *European journal of pharmaceutical sciences : official journal of the European Federation for Pharmaceutical Sciences* 2007, *30* (5), 424-31.

Conclusions and future perspectives

The ease of preparation, scale-up and biocompatibility of TyroSpheres make them a promising drug carrier for topical delivery. They have been shown to enhance drug delivery to the epidermis as well as the pilosebaceous unit in both *ex vivo* and *in vivo* studies and improve the comedolytic effect of adapalene. These nanocarriers were also found to decrease irritation potential of their payload in *in vitro* models by forming a protective layer around the lipophilic drug that can also protect it against environmentally-induced degradation. Therefore, TyroSpheres have a considerable potential for translation to clinical medicine and can be employed as an innovative and effective approach for topical acne therapy.

Generally there are concerns about the long-term toxicity and fate of nanoparticles in the human body. Based on the skin distribution study using fluorescently-labeled TyroSpheres, these nanoparticles were shown not to penetrate to the intact epidermis but accumulated in the follicular cavity. It is assumed that the nanoparticles are depleted from the hair follicles by a slow process of sebum flow and hair growth. Despite our general knowledge about potential skin penetration of these nanocarriers, there still remain significant questions about the exact clearance mechanism of TyroSpheres from the skin, the influence of gender, skin age and site of application on their biodistribution, the possibility of nanoparticles penetration to the viable skin layers and blood vessels from the follicular epithelium, and the potential irritation and risks following their chronic application. Moreover, further studies are required to assess stability of the drug-loaded TyroSpheres in topical formulations during long-term storage at various temperatures. These major concerns will have to be addressed before

nanoparticle-based topical drug delivery finds an application in treatment of dermatological disorders in human subjects.